BEFORE AND AFTER STUDIES OF THE EFFECTS OF A POWER PLANT INSTALLATION ON LAKE LBJ

A Numerical Temperature Model for Lake LBJ

Interim Technical Report No. 1
to the
Lower Colorado River Authority
Austin, Texas

by

Gordon G. Park, Project Research Engineer
Philip S. Schmidt, P.E., Project Supervisor

THE UNIVERSITY OF TEXAS AT AUSTIN
DEPARTMENT OF MECHANICAL ENGINEERING
ADVANCED ENERGY SYSTEMS LABORATORY
CENTER FOR RESEARCH IN WATER RESOURCES

AESL-1
CRWR 80

December 1971

ACKNOWLEDGEMENTS

The author is grateful to his supervising professor, Dr. Philip S. Schmidt, for his suggestion of this research and guidance throughout the investigation. He also wishes to express his gratitude to Dr. E. Gus Fruh for his assistance during the investigation and to Dr. Hugh A. Walls for his help toward preparation of the final draft.

The author is also grateful to Allen White of the Texas Water Development Board for his assistance in developing the mathematical model and acquiring data. He also wishes to thank Beatrice Mladenka for typing the original manuscript. The author gratefully acknowledges the financial support of the National Science Foundation. Additional support was provided by the Lower Colorado River Authority under Interagency Contract ICA (70-71) - 533.

Gordon George Park

The University of Texas
Austin, Texas
September, 1971

ABSTRACT

A one-dimensional mathematical model for predicting the distribution of thermal energy in a deep, stratified reservoir is developed and applied to Lake LBJ. The model takes into account heat transfer through the air-water interface, advection into and out of the reservoir, and advection and diffusion in the vertical direction within the reservoir. A comparison of predicted and observed temperatures profiles shows good agreement.

To predict the physical effects of the thermal discharge from a proposed power plant on a region of Lake LBJ, the model has been modified to account for temperature gradients in the longitudinal direction in addition to the vertical. Although there are limitations to the use of this two-dimensional model, it is a good starting point for more refined analyses of the physical effects of a thermal discharge on a stratified reservoir.

TABLE OF CONTENTS

Page

LIST OF TABLES

LIST OF FIGURES

NOMENCLATURE

Symbol	Description and Units
A_j	average area of the upper and lower surfaces of the j-th element, ft^2
A_s	area of the surface of the reservoir, ft^2
a_j	area of the lower surface of the j-th element, ft^2
C	fraction of the sky covered by clouds, tenths
C_L	cloudiness correction factor for atmospheric radiation
c	heat capacity of water, Btu/lb - $^{\circ}F$
D(z,t)	diffusivity at elevation z and time t, ft^2/hr
D_j	diffusivity at the bottom of the j-th element, ft^2/hr
D_o	diffusivity at the surface of the reservoir, ft^2/hr
e_a	vapor pressure, in. Hg.
e_s	saturation vapor pressure at the water surface temperature, in. Hg.
e_{wb}	saturation vapor pressure at the wet-bulb temperature, in. Hg.
g	acceleration due to gravity, ft/sec^2
H_j	thermal energy content of the j-th element, Btu
h_a	net atmospheric radiative heat flux, $Btu/hr\text{-}ft^2$
h_b	back radiative heat flux, $Btu/hr\text{-}ft^2$
h_c	convective heat flux, $Btu/hr\text{-}ft^2$
h_{d_j}	heat advected in the vertical direction at the bottom of the j-th element, Btu/hr

Symbol

h_e	evaporative heat flux, Btu/hr-ft^2
h_{i_j}	heat advected into the j-th element by a horizontal inflow, Btu/hr
h_l	latent heat of vaporization of water, Btu/lb
h_{net}	net heat flux passing the air-water interface, Btu/hr-ft^2
h_{o_j}	heat advected from the j-th element by a horizontal outflow, Btu/hr
h_s	net short-wave radiative heat flux, Btu/hr-ft^2
h_{s_j}	heat absorbed in the j-th element from solar radiation, Btu/hr-ft^2
h_{v_j}	heat advected in the vertical direction at the bottom of the j-th element, Btu/hr
h'_j	heat flux from external sources (excluding advection) per unit volume absorbed in the j-th element, Btu/hr-ft^2-ft
h'_n	heat flux from external sources (excluding advection) per unit volume to or from the surface element, Btu/hr-ft^2-ft
i	subscript used to denote an inflow
j	subscript used to denote the j-th element or the j-th surface
o	subscript used to denote an outflow
P_a	barometric pressure, in. Hg.
Q_e	evaporation rate, ft^3/hr
Q_{i_j}	horizontal inflow rate into the j-th element, ft^3/hr
Q_{o_j}	horizontal outflow rate from the j-th element, ft^3/hr

Symbol

Q_s	rate of change of the volume of water stored in the surface element, ft^3/hr
Q_{v_j}	vertical flow rate at the bottom of the j-th element, $ft^3 hr$
q	heat flux, $Btu/hr\text{-}ft^2$
R	reflectivity of the water surface for atmospheric radiation
Ri	Richardson number
t	time, hr
u	horizontal component of the current velocity in the reservoir, ft/sec
w	wind speed, mi/hr
z	vertical coordinate
z_d	elevation of the surface of the reservoir, ft
z_j	elevation of the center of the j-th element, ft
z_t	elevation of the thermocline, ft
α_v	coefficient of volumetric expansion of water, $^{\circ}F^{-1}$
β	fraction of the short-wave solar radiation absorbed in the surface element
γ	exponential decay constant for the diffusivity as a function of depth, ft^{-1}
$\Delta\Phi_j$	solar radiation absorbed in the j-th element, Btu/hr
Δz_j	thickness of the j-th element, ft
Δz_n	thickness of the surface element, ft
ϵ	emissivity of water

Symbol

η	exponential decay constant for the absorption of solar radiation with depth, ft^{-1}
θ_a	dry-bulb air temperature, °F
θ_{i_j}	temperature of the inflow to the j-th element, °F
θ_j	temperature of the j-th element, °F
θ_w	temperature of the water surface, °F
θ_{wb}	wet-bulb air temperature, °F
$\dot{\theta}_j$	time derivative of temperature for the j-th element, °F/hr
ρ	density of water, lb/ft^3
σ	Stefan-Boltzmann constant, $Btu/hr\text{-}ft^2\text{-}°R^4$
Φ_j	solar radiative heat flux at the bottom of the j-th element, $Btu/hr\text{-}ft^2$

CHAPTER I

Introduction

This study was conducted in conjunction with a project being undertaken by The University of Texas at Austin for the Lower Colorado River Authority (LCRA) to evaluate the significance of thermal discharges on the water quality and biota of Lake Lyndon B. Johnson (LBJ). The LCRA is constructing a 440 megawatt fossil-fueled steam-electric generating station on the Baird Tract peninsula adjacent to Lake LBJ which is scheduled to go into operation in 1974. The purpose of the LCRA-sponsored project is to determine the ecological effects of this and planned future power generating units on Lake LBJ.

Fruh (7, p.1)* has pointed out that past studies of the effects of thermal discharges on Texas reservoirs have been concerned with fairly shallow reservoirs which are destratified as a result of the circulation of large volumes of cooling water. Lake LBJ has sufficient depth that the circulation of cooling water is not expected to mix the reservoir. Since little is known about the effects of thermal discharges on the water quality and biology of such a stratified reservoir, the objective of this study is the development of a mathematical model which is capable of predicting the annual thermal cycle and the physical effects of the thermal discharge on Lake LBJ as a first step in predicting its ecological effects.

---

*Numbers in parentheses designate References at the end of the report

Description of Lake LBJ and Its Annual Thermal Cycle

Lake LBJ (see Figures 1 and 2) is the third in a series of seven lakes in the Highland Lakes Chain along a 150 mile reach of the Colorado River in Central Texas. The lake is formed by Alvin Wirtz Dam and has a volume of 138,460 acre feet and a surface area of 6,375 acres at the normal constant level of 825 feet above mean sea level (one foot below the top of the flood gates). The lake has a mean depth of 21.7 feet, a maximum depth of about 85 feet, and is 21.15 miles long by the river channel (15; 26, pp. 131-133; and 8, p.5). The annual discharge - reservoir volume ratio is 10.4 (16).

Temperature profiles taken in the deep pool of Lake LBJ are shown in Figure 3 and are tabulated in Appendix D (8, p. 129).By the end of winter the reservoir is at a nearly uniform temperature from top to bottom. During early spring more heat is gained by the lake during the day than is lost at night. Since the lake is at a fairly uniform temperature when the heating cycle begins, wind is able to keep the lake mixed so that it heats uniformly. By late spring the heat flux to the lake has increased to the point that mixing cannot transport heat from the surface to the depths of the reservoir as fast as it is gained; hence, the surface temperature begins to rise. This resulting stable temperature gradient in the reservoir is termed stratification, and it persists until the fall cooling. During the stratified period three more or less distinct layers are observed in the reservoir--the upper layer of warm, fairly well mixed water called the epilimnion, the cooler bottom layer called the hypolmnion, and the region separating these two where the temperature gradient is greatest called the metalimnion. The plane of maximum temperature gradient is called the

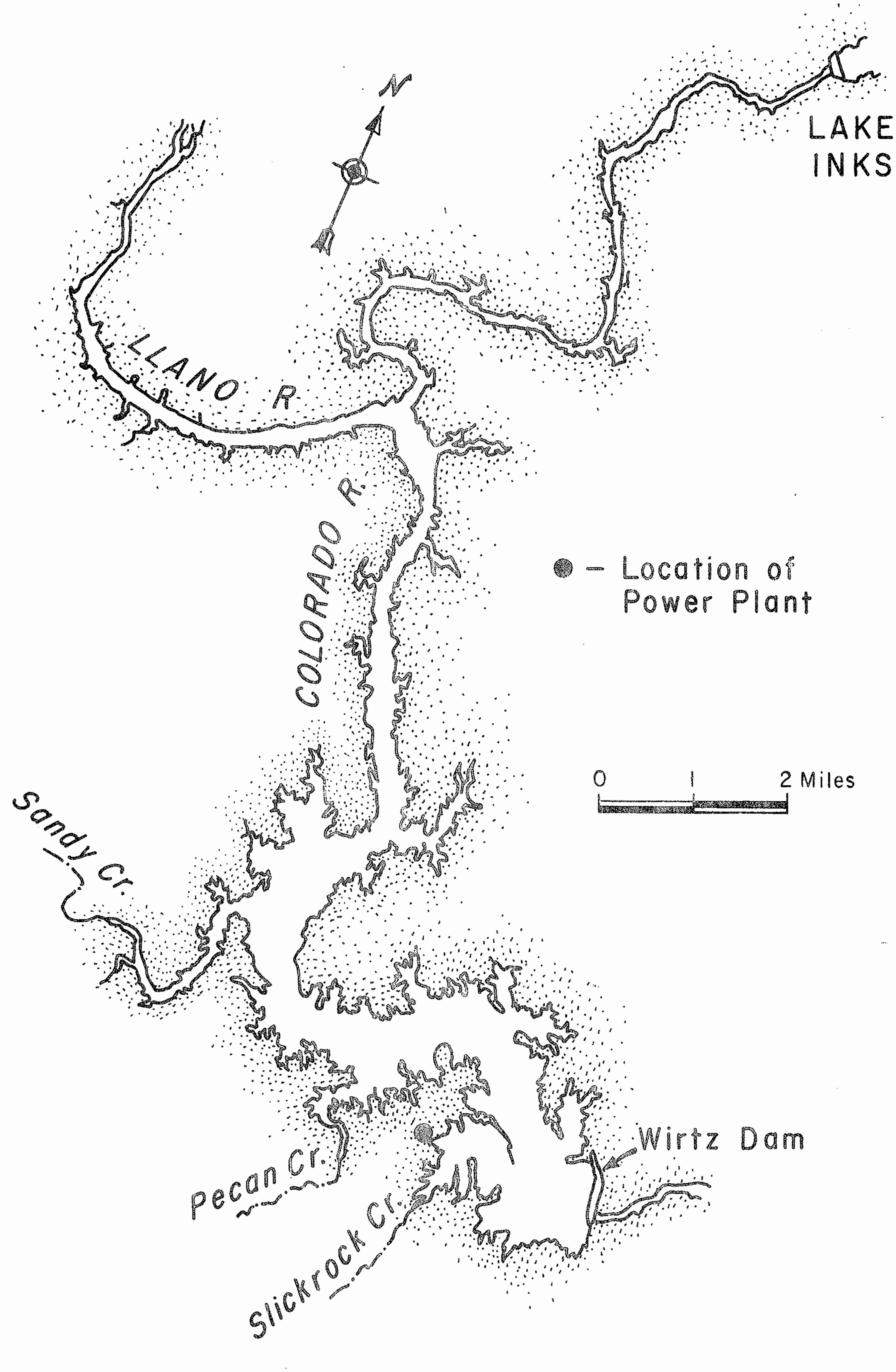

FIG. 1. LAKE LBJ

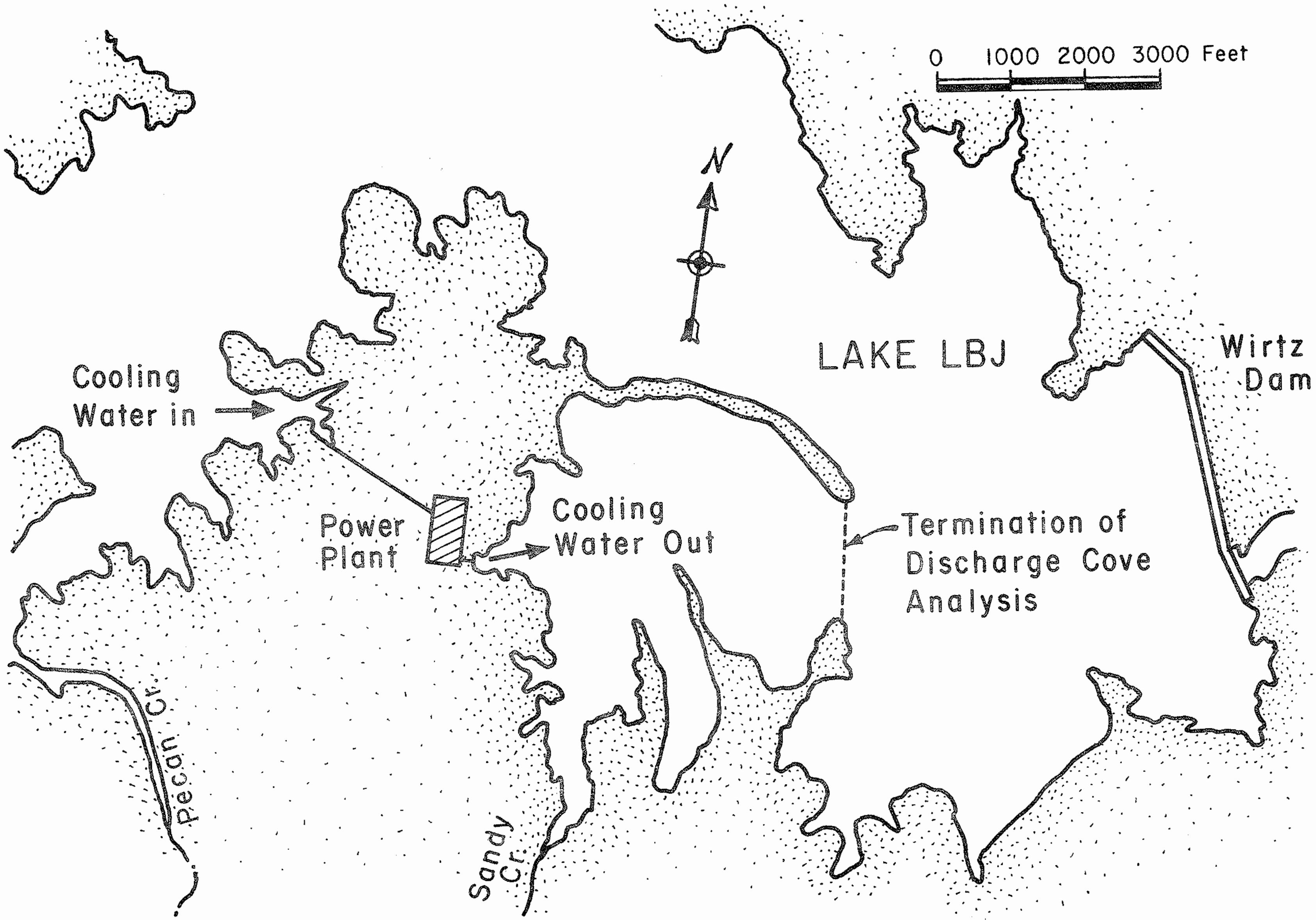

FIG. 2. LAKE LBJ DISCHARGE COVE

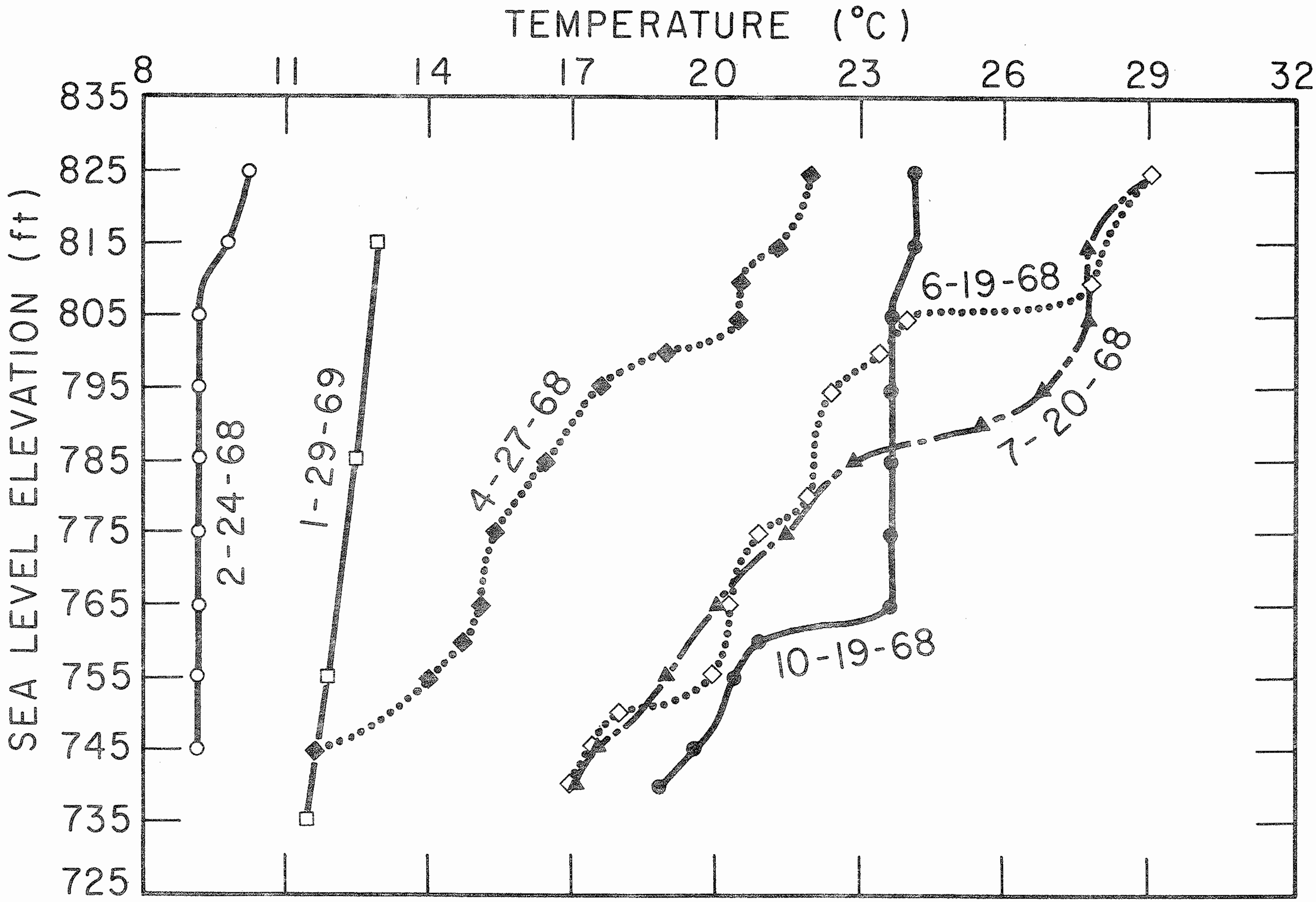

FIG. 3. TEMPERATURE PROFILES FOR LAKE LBJ
(From Reference 8, p.54)

thermocline. As summer progresses heat is absorbed at the surface and mixed downward, increasing the depth of the epilimnion. This process which keeps the epilimnion well mixed is the result of wind induced currents, breaking waves, and convective cooling at night. Convective cooling occurs when the surface water loses heat to the atmosphere and becomes denser than the water below. This causes an unstable gradient and the surface water sinks and mixes with the warmer water below, resulting in an isothermal layer extending down from the surface. In the fall the lake loses more heat during the night than it gains during the day, so it begins to cool. The epiliminon remains well mixed and its lower boundary becomes deeper and deeper. As the cooling process continues the lake becomes fully mixed and then repeats the annual cycle. For a more detailed description of the stratification cycle and other physical and chemical characteristics of impoundments, the reader is referred to Hutchinson (11).

Although Lake LBJ seasonally stratifies, the location of the penstock in the epilimnion causes the thermocline to form at a rather shallow depth. Fruh and Davis (8, p. 50-51) have concluded that due to its depth, penstock location, and power use, Lake LBJ has the characteristics of both a main stream and a storage reservoir. However, the lake's thermal characteristics more closely resemble those of a deep reservoir.

The headwaters of Lake LBJ are formed by the confluence of the Colorado River release from Lake Inks and the Llano River. There is considerable difference in the temperature of these two inflows (8 pp. 89-93). Lake Inks is a main stream reservoir; its detention time based on monthly average inflows for 1968 varied between 2 and 80 days (8 p. 122). Therefore, for certain times of the year, the quality of the water being released from Lake Inks into Lake LBJ is very similar to that coming into Lake Inks from Lake Buchanan (the reservoir upstream from Lake Inks). The release from Lake Buchanan is from the hypolimnion; hence, the water entering Lake LBJ from Lake Inks is usually colder than that from the Llano River. Based on their 1968 study of the Highland Lakes (8, pp. 92-93), Fruh and Davis stated that it appeared that during the summer the cold water from the Lake Inks release does not become much warmer during its travel to the Lake LBJ headwaters and slides under the warmer Llano River waters. This seemed to be verified by the silica data of the summer samplings, as there was an inverse silica stratification that was apparently caused by the Llano River with high silica content flowing over the Inks release water with a low silica content.

Direct and Indirect Effects of Heated Effulents

Since the temperature of a reservoir has a marked effect on its water quality and biota, it is an important parameter to study in the development and operation of a reservoir. The temperature of water directly affects many important physical, chemical, and biological properties, as pointed out by Christianson (3, pp 13-50). Physical effects resulting from an increase in temperature include an increase in evaporation and stratification and a decrease in the solubility of oxygen. An increase in temperature also causes an increase in chemical reaction rates, possible changes in tastes and odors of the water, and a decrease in the time required to biodegrade organic material. Biological effects of increased temperatures include a possible shift in the population structure, increase in metabolism rates of aquatic organisms, decrease in their resistance to toxic substances, possible failure to reproduce, and beyond a certain temperature, death. For a more detailed description of the effects of temperature in a reservoir, the reader is referred to (13) and (19, pp II-1 to IV-23).

In addition to the direct effects of an increase in water temperature, there are also many indirect effects or combinations of effects which could cause problems. One example is the fact that increased temperature reduces the amount of dissolved oxygen in the water by both decreasing its solubility and increasing the rate of the biodegrading of organic material. At the same time aquatic organisms require more oxygen due to their increased metabolic rate caused by the increase in temperature. Another problem which could cause widespread effects is the elimination of a critical segment of the food chain which could drastically hinder other forms of life.

A further example of the compound effect of a temperature increase is the decrease in density of water which leads to stratification and subsequently to other effects. According to Wunderlich and Elder (33, p. 1-2), stratification in a reservoir is the main factor responsible for the movement and quality changes of impounded waters. Thus, in order to predict water quality in a reservoir, it is necessary to know the path followed by the incoming water and the location from which the discharge is withdrawn.

Stratification has an effect on the movement of water in a reservoir, which in turn affects the detention time of incoming water. Water which enters from streams during the spring and summer tends to be warmer than most of the water in the reservoir; hence, it will enter and stay near the surface. Later in the year the incoming water tends to cool faster than the reservoir surface water, so it enters and stays below the surface. If an outlet is located deep in the reservoir, water which entered during the fall may be discharged before water which entered earlier. Since water quality changes as water is detained in a reservoir, the length of the detention time affects the water quality.

Stratification also affects water quality by creating a barrier between the hypolimnion and the epilimnion. The epilimnion of a stratified reservoir is kept well mixed and exposed to surface conditions; however, the hypolimnion is kept isolated from surface conditions due to the strong, stable density gradient at the thermocline which tends to suppress vertical motion. This situation causes the bottom water to become depleted in oxygen, resulting in poor water quality.

Since temperature is one of the most important parameters affecting the water quality in a reservoir, it is necessary to determine the thermal structure of a reservoir before the ecological effects of a thermal discharge from a power plant can be predicted. In order to predict temperature, mathematical models are used to simulate the annual natural thermal cycle of Lake LBJ and the effect of a thermal discharge on the cycle.

Concepts of a Mathematical Model

A mathematical model is a functional representation of a physical system and is usually designed so as to divide the complex prototype (which in this case is the reservoir) into a number of subsystems which are easier to describe mathematically. In this study the thermal behavior of the reservoir is simulated by using a mathematical model which is coded for solution on a digital computer.

Since the actual energy transport and exchange processes within a reservoir are quite complex, it is necessary to make some assumptions in the development of the model. It is not possible to verify independently each assumption; therefore, an assumption's validity must be inferred from the model's ability to satisfactorily describe prototype behavior.

It should be emphasized that there are limitations to the predictive ability of a mathematical model. Due to limitations on the accuracy of input data and the assumptions made, the model will generally be capable of predicting overall gross trends, but will probably not be satisfactory for predicting accurately day to day variations. For example, the model might reasonably be expected to predict the approximate depth of the thermocline at a given time of year or to estimate the date on which the "turn over" of the reservoir might begin, whereas the absolute value of the surface temperature on a given day, or its variation from one day to the next, might be in error.

Objective and Scope

The objective of this study is the development of a mathematical model which is capable of predicting the annual thermal cycle of Lake LBJ and the physical effects of a thermal discharge on a section of the lake.

The scope of this study is concerned with two distinct, but related, problems which are listed below.

1. The development of a one-dimensional model for

simulating the annual thermal cycle of Lake LBJ is carried out. An evaluation of the state-of-the-art of modeling of reservoirs is presented in Chapter II. From this evaluation it is concluded that a model of the type developed by Water Resources Engineers (32) is best suited for the present application.

In the course of the development of the model, the importance of the following parameters is analyzed:

a. the diffusion of thermal energy,

b. the advection of thermal energy, and

c. the importance of the surface heat flux terms.

2. A method of predicting the physical effects of the thermal discharge on a section of Lake LBJ is developed. To accomplish this, the model has been modified to account for temperature gradients in both the vertical and longitudinal directions. This method allows a more accurate prediction of the physical effects of the thermal discharge than could be obtained using a one-dimensional model.

Chapter II

Literature Evaluation

In this chapter a review of the literature pertaining to the prediction of the thermal energy distribution in deep reservoirs is given. This review is not intended to trace the development of methods for predicting temperature from the first attempt to present techniques; instead, only those references which represent the present state-of-the-art are given in detail. These references include the work of Water Resources Engineers (32), Huber and Harleman (10), Markofsky and Harleman (18), and Clay and Fruh (4). A comparison between the works reviewed is summarized in Table 1.

A detailed review of the literature pertaining to the prediction of the temperature distribution in reservoirs is given by Huber and Harleman (10). Other authors who have made significant contributions to the field, and will only be mentioned briefly here, are Dake and Harleman (5) and Edinger and Geyer (6). Dake and Harleman solved the one-dimensional heat conduction equation by superposition of the solutions for surface absorbed radiation and internally absorbed radiation. In their work they showed the importance of considering solar radiation to be partially absorbed at the surface, with the remaining radiation absorbed exponentially with depth. Edinger and Geyer developed a method for predicting the thermal properties of cooling ponds. Their method was not primarily intended for application to large, deep reservoirs; however, many of their concepts, particularly those for describing the exchange of energy at the water surface, are applicable to such a problem.

Table 1

Comparison of Models Reviewed

	WATER RESOURCES ENGINEERS	HUBER and HARLEMAN MARKOFSKY and HARLEMAN	CLAY and FRUH
INFLOWS	Enter at a single layer	Normally distributed among layers	Enter at a single layer
OUTFLOWS	Withdrawn from layers at the elevation of the outlet	Normally distributed within the withdrawal layer, whose thickness is a function of the reservoir	Normally distributed within the withdrawal layer whose thickness is a function of the stratification of the reservoir
EXTERNAL HEAT FLUXES	All exchange with the surface layer, except solar radiation which is absorbed exponentially with depth	All exchange with the surface layer, except solar radiation which is absorbed exponentially with depth	All exchange with the surface layer
INTERNAL DIFFUSION	Diffusivity is decreased exponentially from the surface to the thermocline and is constant below the thermocline	Diffusivity is constant and equal to the molecular diffusivity	Diffusivity is decreased exponentially from the surface to the bottom

Water Resources Engineers (WRE)

One of the first attempts to predict temperature in a stratified reservoir which accurately accounted for the coupling of the hydrometeorological phenomena controlling the heat transfer at the surface with the mechanisms responsible for distributing the heat energy internally was developed by Water Resources Engineers (32). This model accounts for heat transfer through the surface, internal absorption of solar radiation, heat transport by molecular and turbulent diffusion in the vertical direction, horizontal advection into and out of the reservoir, and vertical advection within the reservoir. The heat transfer at the water surface is calculated by using data on the meteorological conditions and the water surface temperature.

The basic assumption of the WRE model is that horizontal isotherms exist in the reservoir at all time, i.e., at any given level the temperature is uniform throughout. The reservoir is divided into a number of horizontal control volumes of small thickness, extending over the entire length and width of the reservoir. For each element the equations of conservation of mass and energy are written, and then the temperature distribution with depth and time is found by numerically integrating the energy equation with the mass conservation equation as a boundary condition. Inflows are assumed to enter the reservoir at a level corresponding to their density and are instantaneously spread over the entire horizontal layer with no mixing. The outflow withdrawal layer is assumed to extend only over the elevation of the outlet and water is withdrawn over the entire horizontal area at that elevation.

The WRE model treats diffusion by assuming that the diffusivity decreases exponentially from the surface of the reservoir to the thermocline and is constant below the thermocline. WRE determined the coefficient by solving for it in the energy equation with the use of field data. This method requires knowledge of two successive temperature profiles, hydrologic inputs, and external energy sources. This diffusivity is a result of the hydrodynamic mixing process and is not a description of the actual mixing mechanism itself. Since this method is an empirical fitting of observed data, it is useful only if sufficient field data for the particular reservoir being modeled are available.

The WRE model has been tested against field data for Fontana Reservoir in the TVA system and found to give good agreement, even though some of its inherent assumptions are highly idealized. In particular, the assumptions regarding the treatment of inflows and outflows and the assumption that no longitudinal or lateral temperature gradients exist are rather idealized. The ratio of Fontana Reservoir's annual discharge to reservoir volume is 2.2 (10, p. 14) compared to 10.4 for Lake LBJ (16); therefore, the inflows and outflows are more important in determining the thermal structure of Lake LBJ, and the prediction of temperature in this reservoir should suffer more from the simplifying assumptions regarding inflows and outflows.

Huber and Harleman

The Huber and Harleman model (10), while developed independently of the WRE model, is similar in several respects. Both models assume the reservoir is characterized by horizontal isotherms and include the effects of surface and internal radiation absorption, surface heating and cooling, vertical advection within the reservoir, horizontal advection into and out of the reservoir, and vertical diffusion of thermal energy within the reservoir.

There are several major differences in the two models. The main refinement in Huber's model is in the treatment of inflows and outflows. The outflow velocity profile is calculated by using Koh's method (12). This method allows for a withdrawal layer thickness which depends on the degree of stratification and assumes a normally distributed velocity profile within the withdrawal layer. The Huber model also allows a distributed inflow which includes mixing. When an inflow enters a reservoir, it is mixed with a volume of surface water which is an arbitrarily determined fraction of the inflow volume. The center of the normally distributed velocity profile is located at the elevation where the density of the reservoir water is the same as the density of the mixed inflow. The shape of the velocity profile is determined by assuming that one standard deviation of the inflow is contained within an arbitrarily chosen vertical distance. While the determination of the inflow and outflow velocity profiles employs some uncertainty, Huber's method is more realistic than WRE's and the degree of uncertainty could be reduced through the use of field data.

The other main difference between the two models is the evaluation of the diffusivity. Instead of calculating a diffusivity based on field measurements, Huber assumes that the thermal diffusion process can be treated by considering only molecular diffusion within the reservoir and convective mixing at the surface when the temperature gradient is unstable. The reasoning behind this method is that convective mixing is assumed to be the major mechanism responsible for causing the large value of the diffusivity near the surface. Since convective mixing is accounted for separately, the value of the diffusivity should not account for this effect, and it is assumed that all other diffusion effects can be accounted for by the molecular diffusivity. This method neglects turbulence caused by wind induced currents, breaking waves, and convective cooling at night during the heating cycle if a time interval of one day or greater is used in the simulation. This simplification has the advantage of not relying on field results and hence can be used in the planning stages of reservoirs.

The Huber model has been tested with both laboratory data and with field data from Fontana Reservoir. In both cases good agreement was obtained between observed and predicted temperatures.

Markofsky and Harleman

Markofsky and Harleman (18) have taken the Huber model and extended its scope to include prediction of conservative and non-conservative water quality parameters. The model also was modified in the way inflows are handled. Subsurface inflows are treated in the same way as Huber's model; however, surface inflows are assumed to enter uniformly over a thickness at the top of the reservoir equal to the depth of the entering stream. Huber's model assumes that inflows are instantaneously spread out over the entire horizontal area of the reservoir at which they enter. Since time is required for water to flow through the reservoir to the dam, this assumption will result in inaccuracies in the prediction of outflow temperatures. Markofsky's model calculates the time required for an inflow to enter the reservoir and flow to the dam. The inflow is then treated as if it entered the reservoir when it actually should have reached the dam. This lagging of the inflow results in an improvement of the outflow temperature predictions.

Clay and Fruh

Clay and Fruh (4) have developed a reservoir model similar to the WRE model, but which emphasizes selective withdrawal; temperature prediction was important only for its effect on selective withdrawal. This objective means that it was necessary to make several modifications to the WRE model; also it was possible to make some simplifications consistent with the objectives of the study. The principal change was the incorporation of a method for calculating the outflow velocity profile. Clay and Fruh evaluated both the Bohan-Grace (1) and the Koh (12) methods, and found that the Bohan-Grace method predicted results as well or better than the Koh method and required less stringent input data. They also modified the reservoir model to account for prediction of conservative chemical concentrations.

Since the main purpose of this model was to study selective withdrawal, it was possible to make several simplifications to the WRE model. One of these was in the calculation of the external heat transferred to the reservoir. The net heat flux was calculated from changes in observed temperature profiles. Then the heat flux caused by advection and evaporation was separated from the surface heat flux and considered independently. This method has the advantage of limiting the quantity of input data because the external heat sources and sinks are not calculated from meteorological data. In Clay and Fruh's model all external heat exchange, except by advection, is assumed to take place in the surface layer. Heat exchange in the other layers takes place by advection and diffusion in the vertical direction. They found that for the reservoirs studied (which included Lake LBJ) that the results are equally good with the diffusivity decreased exponentially from the surface to the bottom instead of from the surface to the thermocline. This conclusion, which is probably a result of the reservoirs being fairly shallow, means that it is not necessary to locate the thermocline and hence it is possible to save some computation time.

One final difference in the two models is the method of solution. The WRE model uses an equation of conservation of energy for each element to simultaneously account for all heat gains and losses in the element. In the Clay and Fruh model the effect of each component is treated individually. The inflow is added, the external heat source is added to the surface layer, heat is diffused throughout the reservoir, and the outflow is taken from the reservoir. After each of these individual steps, a new temperature profile is calculated. Since each process is accounted for successively instead of simultaneously accounting for all, this method seems to limit the maximum allowable time interval used in the computation.

By using their model, Clay and Fruh obtained reasonable accuracy in their prediction of outflow temperatures and temperature profiles for several Texas reservoirs of different sizes and depths, using a time interval of one day and an element thickness of ten feet.

Summary

From the evaluation of the state-of-the-art of modeling of temperature in reservoirs, a model similar to that developed by Water Resources Engineers (32) has been chosen as the type to use to simulate the thermal behavior of Lake LBJ. This model has the following characteristics:

1. It is discretized into elements of uniform depth, extending over the entire length and width of the reservoir.

2. It treats heat transfer at the surface due to solar radiation, atmospheric radiation, back radiation, evaporation, and convection. Each of these terms is calculated from meteorological data and the water surface temperature.

3. It treats advection into and out of the reservoir in the horizontal direction.

4. It treats advection and diffusion of energy along the vertical axis within the reservoir.

This model strictly applies only to deep, stratified reservoirs with a low discharge-volume ratio. Although Lake LBJ has the characteristics of both a deep and a main stream reservoir (8; pp. 50-51), its thermal characteristics more closely resemble those of a deep reservoir, so it is assumed that the model for a deep, well stratified reservoir will adaquately describe the lake.

Chapter III

Model Development

In this chapter the development of the mathematical model which simulates the thermal behavior of a deep reservoir with seasonal stratification is presented. This model accounts for heat gains and losses at the surface, internal absorption of short-wave solar radiation, advection of heat in the horizontal and vertical directions, and molecular and turbulent diffusion of heat in the vertical direction. Advection is the transport of heat associated with the mass flow of water and is expressed mathematically in terms of the temperature and flow rate of the water. Molecular diffusion results from the random motion of molecules and turbulent diffusion results from the mixing of fluid masses known as eddies. The heat transfer by diffusion is expressed mathematically in terms of the temperature gradient and the diffusion coefficient. For convenience the coefficients of molecular and turbulent diffusion are combined to form a single effective coefficient. This coefficient is commonly referred to as the diffusivity, effective diffusion coefficient, thermal diffusivity, or thermal diffusion coefficient. The terms eddy diffusivity and eddy diffusion coefficient are used to refer to just the turbulent component of diffusion.

The prediction of temperature in a reservoir involves two separate but dependent components - the external energy exchange between the reservoir and its surroundings, known as the energy budget, and the internal energy exchange within the reservoir. These two components are dependent because the energy depends upon the surface temperature, which in turn depends upon the rate at which heat is transported downward from the surface. In the computer simulation of the reservoir, the heat budget over a short period of time is calculated based on the temperature distribution at the beginning of the time period. Then a new temperature distribution for the end of the time period is determined by the external and internal energy exchange during the period. The process is repeated for each succeeding time interval.

The conceptual representation of the reservoir is presented in the next section. This representation involves dividing the reservoir into elements which can be easily described mathematically and then coupling the elements so that the entire reservoir is simulated. The mathematical description of each element, which involves mass and heat balances, is described in the next two sections. Following this a discussion of the evaluation of the diffusivity is given. Then the method of accounting for the convective mixing process is presented.

Conceptual Representation of a Reservoir

The development of a mathematical model which accounts for the complex interaction between the external heat sources to a reservoir and the internal hydrodynamics is a complicated problem. Theoretically the thermal behavior of a reservoir can be described by solving the equations of mass, momentum, energy, and state for the reservoir. However, these are non-linear partial differential equations, and their solution for a stratified reservoir in closed form is impractical. In order to solve the problem the differential equations can be approximated by their finite-difference form which reduces them to a set of simultaneous algebraic equations. With certain simplifying assumptions it is possible to solve these equations by using standard matrix solution techniques, as described in Chapter V.

The first step in solving the problem consists of dividing the reservoir into a number of control volumes so that the appropriate finite-difference equation, which governs the temperature of each element, can be written. In order to specify the most convenient geometry of the control volumes, it is necessary to consider the physical behavior of a stratified reservoir.

In a deep reservoir the velocities in the horizontal direction are small; however, over long periods of time they are large enough to eliminate horizontal temperature gradients which may arise as the result of large inflows, wind, or other causes. For this reason it is assumed that the reservoir will always be characterized by horizontal isotherms. This assumption is in good agreement with field results for deep reservoirs. However, this means that only long time averages can be predicted with the model, since time is needed to smooth out horizontal gradients which may exist locally. Since the reservoir is assumed to have horizontal isotherms it is convenient to sectionalize it into horizontal, isothermal elements of small, uniform thickness, extending over the entire length and width of the reservoir. This physical representation of the reservoir is shown in Figure 4. In this figure the j-th element, which is at elevation z_j and has thickness Δz_j, is shown removed from the remainder of the reservoir. The notation used in both this report and the computer program numbers the elements successively from the bottom of the reservoir, so that j = 1 refers to the bottom

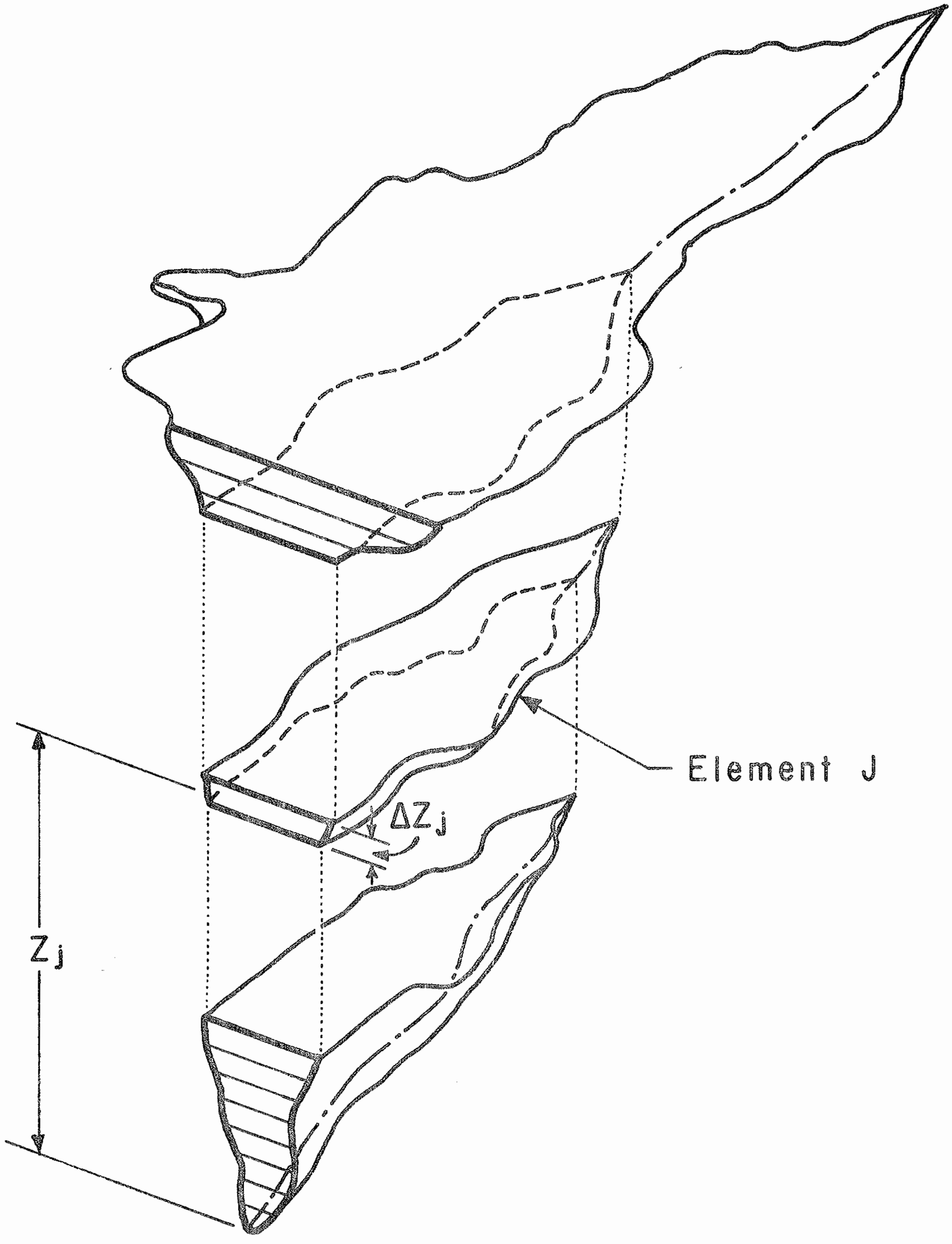

FIG. 4. CONCEPTUAL REPRESENTATION OF A RESERVOIR
(After Water Resources Engineers, Reference 32)

element. Elevations to each element are given to the point half-way between the upper and lower surfaces. Also, subscripts referring to surfaces of the elements are such that the subscript j refers to the bottom of the j-th element and j+1 refers to the top of the same element.

An element may receive water entering the reservoir or lose water discharged from the reservoir. It is assumed that each inflow enters the reservoir at a level corresponding to its own density; hence, the amount of water entering each element is determined by the density structure of the reservoirs. It is also assumed that the density of water is a function only of temperature and is not significantly influenced by dissolved and suspended solids. This assumption means that the inflow will enter the reservoir at an element which has the same temperature as the inflow. Also it is assumed that the inflow enters with no mixing and instantaneously spreads out over the entire horizontal layer which it enters. When an inflow enters an element, continuity requires that the same amount of flow must pass upwards through each element surface above the level where the inflow enters. The model treats discharges from the reservoir by assuming that water is withdrawn only from the elements which are at the level of the outlet. Similar to the case of an inflow, an outflow requires that there be a vertical flow through all surfaces above the outlet. At a glance it appears that the model ignores momentum considerations, although in a very simple fashion momentum is being accounted for via the inflow-layering scheme. More sophisticated possibilities will be discussed in Chapter IX.

The temperature of each element is determined by the one-dimensional heat transport equation with appropriate heat sources and sinks. The heat sources are short-wave solar radiation, atmospheric radiation, and inflows. The heat sinks are surface losses and outflows. Heat is distributed within the reservoir by advection, diffusion, and absorption of solar radiation with depth. Atmospheric radiation, back radiation (i. e., long-wave radiation to the environment from the water surface), evaporation, and convection affect only the surface layer of the reservoir.

Mass Balance for the Control Volume

One of the two equations which govern the thermal behavior of each element in the reservoir is the equation of conservation of mass for an incompressible fluid. Writing this equation for the j-th element, shown in Figure 5, results in

$$Q_{i_j} - Q_{o_j} + Q_{v_j} - Q_{v_{j+1}} + Q_s = 0 \quad \ldots\ldots\ldots \quad (3.1)$$

where

Q_{i_j} = horizontal inflow rate into the j-th element, ft^3/hr

Q_{o_j} = horizontal outflow rate from the j-th element, ft^3/hr

Q_{v_j} = vertical flow rate at elevation j, ft^3/hr

$Q_{v_{j+1}}$ = vertical flow rate at elevation j + 1, ft^3/hr

Q_s = rate of storage of water in the j-th element, ft^3/hr

The storage term is zero for all elements except the surface element, whose volume changes with changes in the water surface elevation. In Figure 5 the vertical flows are shown

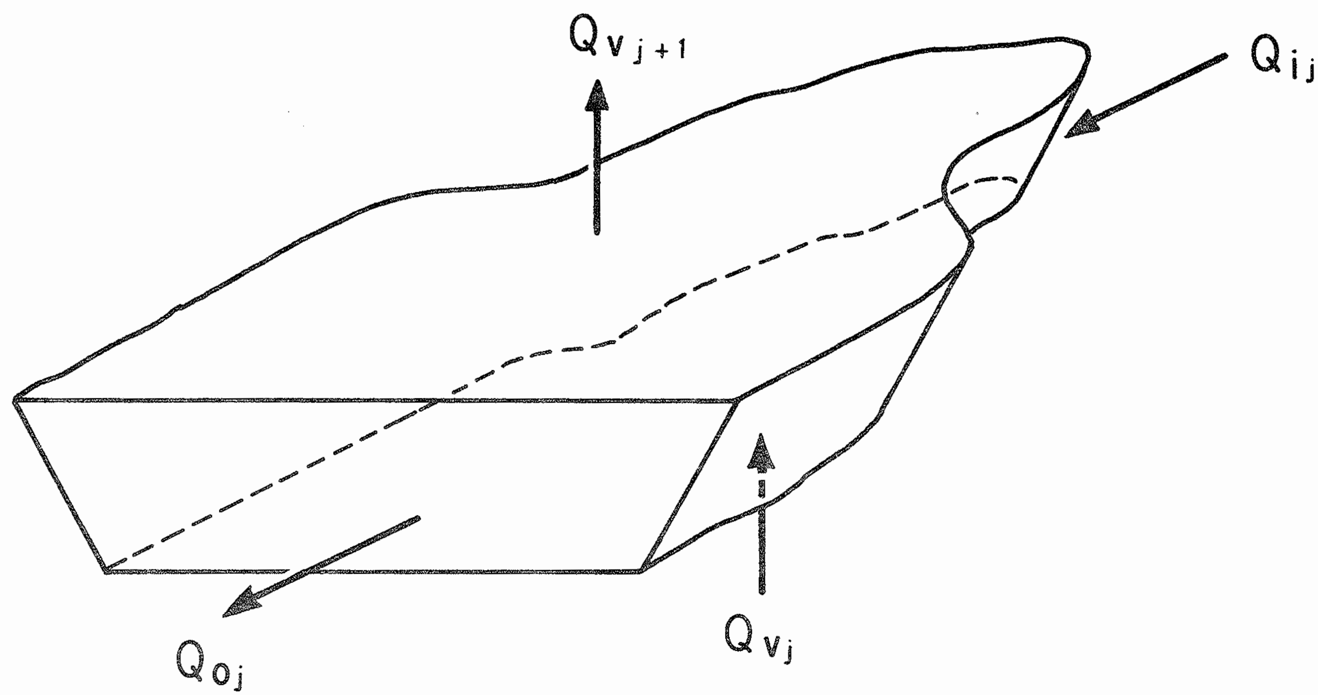

FIG. 5. MASS BALANCE FOR ELEMENT J
(After Water Resources Engineers, Reference 32)

flowing upwards, or in the positive direction. If one or both of these flows is in the downward direction, Equation 3.1 still applies by simply substituting a negative flow rate into the equation. The magnitude and direction of the flow rate at each surface are calculated by noting that the flow rate at each elevation is the sum of all inflows minus all outflows below that elevation. This is stated mathematically as

$$Q_{v_j} = \sum_{k=1}^{j-1} \left(Q_{i_j} - Q_{o_k}\right) \quad \ldots\ldots\ldots\ldots \quad (3.2)$$

The vertical flow rate at the surface is modified to include evaporation and precipitation.

Energy Balance for the Control Volume

The second equation which governs the temperature of each element in the reservoir is the equation of conservation of energy which accounts for energy advected by horizontal and vertical flows, energy diffused at the upper and lower boundaries of the element, and short-wave radiation absorbed within the element. In this development the bottom of the reservoir is assumed to be insulated. For the surface element hear transfer by atmospheric radiation, back radiation, evaporation, and convection must also be included. These terms are described in detail in Chapter IV. For the control volume shown in Figure 6 the energy equation is

$$\frac{dHj}{dt} = h_{s_j} + h_{i_j} - h_{o_j} - \left(h_{v_{j+1}} - h_{v_j}\right) - \left(h_{d_{j+1}} - h_{d_j}\right) \quad \ldots (3.3)$$

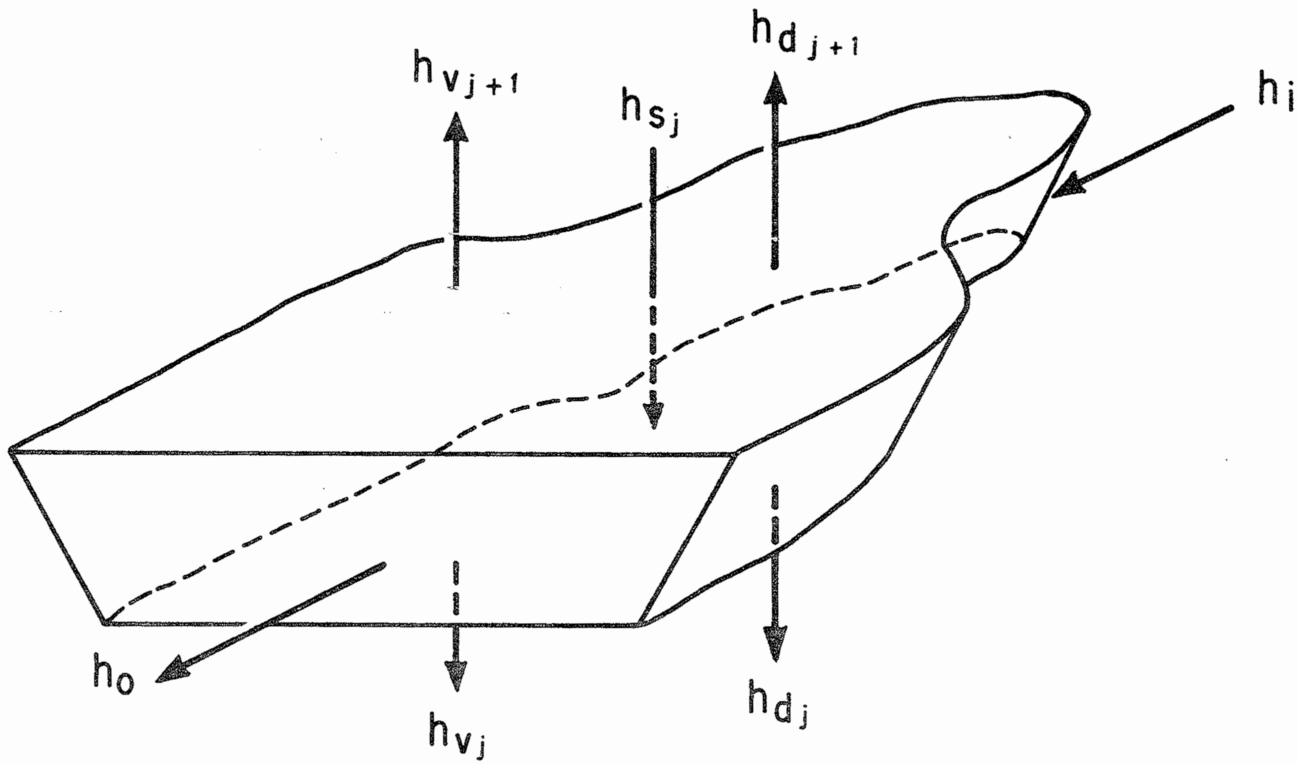

FIG. 6. ENERGY BALANCE FOR ELEMENT J
(After Water Resources Engineers, Reference 32)

where

$\frac{dH_j}{dt}$ = time rate of change of stored heat energy in j-th element, Btu/hr

h_{s_j} = heat absorbed in the j-th element from short-wave solar radiation, Btu/hr

h_{i_j} = heat advected into the j-th element by a horizontal inflow, Btu/hr

h_{o_j} = heat advected from the j-th element by a horizontal outflow, Btu/hr

h_v = heat advected in the vertical direction, Btu/hr

h_d = heat diffused in the vertical direction, Btu/hr

Assuming that each element is completely mixed, the terms of Equation 3.3 can be expressed for the j-th element in terms of water temperatures, fluid flows, and cross sectional areas as follows:

$$\frac{dH_j}{dt} = \rho c \; A_j \; \Delta z_j \; \frac{d\theta_j}{dt} \quad \ldots\ldots\ldots\ldots\ldots \quad (3.4a)$$

$$h_{s_j} = A_j \; \Delta z_j \; h'_j \quad \ldots\ldots\ldots\ldots\ldots \quad (3.4b)$$

$$h_{i_j} = \rho c \; Q_{i_j} \; \theta_{i_j} \quad \ldots\ldots\ldots\ldots\ldots \quad (3.4c)$$

$$h_{o_j} = \rho c \; Q_{o_j} \; \theta_j \quad \ldots\ldots\ldots\ldots\ldots \quad (3.4d)$$

$$h_{v_{j+1}} - h_{v_j} = \rho c\, Q_{v_{j+1}}\, \theta_j - \rho c\, Q_{v_j}\, \theta_{j-1} \quad \ldots\ldots\ldots \quad (3.4e)$$

$$h_{d_{j+1}} - h_{d_j} = -\rho c a_{j+1}\, D_{j+1}\, \frac{2(\theta_{j+1} - \theta_j)}{(\Delta z_{j+1} + \Delta z_j)}$$

$$+ \rho c a_j D_j\, \frac{2(\theta_j - \theta_{j-1})}{(\Delta z_j + \Delta z_{j-1})} \quad \ldots\ldots\ldots\ldots\ldots \quad (3.4f)$$

where

ρ = Density of water, lb/ft^3

c = heat capacity of water, Btu/lb - $^{\circ}$F

a_{j+1} = area of upper surface of the j-th element, ft^2

a_j = area of lower surface of the j-th element, ft^2

A_j = average area of upper and lower surfaces of the j-th element, ft^2

D_{j+1} = diffusion coefficient at the upper surface of the j-th element, ft^2/hr

D_j = diffusion coefficient at the lower surface of the j-th element, ft^{2}hr

h'_j = absorption of solar heat energy per unit volume in the j-th element, Btu/hr ft^{2}ft (for the surface element this term will include all other heat fluxes which pass through the air-water interface)

θ_j = temperature of the j-th element, $^{\circ}$F

θ_{i_j} = temperature of the inflow into the j-th element, $^{\circ}$F

Substituting Equations 3.4a through 3.4f into Equation 3.3 results in:

$$A_j \frac{d\theta_j}{dt} = A_j \frac{h'_j}{\rho c} + \frac{1}{\Delta z_j}\left(Q_{i_j}\theta_{i_j} - Q_{o_j}\theta_j\right) - \frac{1}{\Delta z_j}\left(Q_{v_{j+1}}\theta_j - Q_{v_j}\theta_{j-1}\right)$$

$$+ \frac{1}{\Delta z_j}\left\{a_{j+1}D_{j+1}\frac{2(\theta_{j+1}-\theta_j)}{(\Delta z_{j+1}+\Delta z_j)} - a_j D_j \frac{2(\theta_j - \theta_{j-1})}{(\Delta z_j + \Delta z_{j-1})}\right\}. \quad .(3.5)$$

For Δz constant this equation becomes

$$A_j \frac{d\theta_j}{dt} = A_j \frac{h'_j}{\rho c} + \frac{1}{\Delta z}\left(Q_{i_j}\theta_{i_j} - Q_{o_j}\theta_j\right) - \frac{1}{\Delta z}\left(Q_{v_{j+1}}\theta_j - Q_{v_j}\theta_{j-1}\right)$$

$$+ \frac{1}{\Delta z}\left\{a_{j+1}D_{j+1}\frac{\theta_{j+1}-\theta_j}{\Delta z} - a_j D_j \frac{\theta_j - \theta_{j-1}}{\Delta z}\right\}. \quad . \quad . \quad . \quad . \quad . \quad (3.6)$$

Since the thickness of all control volumes in the reservoir is taken to be the same, Equation 3.6 applies to all elements except the surface element where Δz is not constant, because the amount of water in this element will change with changes in the lake level. For the surface element Equation 3.5 must be used.

In the energy balance equations it was assumed that the vertical flows were upward or in the positive direction. It is important to note that a downward flow will not only change the sign of the advective heat transport term but will also change the temperature used in calculating the term, because a change in direction of the vertical flow means the water is flowing from a different element; hence, it is at a different temperature.

Diffusion of Thermal Energy

The dominant mechanisms of heat, mass, and momemtum transport which control the natural annual thermal cycle of a reservoir and the effects of heated discharges are turbulent, and hence, difficult to analyze. The diffusivity can be considered to consist of several additive components: molecular, free convection, and forced convection. Only the molecular thermal conductivity is easily determined. It is always present, but is usually very small relative to the other components. The other two components may or may not be present simultaneously, and when they are present their values can vary considerably with changing environmental conditions and temperature and velocity gradients in the reservoir. Since no theory exists for adaquately describing the various components of the diffusivity, field data are used in this study to determine its value.

As Sundaram, et. al (22, pp. 99-128) point out, the mechanisms of generation of turbulence in the epilimnion and the hypolimnion are quite different. The diffusivity in the epilimnion is determined mainly by surface-induced effects, one of which is wind shear. The transfer of momentum and energy from the wind to the water takes place by the direct generation of currents and by the breaking of wind induced waves. Currents affect the diffusivity in the entire epilimnion, while the effects of waves are limited to the top few meters of the lake. This has been confirmed by Lee and Masch (14) and Gebhard and Masch (9). The other major driving force for the creation of turbulence in the epilimnion is convective mixing. This phenomenon is much more important during the fall when the reservoir begins to cool than during the summer, since as the lake cools the wind generated turbulence is augmented rather than suppressed by the buoyancy gradient. This fact also means that the rate of descent of the thermocline will be greater during the cooling period than during the warming period.

Turbulence in a reservoir is controlled by inertia forces and the buoyancy forces produced by thermal gradients, the latter tending to suppress turbulence when a stable gradient exists. Near the surface the inertia force due to the wind predominates and the diffusivity is large. At a certain depth the buoyancy forces are sufficient to damp out the inertia forces so that turbulence is reduced to a fraction of the surface value. This depth, which is the boundary of the region of surface induced turbulence and currents, is the thermocline. The effect of these two phenomena, inertia forces and buoyancy forces, can be seen by examining the gradient form of the Richardson number which is defined as

$$Ri = -\alpha_v g \frac{\frac{\partial \theta}{\partial z}}{\left(\frac{\partial u}{\partial z}\right)^2} \quad \ldots\ldots\ldots\ldots\ldots\ldots (3.7)$$

where

Ri = Richardson number

α_v = coefficient of volumetric expansion of water, $^\circ F^{-1}$

g = acceleration due to gravity, ft/sec^2

θ = temperature, $^\circ F$

u = horizontal component of velocity, ft/sec

z = vertical coordinate measured downward from the surface, ft.

In the expression for the Richardson number, the term $(\partial u/\partial z)^2$ represents the rate of production of turbulence by Reynolds' stresses and the term $\partial\theta/\partial z$ represents the rate of production or suppression of turbulence by the buoyancy field. The Richardson number is positive for stable stratification, i.e., temperature decreasing with depth, and negative for unstable stratification, with its absolute value increasing with increasing stratification (23, p. 4). Since the value of the Richardson number for stable stratification is inversely proportional to the degree of turbulence, it should also be inversely proportional to the diffusivity. As discussed above, the degree of turbulence is a maximum at the surface and decreases to a minimum at the thermocline. As expected, the inverse of the Richardson number follows this same pattern. For this reason, in the literature the diffusivity is usually assumed to be a maximum at the surface and a minimum at the thermocline, with an exponential decrease with depth in the epilimnion (4 and 32).

The strong stable gradient at the thermocline tends to suppress the influence of surface effects in the hypolimnion; hence, the turbulence is caused primarily by indirect effects such as the degradation of internal waves of hypolimnic currents caused by seiches (22, pp. 109-112). Internal waves at the thermocline may be caused by an irregular lake bottom, local atmospheric disturbances, the cooling water intake for a power plant, or discharges from the reservoir. Turbulence also is caused by seiches, which are internal standing waves. Since these currents are oscillatory in the horizontal direction, they do not cause any significant net horizontal transport but do result in vertical transport due to turbulent mixing. Since both seiches and internal currents are intermittent phenomena, the turbulence produced by them will also be intermittent. As expected, values of the diffusivity in the hypolimnion have been found to decrease as stratification progresses and stability increases (22, p.128). Most authors have assumed that the eddy diffusivity in the hypolimnion is constant with depth and equal to the epilimnic value at the thermocline (4, 10, and 32). In the hypolimnion the stability is greatest at the thermocline and decreases with depth, which would seem to indicate that the diffusivity should increase with depth.

Accurate determination of the diffusivity is complicated by uncertainties in field data. This may be seen by examining the heat flux equation which, neglecting advection and direct absorption of solar radiation, becomes

$$q = -\rho c D \frac{\partial \theta}{\partial z} \quad . \; . \; . \; . \; . \; . \; . \; . \; . \; . \; . \quad (3.8)$$

where

q = heat flux, Btu/hr-ft^2

ρ = density of water, lb/ft^3

c = heat capacity of water, Btu/lb-$^{\circ}$F

D = coefficient of thermal diffusion, ft^2/hr

$\frac{\partial \theta}{\partial z}$ = vertical temperature gradient, $^{\circ}$F/ft.

From this equation it should be possible to solve for the diffusivity, which is proportional to the heat flux at a plane divided by the temperature gradient at the plane. However, since both of these quantities are very small in the hypolimnion, it is difficult to calculate the diffusivity in the hypolimnion with much precision, and the variation of diffusivity with depth in this region remains in doubt.

To account for the effects of the advection of thermal energy and the absorption of solar radiation in the present study, Equation 3.6 is used to solve for the diffusivity instead of using Equation 3.8; however, the general procedure is the same. The method described here follows that presented by Water Resources Engineers (32, pp. 25-33).

An expression for the diffusivity as a function of depth and time is found by solving Equation 3.6 for D using field measurements. If Equation 3.6 is taken in the limit as $z \rightarrow 0$, subscript $j+1$ will merge to j and

$$A_j = \frac{a_{j+1}+a_j}{2} \rightarrow a_j$$

$$\frac{d\theta_j}{dt} \rightarrow \frac{\partial\theta_j}{dt}$$

$$\frac{1}{\Delta z}\left(Q_{i_j}\theta_{i_j} - Q_{o_j}\theta_j\right) \rightarrow \frac{\partial}{\partial z}\left(Q_{i_j}\theta_{i_j} - Q_{o_j}\theta_j\right)$$

$$\frac{1}{\Delta z}\left(Q_{v_{j+1}}\theta_j - Q_{v_j}\theta_{j-1}\right) \rightarrow Q_{v_j}\frac{\partial\theta_j}{\partial z}$$

$$\frac{1}{\Delta z}\left(a_{j+1}D_{j+1}\frac{\theta_{j+1} - \theta_j}{\Delta z} - a_j D_j\frac{\theta_j - \theta_{j-1}}{\Delta z}\right) \rightarrow \frac{\partial}{\partial z}\left(a_j D_j\frac{\partial\theta_j}{\partial z}\right)$$

Making these substitutions and rearranging, Equation 3.6 becomes

$$\frac{\partial}{\partial z}\left(a_j D_j\frac{\partial\theta_j}{\partial z}\right) = a_j\frac{\partial\theta_j}{\partial t} - a_j\frac{h_j'}{\rho c} - \frac{\partial}{\partial z}\left(Q_{i_j}\theta_{i_j} - Q_{o_j}\theta_j\right) + Q_{v_j}\frac{\partial\theta_j}{\partial z} \quad \ldots\ldots(3.9)$$

Integrating Equation 3.9 with respect to z from $z = 0$ to $z = z_j$, where $z = 0$ corresponds to the bottom of the reservoir, results in

$$\left| a_j D_j \frac{\partial \theta_j}{\partial z} \right|_0^{z_j} = \int_0^{z_j} a_j \left(\frac{\partial \theta_j}{\partial t} - \frac{h'_j}{\rho c} \right) dz$$

$$- \sum_{j=1}^{j} \left(Q_{i_j} \theta_{i_j} - Q_{o_j} \theta_j \right) + \left| Q_{v_j} \theta_j \right|_0^{z_j} \quad \ldots\ldots\ldots \quad (3.10)$$

The second term on the right hand side of Equation 3.10 appears as a summation instead of an integral because the inflows and outflows are defined only at discrete points. Assuming that there is neither advection or diffusion at the bottom of the reservoir, the lower limits of the term on the left and the last term on the right are zero. Making this substitution and solving for D_j results in

$$D_j = \frac{\int_0^{z_j} a_j \left(\frac{\partial \theta_j}{\partial t} - \frac{h'_j}{\rho c} \right) dz - \sum_{j=1}^{j} \left(Q_{i_j} \theta_{i_j} - Q_{o_j} \theta_j \right) + Q_{v_j} \theta_j}{a_j \frac{\partial \theta_j}{\partial z}} \quad \ldots \quad (3.11)$$

Writing Equation 3.11 in finite difference form gives

$$D_j = \frac{\sum_{j=1}^{j} a_j \left(\frac{\Delta \theta_j}{\Delta t} - \frac{h'_j}{\rho c} \right) \Delta z_j - \sum_{j=1}^{j} \left(Q_{i_j} \theta_{i_j} - Q_{o_j} \theta_j \right) + Q_{v_j} \theta_j}{a_j \frac{\Delta \theta_j}{\Delta z}} \quad \ldots \quad (3.12)$$

Equation 3.12 can be solved for D_j if there exist two successive temperature profiles, hydrologic inputs, and external energy sources between the times of the two profiles. In evaluating Equation 3.12 for D_j, all terms are taken as mean values over the time interval considered.

Water Resources Engineers (32, pp. 28-30) present calculated values for the effective diffusion coefficient for four stratified reservoirs - - Fontana Reservoir in North Carolina, Hungry Horse in Montana, and Castle Lake and Lake Tahoe in California. Although the values and variation of the coefficient with depth are unique for each reservoir studied, certain similar characteristics are noted in each. In all cases the coefficient was greatest near the surface and declined rapidly to a minimum near the thermocline. From the thermocline the coefficient increased with depth to about the mid-depth of the hypolimnion, then decreased to a value close to that at the thermocline. Based on these observations, Water Resources Engineers assumed that the effective diffusion coefficient can be represented by a decaying exponential in the epilimnion and a constant, equal to the value at the thermocline, in the hypolimnion. This is expressed as

$$D(z,t) = D_o(t)e^{-\gamma(z_d - z)} \qquad \text{for } z \geq z_t \quad \ldots\ldots (3.13)$$

and

$$D(z,t) = D(z_t,t) \qquad \text{for } z \leq z_t \quad \ldots\ldots (3.13)$$

where

$D(z,t)$ = coefficient of effective diffusion, ft^2/hr

$D_o(t)$ = value of the coefficient at the reservoir surface, ft^2/hr

z_d = elevation of the surface, ft

z_t = elevation of the thermocline, ft

z = vertical coordinate, ft

γ = decay coefficient, ft^{-1}.

The decay coefficient is determined by the values of the diffusivity at the surface and at the thermocline. The diffusivity is determined by solving for it as a function of depth in Equation 3.12. An equation of the form of Equation 3.13, which is the assumed form, is then fitted to the calculated values. Water Resources Engineers found fairly large variations between the assumed shape in the hypolimnion and the values of the coefficient calculated using Equation 3.12. This discrepancy was probably primarily caused by inaccuracies in the temperature gradient data in this region of the lake. Thus, the specification of an assumed shape of the diffusion coefficient profile helps to smooth out errors caused by inaccuracies in measurements.

Convective Mixing

During the fall and winter the surface layer of a reservoir cools more rapidly than lower layers. This cooling process causes the surface water to become denser than the water below it, and hence it sinks and mixes with the warmer subsurface water. When the model generates this type of unstable temperature distribution, it simulates convective mixing in order to eliminate the instability.

The mixing is accomplished by checking the temperature distribution and whenever an unstable gradient of more than 0.1 $^{\circ}F$ per foot is found all layers from the top of the reservoir to the point of instability are mixed. The new temperature of the mixed layer is found by taking the volume-weighted average temperature of the mixed elements in order to maintain the energy balance. If an instability still exists between the mixed layers and the element below, the element below is mixed. This process is repeated until a stable temperature gradient exists in the entire reservoir. An unstable gradient of $0.1^{\circ}F$ per foot is allowed to avoid mixing slight instabilities which result from inaccuracies in the numerical calculations.

In actuality, the convective mixing process takes place not only during the fall and winter but also at night during the warming period when the surface cools. In the computer model this nightly mixing is not taken into account directly because a time interval of one day is used in the simulation. This results in an averaging of the diurnal heating and cooling of the reservoir so that there is no convective cooling at night during the heating period; however, the mixing process is accounted for indirectly in computing the value of the turbulent diffusivity for heat.

Chapter IV

Energy Budget

The main factor accounting for the temperature distribution of a deep reservoir is the exchange of heat energy between the reservoir and the atmosphere. The mechanisms of heat exchange which represent energy gains and are independent of surface temperature are short-wave solar radiation and long-wave atmospheric radiation. Mechanisms of heat transfer which depend on the surface temperature are long-wave back radiation, evaporation, and convection. These are heat losses except for convection which can be a gain or a loss depending on the air and water surface temperatures. The algebraic sum of these terms, which is equal to the net rate of surface heat exchange and is referred to as the energy budget, is expressed mathematically as

$$h_{net} = h_s + h_a - h_b - h_e + h_c \quad \ldots \ldots \ldots (4.1)$$

where

h_{net} = net heat flux passing the air-water interface, Btu/hr-ft^2

h_s = net short-wave radiative flux, Btu/hr-ft^2

h_a = net atmospheric radiative flux, Btu/hr-ft^2

h_b = back radiative flux, Btu/hr-ft^2

h_e = evaporative energy flux, Btu/hr-ft^2

h_c = convective energy flux, Btu/hr-ft^2

The magnitudes of some of the components of the energy budget depend upon the reservoir surface temperature, which in turn depends upon the rate at which thermal energy is transported downward from the surface; therefore, it is not possible to calculate the energy budget from meteorological data independently of the internal energy transfer in the reservoir. The terms of the energy budget for Lake LBJ, as calculated in the simulation of the thermal behavior of the reservoir, are plotted in Figure 10 of Chapter VI.

Short-Wave Solar Radiation

Short-wave solar radiation is radiant energy which passes directly from the sun to the earth and has a wavelength between 0.14 and 4.0 microns with a maximum intensity at 0.5 microns (6, pp. 19-20). The short-wave radiation incident upon the surface of the water is the radiation reaching the top of the atmosphere less losses in the atmosphere. These losses include absorption by ozone in the upper atmosphere, scattering by dry air, and absorption and scattering by particles and water vapor. The radiation reaching the water surface, which is a function of the latitude and elevation of the site, time of day, season, and cloud cover, can be calculated as described by Water Resources Engineers (32,pp. 37-43) or Raphael (21, pp. 160-166). This calculation is rather complex and requires the use of several quantities which are not usually available for the site under consideration. For these reasons it is best to use measurements of solar radiation recorded by a pyrheliometer, if available, as was done in this study.

The solar radiation which reaches the water surface is further reduced by reflection at the water surface and from bubbles and suspended material just below the surface. The percentage of reflection is mainly a function of the sun's altitude angle and the amount and type of cloud cover. Two slightly different methods for calculating this quantity are reported in the literature (32, p. 43; 2, pp. 46-48). Since the reflected short-wave radiation depends on the sun's altitude angle, it will vary during the day. In the present study a daily average value for solar radiation arriving at the water surface was used; therefore, to be consistent, an average value of reflected radiation was also used. A yearly average value of 6% reflection of incident short-wave radiation, as reported by Parker and Krenkel (19, p. VI-7), was used instead of using a formula for calculating an instantaneous value of reflection.

Long-Wave or Atmospheric Radiation

Atmospheric radiation is radiant energy which is absorbed in gases in the atmosphere, mainly water vapor, and then radiated to the earth. It has a range of wavelengths from 4 to 120 microns with a peak intensity at about 10 microns (6, p. 22). Its magnitude depends on the air temperature and humidity, and ozone, carbon dioxide, and other matter in the atmosphere. This quantity can be measured with a flat plate radiometer; however, these measurements are seldom available. The atmospheric radiation can also be calculated as described by Water Resources Engineers (32, p.44) and Edinger and Geyer (6, pp. 22-23, 26). The method described in (32), which uses the following formula, was used:

$$h_a = 2.89 \times 10^{-6} \sigma \theta_a^6 C_L (1 - R) \quad . . . . . (4.2)$$

where

h_a = atmospheric radiative flux, Btu/hr-ft^2

σ = Stefan-Boltzmann constant - 0.1713 x 10^{-8} Btu/hr-ft^2 - $^{\circ}R^4$

θ_a = Absolute air temperature at a level of 2 meters about the water surface, $^{\circ}R$

C_L = Correction factor for cloudiness given by $C_L = 1.0 + 0.17 C^2$

C = Fraction of sky occupied by clouds

R = Reflectivity of water surface for atmospheric radiation = 0.03

Back Radiation

One of the mechanisms by which a reservoir loses thermal energy is by radiation to the atmosphere, called long-wave back radiation. The rate of this heat loss is calculated by Stefan-Boltzmann fourth power radiation law, which is presented by Water Resources Engineers (32, p. 44) as

$$h_b = \epsilon \sigma \theta_w^4 \quad . . . . (4.3)$$

where

h_b = back radiative flux, Btu/hr-ft^2

ϵ = emissivity of water $\cong$ 0.97

σ = Stefan-Boltzmann Constant = 0.1713×10^{-8} Btu/hr-ft^2 - $^\circ R^4$

θ_w = Absolute water surface temperature, $^\circ R$

Evaporation

Another important mechanism by which a reservoir loses thermal energy to the environment is through evaporation. Each pound of water which evaporates carries with it its latent heat of about 970 Btu. There are many different methods of calculating the evaporative heat loss, most of which use the general relation

$$h_e = f(w)\ (e_s - e_a) \quad . \ . \ . \ . \ . \ . \ . \ . \ . \ . \ (4.4)$$

where

h_e = evaporative heat flux, Btu/hr-ft^2

w = wind speed, miles/hour

$f(w)$ = function of wind speed

e_s = saturation vapor pressure at the water surface temperature, in. Hg.

e_a = water vapor pressure, in. Hg.

The wind speed function (mass transfer coefficient) has been determined empirically by a number of investigators, and its value varies considerably depending on the time period over which data was averaged, the standard reference height for the wind speed and vapor pressure, and the local topography of the site studied (6, p. 36).

In this study the mass transfer coefficient determined in the noted Lake Hefner studies is used. This results in the following (6, p. 34):

$$h_e = 12.1w\ (e_s - e_a) \quad \text{. . . . .(4.5)}$$

The vapor pressures are calculated by the following formulas (27, p.13):

$$e_s = 0.1001 \exp(0.03\theta_w) - 0.087$$

$$e_a = e_{wb} - 0.000367\ P_a \left(\theta_a - \theta_{wb}\right)\left(1 + \frac{\theta_{wb} - 32}{1571}\right)$$

$$e_{wb} = 0.1001 \exp(0.03\theta_{wb}) - 0.0837 \quad \text{. . . . .(4.6)}$$

where

θ_w = water surface temperature, $^\circ$F

θ_{wb} = wet bulb air temperature, $^\circ$F

θ_a = dry bulb air temperature, $^\circ$F

e_{wb} = saturation vapor pressure at the wet bulb air temperature, in. Hg.

P_a = atmospheric pressure, in. Hg.

The rate of water loss by evaporation is calculated from

$$Q_e = \frac{h_e A_s}{\rho\ h_1} \quad \text{. . . . .(4.7)}$$

where

Q_e = rate of evaporation, ft^3/hr

A_s = area of the surface of the reservoir, ft^2

ρ = density of water, lb/ft^3

h_l = latent heat of vaporization of water, Btu/lb given hy $h_l = 1084 - 0.5\theta_w$ (27, p. 13)

Convection

The reservoir can either gain or lose heat by convection depending on whether the air temperature is greater or less than the water surface temperature. The calculation of the convective heat flux is similar to the evaporative flux, since the heat transfer coefficient for convection is assumed to be proportional to the coefficient for evaporation. Thus, the convective heat flux is given (6, pp. 37-38) as

$$h_c = \frac{0.0102\ h_e\ (\theta_a - \theta_w)}{(e_s - e_a)}\ \frac{P_a}{29.92} \quad . . . . (4.8)$$

where

h_c = convective heat flux, Btu/hr-ft^2

Internal Absorption of Thermal Energy

In order to calculate the temperature of a reservoir it is necessary to link the external thermal energy flux with its absorption within the reservoir. Atmospheric radiation, back radiation, evaporation, and convection are heat gains and losses which affect only the surface element of water in the reservoir. Short-wave solar radiation is assumed to be absorbed exponentially with depth, according to the extinction properties of visible light in water.

The rate of gain or loss of heat energy per unit volume in the surface element is expressed as

$$h_n' = \frac{\beta\, h_s + h_a - h_b - h_e + h_c}{\Delta\, z_n} \qquad \ldots\ldots\ldots (4.9)$$

where

h_n' = heat flux per unit volume to or from the surface element, Btu/hr-ht^2-ft

β = fraction of short-wave radiation absorbed in the surface element

$\Delta\, z_n$ = thickness of surface element, ft.

The remaining solar radiation, $(1 - \beta)\, h_s$, is absorbed exponentially with depth in the reservoir. This flux below the surface element is expressed as

$$\Phi\,(z) = (1-\beta) h_s\, e^{-\eta(z_n - z)} \qquad \ldots\ldots\ldots (4.10)$$

where

$\Phi(z)$ = solar radiative flux at elevation z, Btu/hr ft^2

η = light extinction coefficient in water, ft^{-1}

z_n = elevation of bottom of surface element

The solar radiative flux, $\Phi\,(z)$, is a continuous function of z and the difference between its value at the top and bottom of an element gives the amount of thermal energy absorbed in the element. This is expressed as

$$\Delta\Phi_j = \Phi_{j+1}\, a_{j+1} - \Phi_j\, a_j \qquad \ldots\ldots\ldots (4.11)$$

where

$\Delta\Phi_j$ = solar radiation absorbed in the j-th element, Btu/hr

Φ_{j+1} = solar radiative flux at the top of the j-th element, Btu/hr-ft^2

Φ_j = solar radiative flux at the bottom of the j-th element, Btu/hr-ft^2

a_{j+1} = area of top surface of j-th element, ft^2

a_j = area of bottom surface of j-th element, ft^2

Note that Equation 4.11 implies that all radiation striking the walls of the reservoir is absorbed in the water at that elevation. The Tennessee Valley Authority (24, pp. 3-4) has found that for rock and sand walls about 20 percent of the radiation striking the walls is reflected upwards, sideways, and downward. The rest of the radiation is absorbed by the walls which then warm the adjacent water, so that the simplifying assumption of absorption within the water directly seems reasonable. Since the wall-to-water surface area ratio is usually quite small for elements near the lake surface, where the solar radiation term is most significant, even large departures from this assumption should have a negligible effect on the element temperature.

The absorption of solar radiation per unit volume for the j-th element is found by dividing Equation 4.11 by the volume of the element, of

$$h'_j = \frac{\Phi_{j+1}\, a_{j+1} - \Phi_j\, a_j}{A_j\, \Delta z} \quad \ldots\ldots\ (4.12)$$

where

A_j = average of the upper and lower horizontal surface areas of the j-th element, ft^2

Δz = thickness of each element in reservoir, ft.

Note that in this equation the subsctipt j need not be included in the Δz term, since this quantity is fixed for all elements except the surface element, and the equation is not applied to the surface element.

Chapter V

Solution Technique

In the two previous chapters the governing equations for the temperature distribution in a stratified reservoir have been developed. In this chapter the method used to solve these equations by means of a digital computer is presented. A listing of the program is given in Appendix A and instructions for its use are given in Appendix C.

The three basic governing equations are:

Conservation of energy:

$$A_j \frac{d\theta_j}{dt} = A_j \frac{h_j'}{\rho c} + \frac{1}{\Delta z}\left(Q_{i_j}\,\theta_{i_j} - Q_{o_j}\,\theta_j\right) - \frac{1}{\Delta z}\left(Q_{v_{j+1}}\,\theta_j - Q_{v_j}\,\theta_{j-1}\right)$$

$$+ \frac{1}{\Delta z}\left\{a_{j+1}\,D_{j+1}\,\frac{\theta_{j+1} - \theta_j}{\Delta z} - a_j\,D_j\,\frac{\theta_j - \theta_{j-1}}{\Delta z}\right\} \quad \ldots (3.6)$$

Conservation of mass:

$$Q_{v_j} = \sum_{k=1}^{j-1}\left(Q_{i_k} - Q_{o_k}\right) \quad \ldots\ldots\ldots\ldots (3.2)$$

Absorption of solar energy:

$$h_j' = \frac{\Phi_{j+1}\,a_{j+1} - \Phi_j\,a_j}{A_j\,\Delta z} \quad \ldots\ldots\ldots\ldots (4.12)$$

For the special case of the surface element the equations of conservation of energy and absorption of energy are:

Conservation of energy:

$$A_j \frac{d\theta_j}{dt} = A_j \frac{h'_j}{\rho c} + \frac{1}{\Delta z_j} \left(Q_{i_j} \theta_{i_j} - Q_{o_j} \theta_j \right) - \frac{1}{\Delta z_j} \left(Q_{v_{j+1}} \theta_j - Q_{v_j} \theta_{j-1} \right)$$

$$+ \frac{1}{\Delta z_j} \left\{ a_{j+1} D_{j+1} \frac{2(\theta_{j+1} - \theta_j)}{(\Delta z_{j+1} + \Delta z_j)} - a_j D_j \frac{2(\theta_j - \theta_{j-1})}{(\Delta z_j + \Delta z_{j-1})} \right\} \quad . \quad . (3.5)$$

Absorption of energy:

$$h'_n = \frac{\beta h_s + h_a - h_b - h_e + h_c}{\Delta z_n} \quad . \; . \; . \; . \; . \; . \; . \; . (4.9)$$

These general expressions represent three equations for the five unknowns, θ_j, Q_{i_j}, Q_{o_j}, Q_{v_j}, and h'_j. The two unknowns, Q_{i_j} and Q_{o_j}, are determined by the assumed inflow and outflow conditions, as explained in Chapter III.

The solution to the equations presented here follows that given by Water Resources Engineers (32, pp. 57, 59-63). When equation 3.6, or equation 3.5 for the surface element, is written for each element in the reservoir, the result is a set of n simultaneous algebraic equations, where n is the number of elements, which can be written conveniently in matrix notation as

$$[A]\{\dot{\theta}\} = [A]\{P\} + \{Q\} + [K]\{\theta\} \quad . \; . \; . (5.1)$$

$[A]\{\dot{\theta}\}$	$[A]\{P\}$	$\{Q\}$	$[K]\{\theta\}$
Time rate of temperature change	Horizontal advection and radiation absorption	Vertical advection	Diffusion

where

$[A]$ = a diagonal matrix of average horizontal surface areas of each element given by $A_{jj} = A_j$

$\{\dot{\theta}\}$ = a vector (column matrix) expressing the time rate of temperature change of each element given by

$$\dot{\theta}_j = \frac{d\theta_j}{dt}$$

$\{P\}$ = a vector giving the thermal load to each element by horizontal advection and absorption of solar radiation. (For the surface element the term h' will also include all other heat fluxes which pass the air-water interface.) The j-th element of the matrix is given by

$$P_j = \frac{h'_j}{\rho c} + \frac{1}{A_j \, \Delta z_j} \left(Q_{i_j} \theta_{i_j} - Q_{o_j} \theta_j \right)$$

$\{Q\}$ = a vector giving the thermal load to each element due to advection in the vertical direction. Assuming positive flows, the j-th element of the matrix is given by

$$Q_j = \frac{1}{\Delta z_j} \left(Q_{v_j} \theta_{j-1} - Q_{v_{j+1}} \theta_j \right)$$

[K] = a tridiagonal matrix of thermal diffusion parameters. The terms of the j-th row are given by

$$K_{j,j-1} = \frac{a_j D_j}{\Delta z_j^2}$$

$$K_{j,j} = -\frac{a_{j+1} D_{j+1} + a_j D_j}{\Delta z_j^2}$$

$$K_{j,j+1} = \frac{a_{j+1} D_{j+1}}{\Delta z_j^2}.$$

Equation 5.1 can be simplified to

$$[A] \{\dot{\theta}\} = \{P'\} + [K] \{\theta\} \quad \ldots\ldots\ldots\ldots\ldots \quad (5.2)$$

where

$$\{P'\} = [A] \{P\} + \{Q\} \quad \ldots\ldots\ldots\ldots\ldots \quad (5.3)$$

In Equation 5.2 θ and $\dot{\theta}$ are unknowns and all other quantities are known. In order to solve this matrix equation an expression for θ in terms of $\dot{\theta}$ will be substituted for θ. The equation is then solved for $\dot{\theta}$ and this value can be used to determine θ by using the relation between θ and $\dot{\theta}$, which is obtained by writing a Taylor series expansion for $\dot{\theta}$. Retaining only the first two terms, this results in

$$\theta_j (t + \Delta t) = \theta_j(t) + \dot{\theta}_j \Delta t \quad \ldots\ldots\ldots \quad (5.4)$$

where time "t" is the beginning of the time interval and time "t + Δt" is the end of the time interval of length Δt. Evaluating the time derivative of temperature at the average of its value at the beginning and the end of the time interval, Equation 5.4 becomes

$$\theta_j (t + \Delta t) = \theta_j(t) + \frac{\dot{\theta}_j (t) + \dot{\theta}_j (t + \Delta t)}{2} \Delta t \quad . . . (5.5)$$

Defining

$$\alpha_j(t) = \theta_j (t) + \dot{\theta}_j(t) \frac{\Delta t}{2} \quad . . . (5.6)$$

and substituting into Equation 5.5 results in

$$\theta_j (t + \Delta t) = \alpha_j (t) + \dot{\theta}_j (t + \Delta t) \frac{\Delta t}{2} \quad . . . (5.7)$$

Since this equation applies to all elements in the reservoir, it can be written in matrix form to describe the entire reservoir. This results in

$$\{\theta (t + \Delta t)\} = \{\alpha (t)\} + \frac{\Delta t}{2} \{\dot{\theta} (t + \Delta t)\} \quad . . . (5.8)$$

By substituting Equation 5.8 into Equation 5.2, the governing equation becomes

$$[A] \{\dot{\theta} (t + \Delta t)\} - \frac{\Delta t}{2} [K(t + \Delta t)] \{\dot{\theta} (t + \Delta t)\}$$

$$= \{P'(t + \Delta t)\} + [K(t + \Delta t)] \{\alpha(t)\} \quad . . . (5.9)$$

Letting

$$[S(t + \Delta t)] = [A] - \frac{\Delta t}{2} [K(t + \Delta t)] \quad . . . (5.10)$$

And

$$\{F(t + \Delta t)\} = \{P'(t + \Delta t)\} + [K(t + \Delta t)] \{\alpha(t)\} \quad . (5.11)$$

equation 5.9 reduces to

$$[S(t + \Delta t)] \{\dot{\theta} (t + \Delta t)\} = \{F(t + \Delta t)\} \quad . . . (5.12)$$

By using the above equations a recursive relationship is established which will yield the temperature at each time step. This procedure is summarized as follows:

1. Set the initial condition that $\{\alpha(o)\} = \{\theta(o)\}$
2. Apply the following recursion formulas in sequence for each time step, Δt,

   a. $[S(t + \Delta t)] = [A] - \frac{\Delta t}{2} [K(t + \Delta t)]$

   b. $[F(t + \Delta t)] = \{P'(t + \Delta t)\} + [K(t + \Delta t)] \{\alpha(t)\}$

   c. Find $\{\dot{\theta}(t + \Delta t)\}$ from $[S(t + \Delta t)] \{\dot{\theta}(t + \Delta t)\}$
      $= \{F(t + \Delta t)\}$

   d. $\{\theta(t + \Delta t)\} = \{\alpha(t)\} + \frac{\Delta t}{2} \{\dot{\theta}(t + \Delta t)\}$

   e. $\{\alpha(t + \Delta t)\} = \{\theta(t + \Delta t)\} + \frac{\Delta t}{2} \{\dot{\theta} (t + \Delta t)\}$

The method of finding $\{\dot{\theta}\ (t + \Delta t)\}$ (part 2c) is given by Ralston and Wilf (20, p. 233) and is presented in Appendix F.

The step forward integration technique presented here is not exact unless $\Delta t \rightarrow 0$. However, Water Resources Engineers (32, p. 63) stated that "...even with Δt quite large, the results obtained are within an accuracy of the assumptions used in formulating the problem." In this study a minimum time interval of one day is used.

Chapter VI

Application of the Temperature Model to Lake LBJ

In 1968 a study of water quality in Lake LBJ was conducted by Fruh and Davis (8). In this chapter the temperature data obtained from this study are compared with the predicted results of the mathematical model developed in the preceeding chapters. The importance of various components of the model in predicting the temperature profiles is also discussed.

Input Data for the Simulation of Lake LBJ

Four types of data are required for the simulation of Lake LBJ: geometry of the reservoir, meteorological data, hydrologic data, and miscellaneous constants. Each of these data types and its source is described below.

1. Geometry of the Reservoir
    a. Elevation of the bottom of the reservoir
    b. Table of the volume of elements of one foot thickness.

Both of these items were obtained from LCRA (17) and are given in Appendix D. These data indicate that the maximum depth of Lake LBJ is 65 feet; however, profiles taken in the deep pool show that the maximum depth is 83 feet. To extend the predictive results of the model to a greater depth, eighteen elements with the same volume as the bottom element from the LCRA data, which is 102 acre feet, were added to the bottom of the lake. This addition has little effect on the total volume of the reservoir, but it does allow the prediction of the lower temperatures near the bottom.

2. Meteorological Data

   a. Dry-bulb air temperature

   b. Wet-bulb air temperature

   c. Wind velocity

   d. Barometric pressure

   e. Cloud cover

   f. Precipitation

   g. Daily average of short-wave solar radiation

The solar radiation data was obtained from the Texas Water Development Board's records of their pyrheliometer located at the Austin Municipal Airport (28). All other meteorological data were obtained from U. S. Weather Bureau measurements taken at the Austin Airport (29). Although this data was measured about forty miles from Lake LBJ, is is not expected to vary much over the distance. The wind velocity, which varies with the local topography and the height at which it is measured, is expected to be the most uncertain.

3. Hydrologic Data

   a. Inflows

   b. Outflows

   c. Water surface elevation

   d. Temperature of inflows

   e. Initial temperature of the reservoir

Four inflows to Lake LBJ were used in the study: the release from Lake Inks, the Llano River, Sandy Creek, and precipitation falling directly on the lake's surface. Daily average outflows from Lake Inks were obtained from LCRA records (16). The daily average flows of the Llano River and Sandy Creek were obtained from U. S. Geological Survey (USGS) records (30). The USGS gauging station on the

Llano River is located at Llano, which is approximately twenty miles upstream from Lake LBJ; no other complete records are available for the flow at any point along the river closer to Lake LBJ. A 1965 USGS study (25) indicates that for the few instances where measurements are available at different places along the river, the flow is fairly constant between Llano and Lake LBJ, so measurements at the USGS gauging ststion should be fairly representative of the flow into Lake LBJ. The gauging station for Sandy Creek is about three miles upstream from Lake LBJ; therefore, it should give fairly accurate measurements of the inflow from that source. Precipitation which falls directly on the lake (not including local runoff) is calculated on the basis of precipitation at the Austin Municipal Airport. The variation in precipitation between Austin and Lake LBJ is not too great, and this source is a very minor contribution to the total inflow, so it is not expected to contribute significantly to the inaccuracy of the total inflow measurements.

Each of the components of the inflows and outflows for Lake LBJ for the year beginning in March, 1968 is shown in Table 2. Monthly values are shown in Table 3. Since the components of the inflow account for 97.92% of the outflow and the outflow is equal to the inflow for a constant level lake, it appears at a first glance that each component of the inflow has been accounted for with sufficient accuracy. However, when the inflow is compared to the volume of the reservoir, it can be seen that the two percent discrepancy between the inflow and outflow is equivalent to twenty percent of the volume of the reservoir. Thus, if only the inflows shown in Table 2 are used in the simulation of Lake LBJ, after one year the lake will be only eighty percent full. To overcome this problem the total inflow volume for each time period of the simulation is calculated on the basis of the measured discharge, evaporation loss, and the change in the surface level. The total inflow is then used to determine a makeup volume of inflow which must be added to the other inflows in order to maintain the correct volume of water in the reservoir. It is desirable to keep the inflows separated instead of lumping them together because different inflows are at different temperatures, so they will enter the reservoir at different levels.

As discussed in Chapter III, the inflows are assumed to enter the reservoir at the level which has the same density as the inflow. The outflow is assumed to be equally divided between the top 30 elements, except for the flow going over the spillway which is assumed to come from the top element.

Little temperature data has been found on the inflows and outflows for Lake LBJ. Discharge temperatures for Lake Inks were measured five times during the period covered by the simulation, and temperatures of the Llano River were measured six times (8, p. 170). The temperatures of the Llano River, which were measured in water which varied between 12 and 15 feet, showed less than 1 °C temperature stratification except for the April 6 measurement which showed a 4.3 °C temperature difference from top to bottom. To obtain an approximate mixed mean temperature, the top and bottom temperatures were averaged. No temperatures were available for Sandy Creek, so it was assumed to be at the same temperature as the Llano River. The same assumption was also made for the makeup flow.

Table 2

Inflows and Outflows for Lake LBJ for

March 1, 1968 to February 28, 1969

Outflows	Acre Feet
Penstock	1,218,251
Spillway	194,504
Evaporation	28,053
Total	1,440,808

Inflows	Acre Feet	% of Outflow
Lake Inks Release	809,898	56.21
Lake Inks Spillway	236,820	16.44
Llano River	297,570	20.65
Sandy Creek	48,684	3.38
Precipitation	17,900	1.24
Total	1,410,872	97.92

$$\text{Ratio of Outflow to Reservoir Volume} = \frac{1,440,808}{138,460} = 10.4$$

Table 3

Monthly Inflows and Outflows for Lake LBJ
for March 1, 1968 to February 28, 1969

(All figures are in acre feet)

	Lake LBJ Discharge	Lake Inks Discharge	Llano River	Sandy Creek
March	304,628	198,564	63,020	14,930
April	217,426	131,804	72,630	6,020
May	424,996	295,244	75,190	17,260
June	118,286	88,166	24,480	3,890
July	38,548	27,252	11,250	856
August	42,666	41,925	6,020	198
September	16,532	10,863	7,890	1,180
October	12,566	6,879	5,520	487
November	6,839	978	6,610	858
December	14,851	0	10,030	1,680
January	10,887	6,397	7,430	570
February	10,026	1,826	7,500	755
Total	1,218,251	809,898	297,570	48,684

Since daily values of the temperature were desirable for use in the simulation, a least squares curve fit was used to determine an equation for the temperature as a function of time. The equations used are:

$$\theta_{Llano} = -0.19481 \times 10^{2} + 0.57918 \times d$$

$$-0.20482 \times 10^{-2} \times d^{2} + 0.20109 \times 10^{-5} \times d^{3} \quad . . . (6.1)$$

$$\theta_{Inks} = -0.17784 \times 10^{1} + 0.22390 \times d$$

$$-0.46808 \times 10^{-3} \times d^{2} \quad . . . (6.2)$$

where

θ_{Llano} = temperature of the Llano River inflow, $^{\circ}C$

θ_{Inks} = temperature of the Lake Inks release, $^{\circ}C$

d = number of the day of the year

and $54 < d < 398$.

These two curves, together with the measured data points, are plotted in Figure 7. Ward (31) has suggested that the annual variation of a stream's temperature follows a sinusoidal curve; however, the parabolas give a better fit of the data for the time period under consideration. The temperature of the rainfall was taken as the wet-bulb air temperature as suggested by Raphael (21, p.174).

The other temperature data which are needed include a temperature profile in the reservoir at the beginning of the simulation and profiles at various times of the year

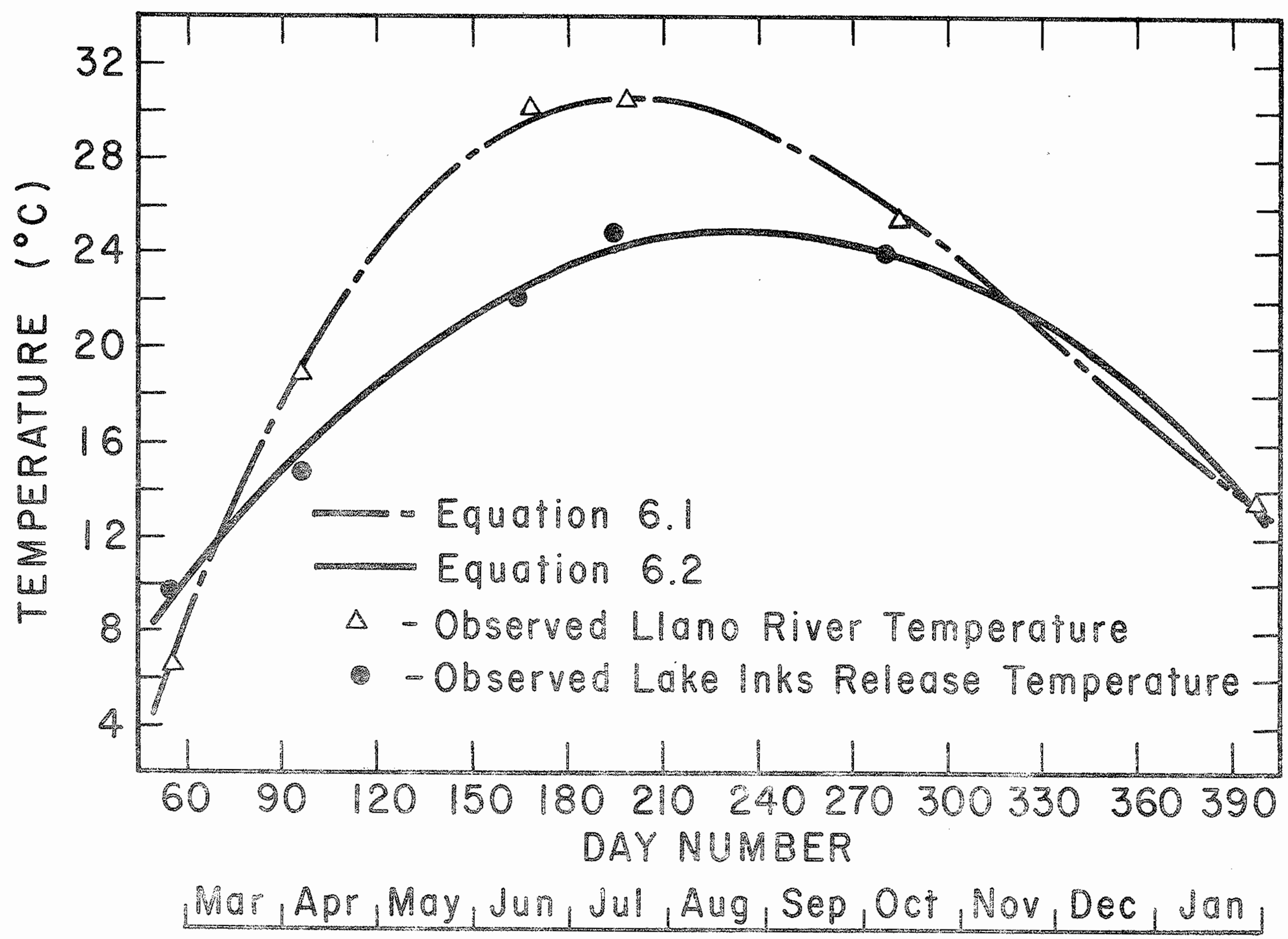

FIG. 7. INFLOW TEMPERATURES FOR THE LAKE INKS RELEASE AND THE LLANO RIVER

for checking the predicted results. Six profiles were available for this purpose during the period of February 24, 1968 to February 1, 1969, the period chosen for the simulation. In addition to checking temperature profiles, predicted and measured outflow temperatures can be compared. However, no outflow temperatures were recorded for the period considered.

4. Miscellaneous constants

   a. Density of water

   b. Specific heat of water

   c. Solar radiation extinction coefficient (η)

   d. Fraction of short-wave solar radiation absorbed in the surface layer (β)

   e. Coefficient of effective diffusion

Within the range of temperatures encountered in the reservoir, the density and specific heat of water vary only slightly and are considered to be constant at ρ = 62.4 lb/ft^3 and c = 1.0 Btu/lb-^{o}F. Note that this assumption does not affect buoyancy effects, which include stratification and convective cooling, since these effects are considered to be a function of temperature directly instead of the density which is a function of the temperature.

The percentage of short-wave solar radiation absorbed in the surface layer is given by β and the remaining radiation is assumed to be distributed vertically as an exponential decay, with a decay constant η . From their studies Dake and Harleman (5, p. 487) have concluded that β appears to be constant for all lakes and equal to 0.4, which is the value used in this study. The decay coefficient η varies with season, weather, and location. It increases as radiation is absorbed faster with depth, which could be caused by plankton growth during the summer or suspended particles during the flood season. Plots of solar radiation with depth for Lake Buchanan (8, pp. 56-57) for two different times are shown in Figure 8. These plots show curves of Φ/Φ_o plotted against depth, where Φ is the radiation at a given depth and Φ_o is the radiation just below the surface. Thus, Φ_o is the radiation remaining after the fraction β is absorbed at surface. In the present study the average values of η = 0.16 for the two curves is used.

The method of determining the diffusivity is described in the next section.

Determination of the Diffusivity

An attempt was made to determine the diffusivity by the method presented in Chapter III; however, this method did not prove to be successful for Lake LBJ. The method determines the diffusivity at a depth under consideration on the basis of the rate of change of heat content below that depth divided by the temperature gradient at the depth. The heat transport due to advection and direct absorption of solar radiation is subtracted in order to account only for the heat transport caused by diffusion. Using this method diffusivities were calculated for the warming period of March and April and the well stratified period of May through August. No attempt was made to calculate diffusivities during the fall when convective mixing effects would further complicate the calculation. The results for both periods showed that the diffusivities varied considerably from one depth to another and followed no consistent pattern. At some depths negative values were calculated, which meant that advection and absorption of solar radiation accounted for more heat transport than that calculated on the basis of

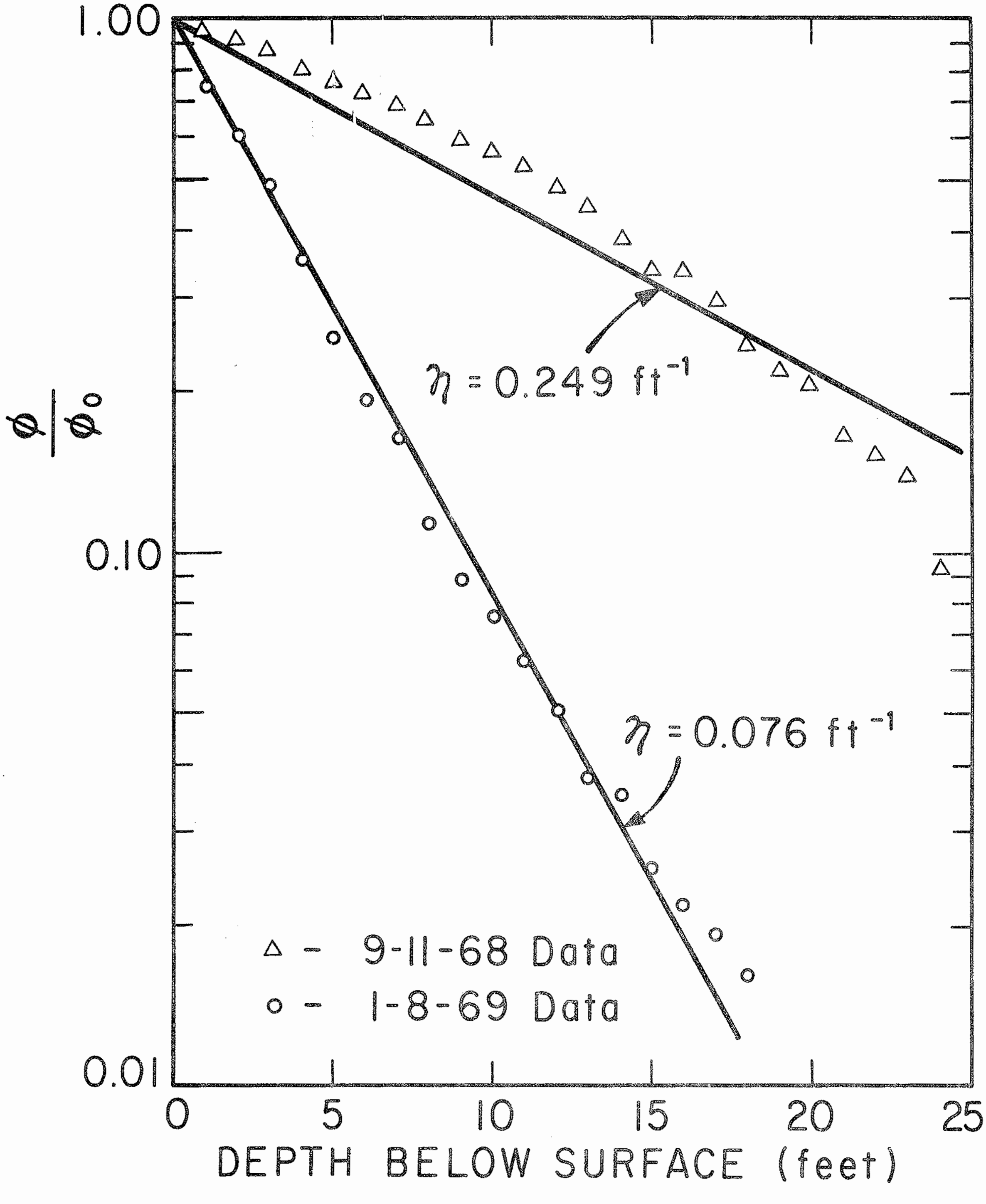

FIG. 8. PENETRATION OF SOLAR RADIATION FOR LAKE BUCHANAN

the change in temperature. This inaccuracy can probably be attributed to the large volume of inflows and outflows and the fact that the heat content of the lake is calculated on the basis of a single temperature profile. Thus, this method of calculating the diffusivity, which involves the calculation of a small difference of large numbers, is extremely sensitive to errors and cannot be applied to Lake LBJ.

To avoid this problem the diffusivity was calculated by simulating the operation of the reservoir with no inflows or outflows. This procedure yielded coefficients which were approximately constant from top to bottom and equal to about 0.6 ft^2/hr for March and April and 0.3 ft^2/hr for May through August. These values were then used as a starting point for a trial and error process of finding the diffusivity which resulted in the best agreement between predicted and observed temperature profiles.

Results of the Computer Simulation of the Annual Thermal Cycle of Lake LBJ

Predicted and observed temperature profiles for Lake LBJ are shown in Figure 9. The simulation to calculate these results used a calculation time step of one day and an element thickness of one foot. Daily averages of inflow, outflow, and meteorological data were used. The following values of the diffusivity gave the best agreement with observed temperatures:

Time Period	Diffusivity (ft^2/hr)
February - April	0.70
May - June	0.45
July - January	0.05

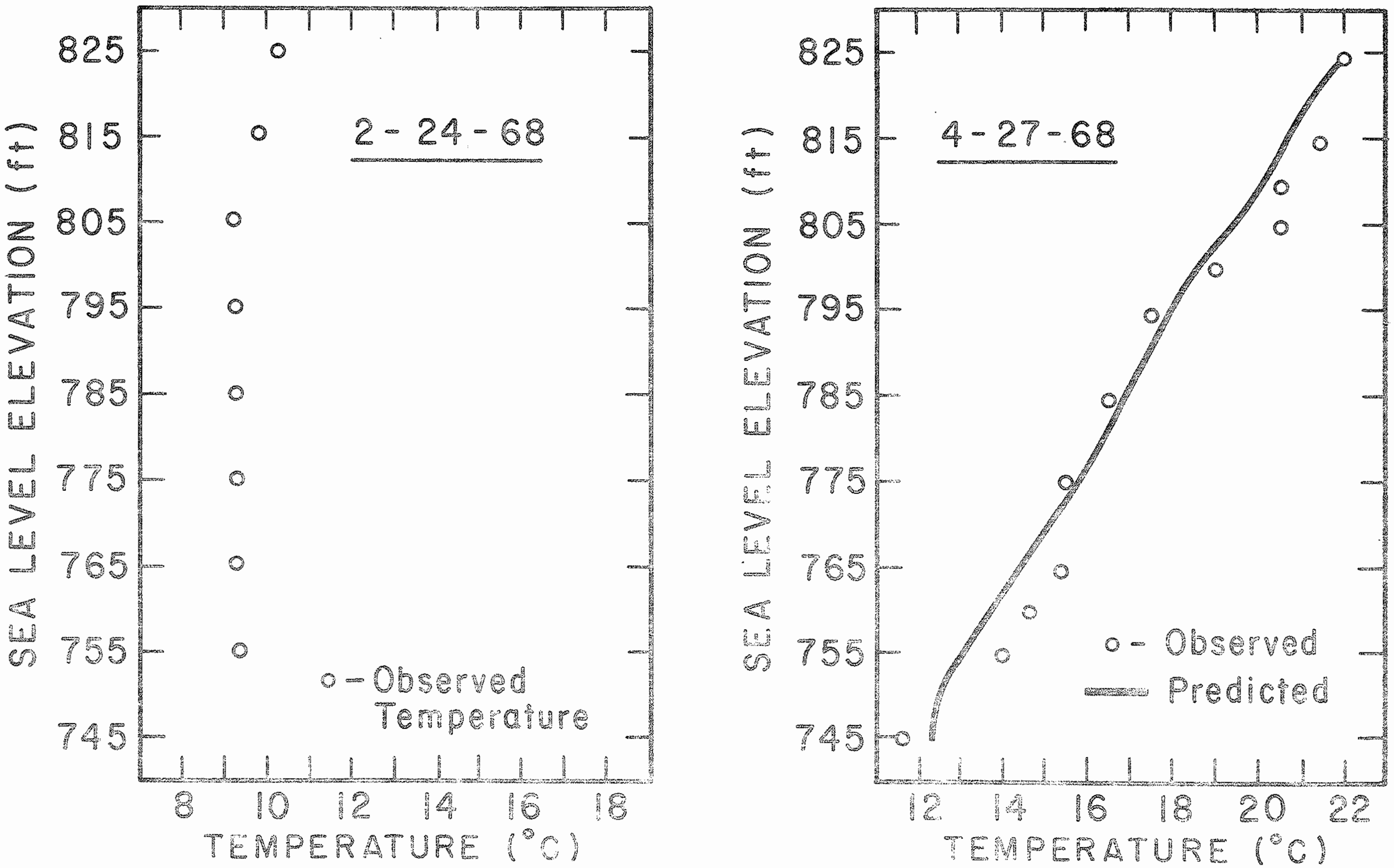

FIG. 9. PREDICTED TEMPERATURE PROFILES FOR LAKE LBJ

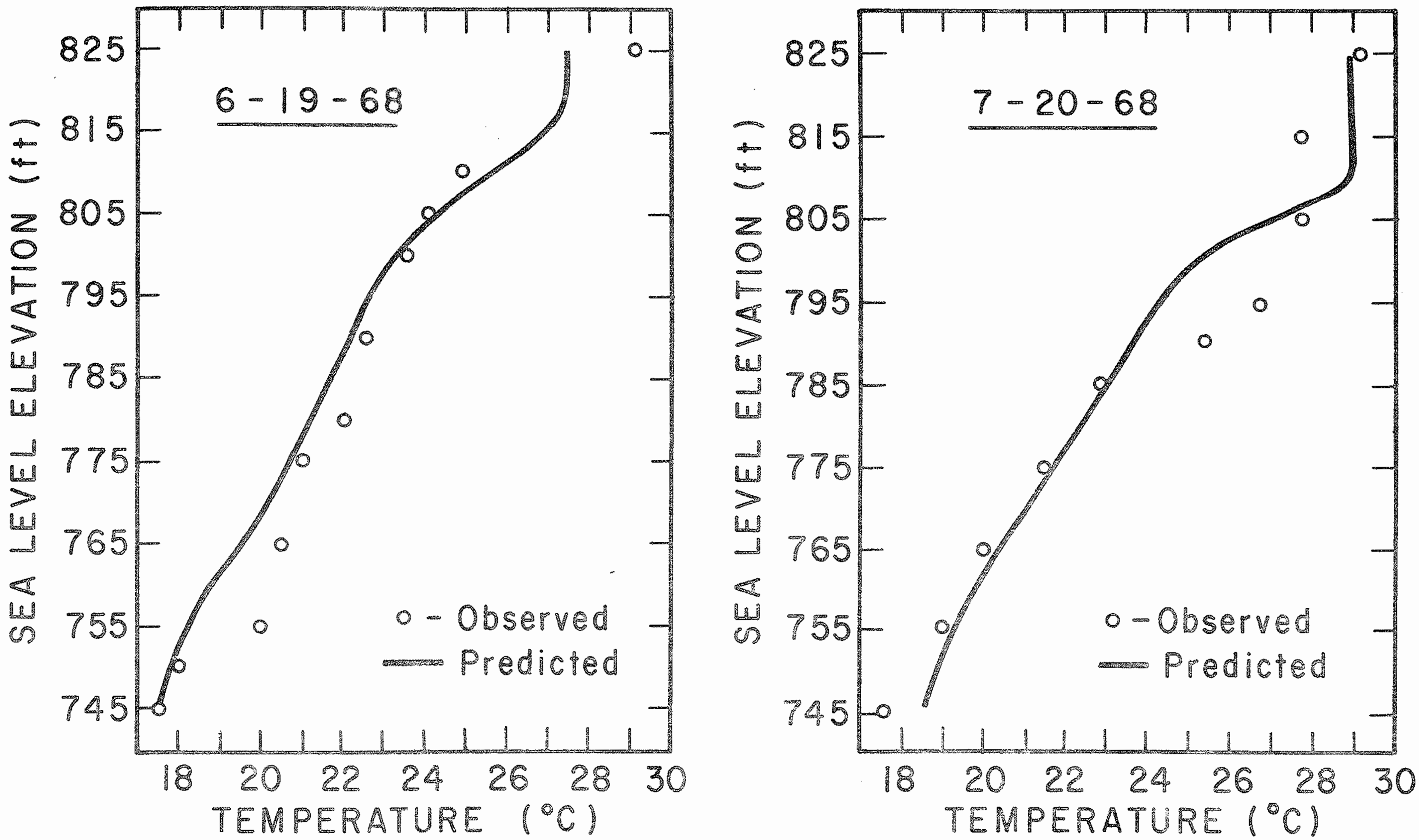

FIG. 9. CONTINUED

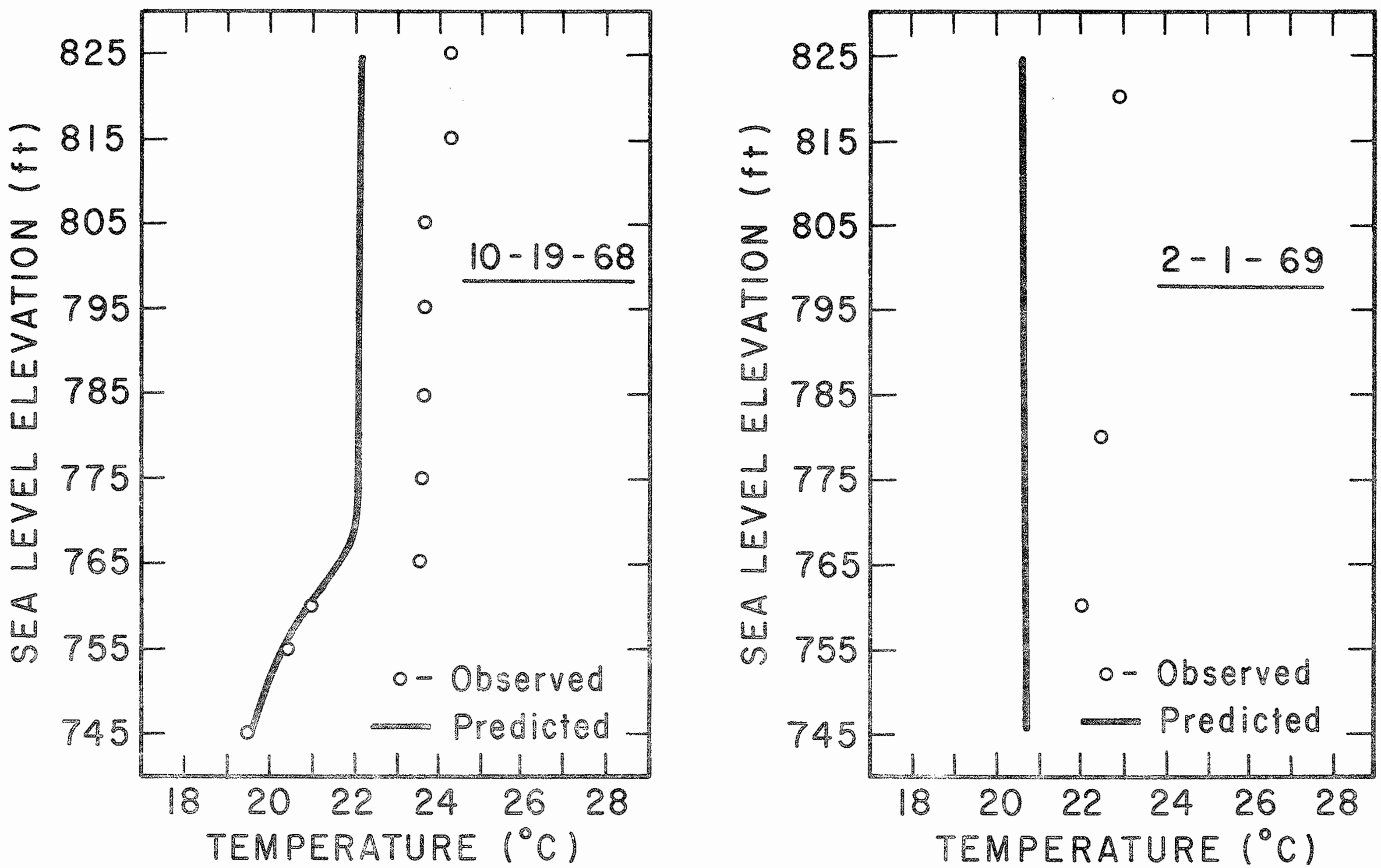

FIG. 9. CONTINUED

These values are consistent with the conclusion of Sundaram (22, p. 128) that the diffusivity in the hypolimnion of most lakes which have been studied decreases by one or two orders of magnitude during the stratification period due to the stabilizing influence of the density gradient.

As discussed in Chapter II, some investigators have used a constant value of the diffusion coefficient from the surface to the bottom, whereas others have found it necessary to use a much larger value at the surface. Although this study used a value that was constant with depth, it varied seasonally from one to two orders of magnitude larger than the molecular diffusivity (0.0055 ft^2/hr).

These diffusivities were taken to be constant from the surface to the bottom of the lake. The results of computer runs using different values of the diffusivity showed that the distribution of thermal energy in Lake LBJ is very sensitive to the value of the diffusivity in the hypolimnion; however, the temperature profiles in the epilimnion show little dependence on the value of the diffusivity. This result can be attributed to the fact that the thermocline is at a fairly shallow depth and the top ten or twenty feet (which includes much of the epilimnion) remains fully mixed during the stratified season. Since the epilimnion remains well mixed, there is no temperature gradient and therefore no diffusion near the surface. Thus, the predicted temperature is essentially unaffected by the choice of the diffusivity near the surface.

The reason that the epilimnion remains well mixed at all times can be seen by examining a plot of the terms which make up the net surface heat exchange, shown in Figure 10. Although the net heat flux passing the air-water interface

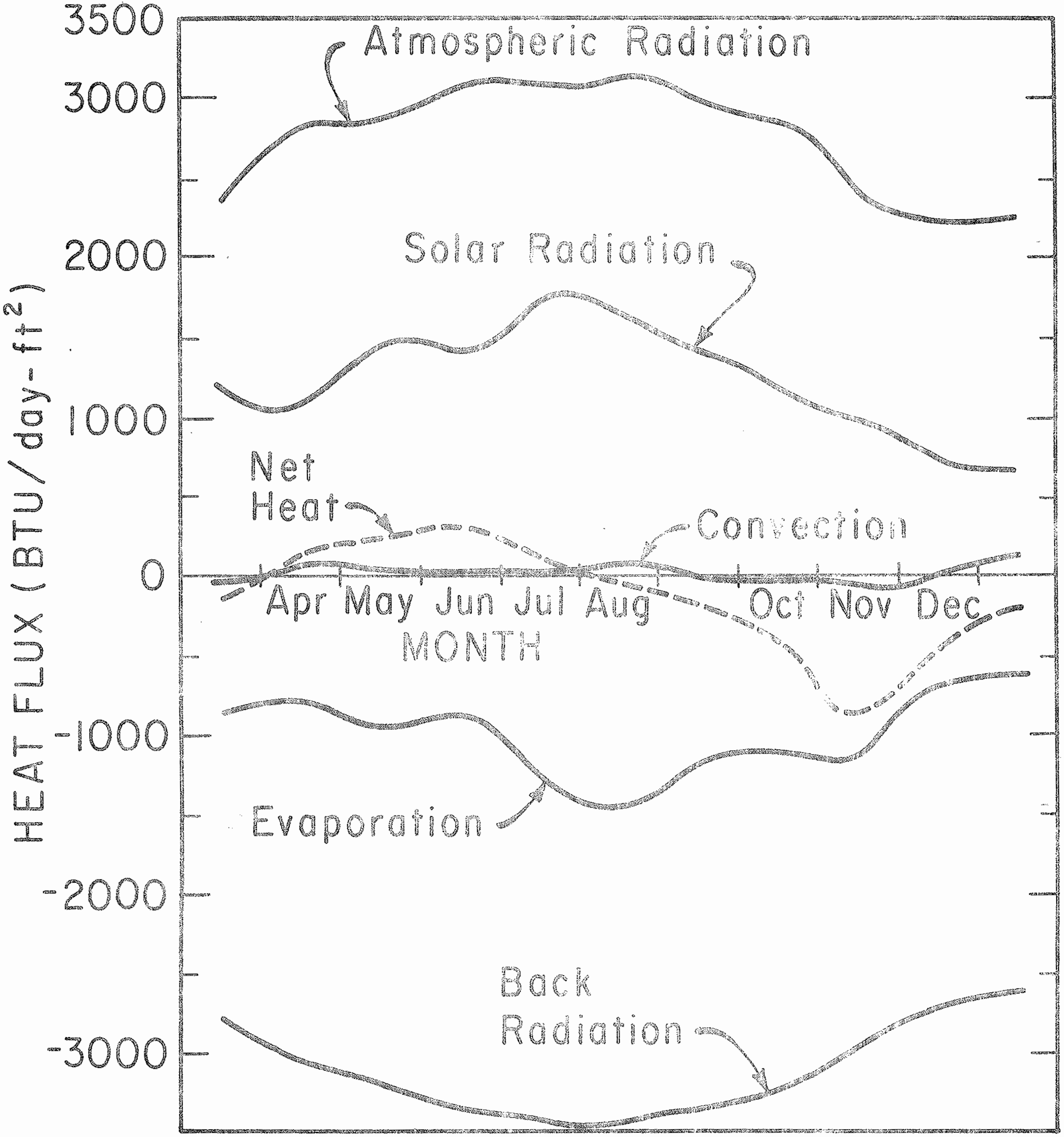

FIG. 10. ENERGY BUDGET TERMS FOR LAKE LBJ - 1968

is positive during the warming period, the heat transfer to the surface layer is not necessarily positive. Only 40% of the short-wave solar energy is absorbed in the surface layer. If the 60% which is absorbed below the surface is subtracted from the net heat flux, it can be seen that the heat exchange with the surface layer is always negative; hence, the surface is always cooling, producing an unstable density gradient. The resulting convective mixing keeps the upper layers of the lake mixed.

An examination of the observed temperature profiles shows that during the warming period there is a small positive temperature gradient at the surface; hence, the computer model seems to be incorrectly predicting the lake's behavior when it is mixing the surface layers due to the cooling at the surface during the heating period. This discrepancy seems to be caused by inaccuracies in the calculation of the surface heat flux and inconsistencies in the time of day at which the observed profiles were measured, as discussed below. Clay and Fruh (4, p. 42) calculated a net heat exchange on the basis of changes in the observed temperature profiles and concluded that the net heat exchange is maximum in mid-April and equal to about 1470 Btu/day-ft^2. Although this result includes the effects of advection in addition to surface heat exchange, it does make the results in Figure 10 appear questionable.

The net heat flux during the fall seems to represent too great a heat loss. This is probably caused by the evaporative heat flux, which appears to be too large during this period. According to Sundaram (22, p. 128), it has been found that the mass transfer coefficient used to calculate the evaporation is not constant, but is actually a function of wind and wave conditions. If this effect were taken into account, it should be possible to improve the calculation of the evaporative heat flux.

The predicted results of the model follow the general trend of events expected to occur within a deep reservoir. The reservoir progresses from a state of neutral equilibrium, through the warming period when the lake becomes stratified, and to the cooling period when the lake cools as the result of the convective mixing process. The cycle is completed when the lake becomes fully mixed at the end of the year.

Although the general shape of the predicted profiles is in good agreement with the observed profiles, some discrepancies do exist. The first observed profile after the beginning of the simulation on February 24 is on April 27. For this day the results are very good. The next profile, which was taken on June 19, shows good agreement except near the surface where the predicted temperature is 1.8 °C too low. This discrepancy seems to be caused by the heat flux being too low during this time of year, as discussed above.

The predicted results for July 20 are good except in the region 25 to 35 feet below the surface. This error could be caused by the assumption that the withdrawal comes only from the top 30 feet and is uniformly distributed over this elevation. If a method of selective withdrawal were used to determine the outflow velocity profile, some water would be withdrawn from the layers below the top 30 feet. Continuity would require warmer water from above to flow down to replace the water withdrawn. This would tend to warm the layers between 25 and 35 feet below the surface; hence, the predicted results would be improved.

The predicted profiles for both October 19 and February 1, show shapes which closely follow the observed temperatures; however, the predicted temperature above the thermocline is too cold. This difference may be mainly attributed to too large an evaporative heat flux, as discussed above.

Another important method of checking the accuracy of the results is to compare the predicted and observed elevations of the thermocline. In all cases the results are quite good.

When evaluating the predicted temperature profiles, it is important to realize that measured temperatures can vary considerably from one day to the next or during a single day. Thus, care must be exercised when comparing predicted and observed results. For example, consider the profile for June 19. The predicted temperature represents a daily average temperature calculated for a particular day. Measurements taken during the afternoon would show temperatures near the surface which were higher than the daily average; hence, this is a possible cause for the apparent low value of the temperature near the surface predicted on that day. This difference could also explain why the predicted profiles show the surface layers to be fully mixed during the summer and the observed profiles, which were taken during the warming period of the day, show a slight positive temperature gradient at the surface.

Another example of possible misinterpretation of results caused by comparing only one day's predicted results with the day's observed results instead of looking at more general trends is seen by examining the predicted profile for October 19. During this time of year the reservoir is cooling rapidly. Although the profile shows the results to be in error by several degrees centigrade, the error can be interpreted in another way. Comparing the observed October 19 profile with the predicted one for October 16, the agreement is seen to be very good, as shown in Figure 11. Thus, the predicted profile at this time of year indicates that the lake is cooling about three days earlier than it actually is.

Another interesting comparison can be made by comparing the results of this study with those predicted by Clay and Fruh (4, p. 57). Although the methods used in these two studies were considerably different in several aspects, the major discrepancies in results are the same in both cases.

The model which has been developed in this study requires about 20 seconds of CDC 6600 computer time to simulate eleven months of the operation of Lake LBJ using a time step of one day and an element thickness of one foot.

The comparison between the predicted and observed temperature profiles for Lake LBJ has demonstrated that the model, although still in the development process, is ready for use as a tool in water resource planning.

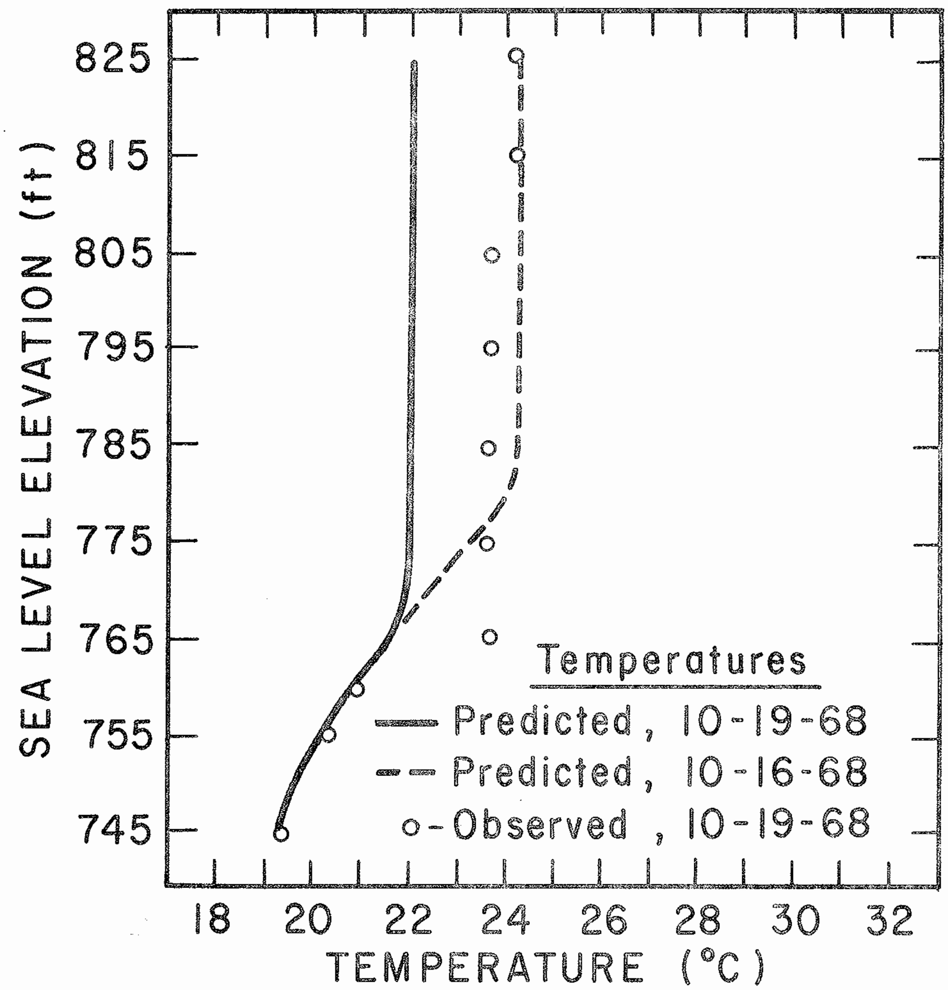

FIG. 11. PREDICTED TEMPERATURE PROFILES FOR LAKE LBJ FOR OCTOBER 16 AND OCTOBER 19, 1968

Chapter VII

Effects of a Thermal Discharge on the Temperature of Lake LBJ

In the preceeding chapter the application of the one-dimensional model for simulating the natural thermal cycle of Lake LBJ was presented. Since this model is not directly applicable to predicting the physical effects of a thermal discharge, the model has been modified to treat temperature gradients in the longitudinal direction in addition to the vertical. The results of the application of this two-dimensional model are discussed in this chapter.

Application of a One-Dimensional Model to Prediction of the Physical Effects of a Thermal Discharge

From the beginning of this study it was recognized that the method of application of the one-dimensional model to predict the effects of a thermal discharge would have to be somewhat modified to yield meaningful results. If the model for the whole of Lake LBJ were used directly, it would be necessary to assume that the thermal plume entered and instantaneously spread out over the entire surface of the reservoir. To improve the quality of the results, the simulation was performed considering the discharge cove separately from the remainder of the reservoir. (The discharge cove is considered to be the region from the discharge point to the dashed line in Figure 2).

To simplify the input requirements, a simplified geometry was used in the simulation. The validity of this assumption is discussed below. The surface area of the cove was found to be 363 acres. Instead of using the actual area versus depth relations (which are not known accurately due to recent excavation) the cove was assumed to have zero area at a depth of 40 feet, (the approximate maximum depth), with area increasing linearly from the bottom to the surface.

The simulation was performed for the discharge from the first unit of the power plant (440 MW) which is 275,000 gpm or 613 cfs at 15 °F above the intake temperature. The heated water is discharged to the reservoir as a six foot deep plume. Since the actual hydrodynamics of the discharge is difficult to specify, it was assumed that the inflow and outflow from the discharge are equally divided amoung the top six feet of the reservoir. Although this assumption may not accurately represent the physical process of the discharge, it seems to introduce little error, since the discharge cove is fairly shallow and it never becomes well stratified. Hence, the temperature varies little with depth and the specification of the hydrodynamics of the discharge is not critical, as will be shown later.

The discharge cove was simulated for one year with no thermal discharge and the annual average surface temperature was calculated as 69.5 °F. With the thermal discharge the average surface temperature was 78.4 °F. The results of the 8.9 °F temperature rise caused by the thermal discharge must be interpreted with care. Obviously, the rise in the region close to the discharge will be greater. Also, the temperature rise farther from the discharge will be less than calculated, since in the actual discharge the heat will be more concentrated than that assumed by spreading it out over the entire cove; thus, more heat will be lost directly to the atmosphere and less will go to raising the temperature of the water. The one-dimensional simulation is thus considered to be overly conservative in the far-field.

Application of a Two-Dimensional Model to Prediction of the Physical Effects of a Thermal Discharge

To more accurately describe the physical process of dissipation of heat from the thermal plume, the one-dimensional model has been modified to include temperature gradients in both the vertical and longitudinal directions. Although temperature gradients are allowed in two directions, diffusion of thermal energy is considered only in the vertical direction. It has been assumed that with a thermal discharge the main mechanism responsible for heat transport in the horizontal direction is advection and diffusion can be ignored in this direction. An approximate calculation, using a diffusion coefficient 1000 times the molecular diffusivity, showed that the rate of heat transport in the discharge cove by advection was still five orders of magnitude greater than that by diffusion; therefore, the assumption that the diffusion of thermal energy in the horizontal direction can be neglected seems to be valid.

Conceptual Representation of the Discharge Cove

The two-dimensional representation involves dividing the discharge cove into a number of subdivisions, each of which is considered as a separate system with the common boundary condition that the outflow from one segment is the inflow to the next. A sketch showing the treatment for one and two subdivisions is shown in Figure 12. In both cases the cove is divided into 40 horizontal elements of one foot thickness.

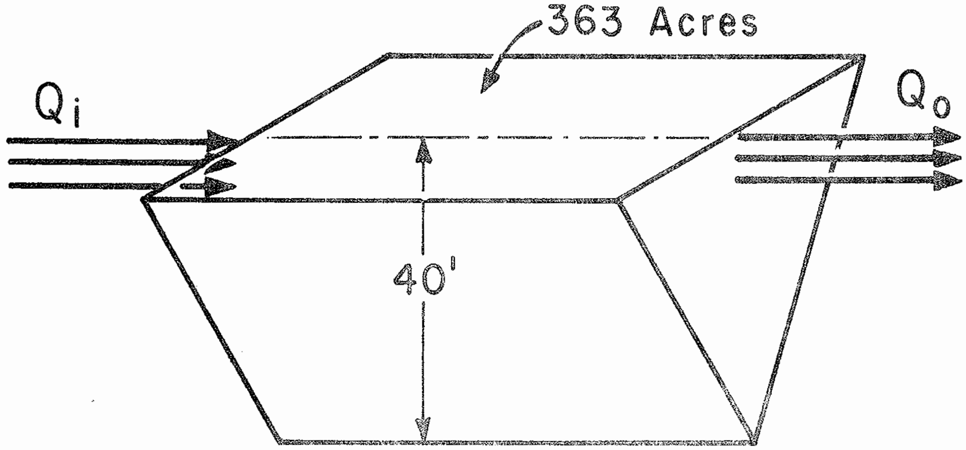

(a) One-Dimensional Simulation of the Discharge Cove

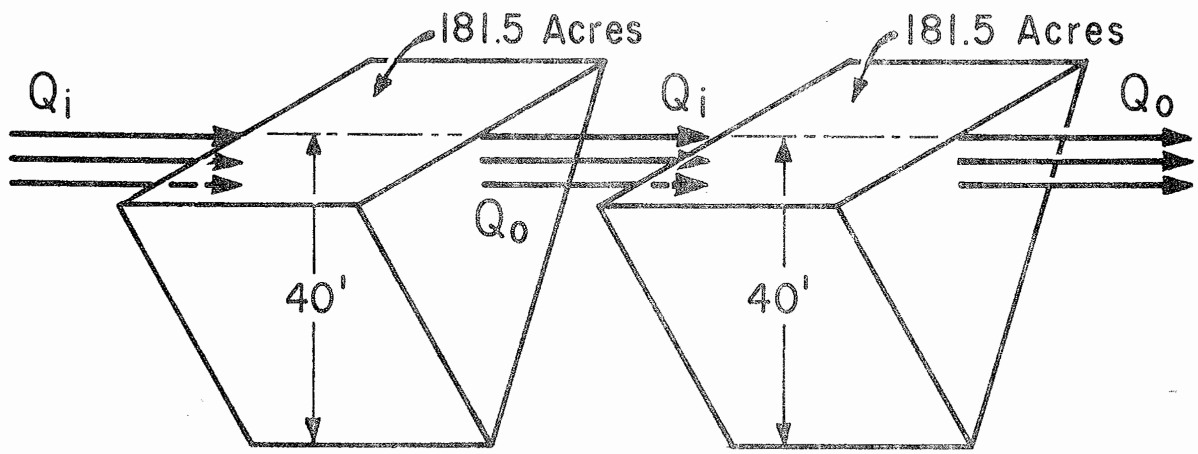

(b) Two-Dimensional Simulation of Discharge Cove with Two Subdivisions

FIG. 12. CONCEPTUAL REPRESENTATION OF THE LAKE LBJ DISCHARGE COVE

Figure 12(a) with one subdivision represents the case of the one-dimensional simulation discussed in the preceeding section. Figure 12(b) represents the case of the simplified two-dimensional model with two subdivisions. The power plant discharge is the inflow to the first subdivision and the outflow from the first subdivision is the inflow to the second. The thermal discharge is assumed to be equally divided among the top six elements of one foot thickness in all the subdivisions. No other flows are assumed to exist in the discharge cove. Thus, the inflow and outflow in each of the top six elements of each subdivision is equal to 1/6 of the cooling water flow and no other inflows, outflows, or vertical flows are present. However, the outflow temperature from an element will be less than the inflow temperature, since in each segment heat is lost to the environment and diffused downward to the cooler underlying layers.

Results of the Two-Dimensional Simulation

This procedure was repeated for the cases of four and eight subdivisions with the idea that as the number of subdivisions is increased the accuracy of the predicted temperatures should improve. Thus, for the subdivision closest to the discharge the temperature will increase as the cove is divided into more regions and should asymptotically approach a constant for a large number of subdivisions. In a similar manner, the temperature of the subdivision farthest from the discharge will decrease and approach the "true" temperature as the number of subdivisions is increased. The results of these calculations using finer and finer subdivisions are shown in Figure 13. As seen in the figure, with eight subdivisions the temperatures of the subdivisions closest to and farthest from the discharge seem to have

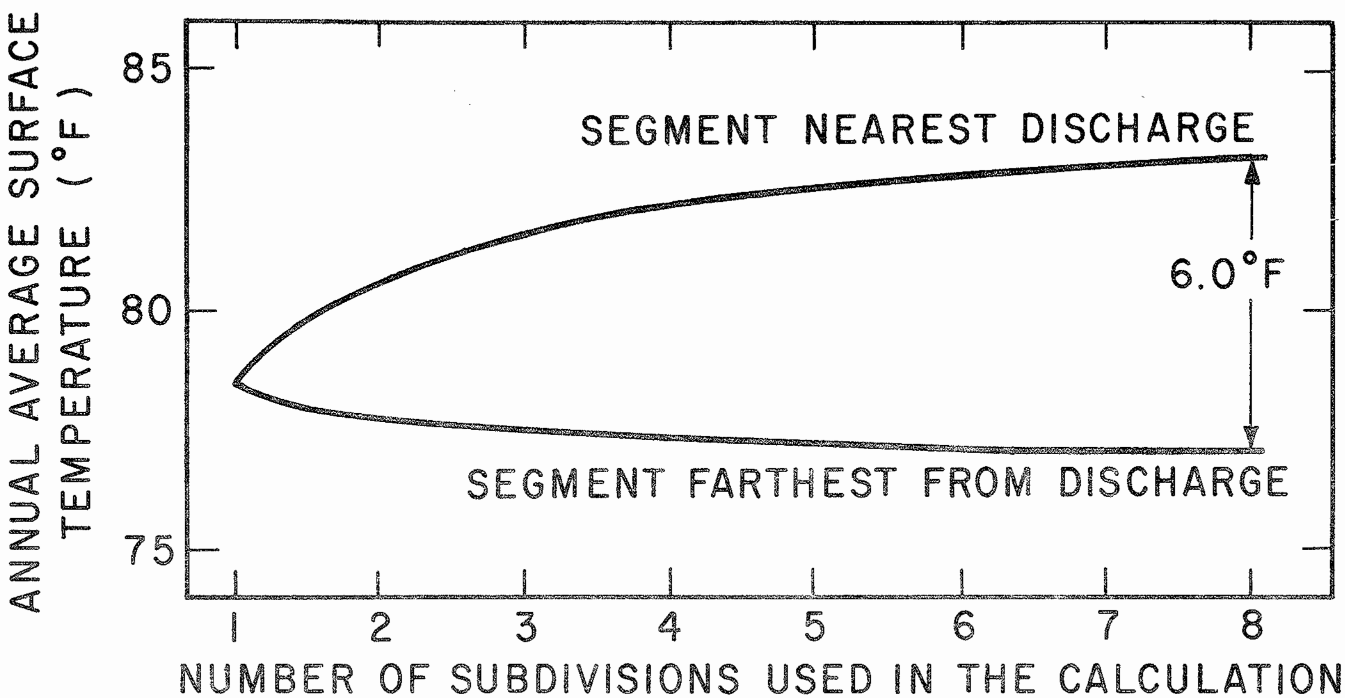

FIG. 13. TEMPERATURE OF THE DISCHARGE COVE WITH A THERMAL DISCHARGE

leveled out to constant values. From these results the annual average temperature at the end of the cove is raised 7.8 ^{o}F by the thermal discharge. This is compared with 8.9 ^{o}F calculated by the one-dimensional simulation. Thus, the use of the two-dimensional approach has changed the temperature in the expected direction.

As seen in Figure 13, the temperature difference from one end of the cove to the other is 6.0 ^{o}F. The remaining difference between the 15 ^{o}F above ambient and the ambient temperature is accounted for in the first subdivision where the average surface temperature is 1.2 ^{o}F less than the discharge temperature.

A plot of the surface temperature at the end of the discharge cove for the cases of no thermal discharge and the 613 cfs discharge at 15 ^{o}F above ambient (using eight subdivisions) is shown in Figure 14. From this figure it can be seen that the effect of the thermal discharge on the temperature is greater during the winter than during the summer. To arrive at these results it has been assumed that the power plant operates at its full load capacity of 440 MW for the entire year. In reality, during the winter the plant might be operating at reduced load or might be shut down for routine maintenance. Thus, during the actual operation of the plant the true temperature rise will be somewhat less than predicted, especially during the winter. It is important to realize that this smaller temperature rise is not necessarily a better situation from an ecological point of view, since the temperature cycling inherent in the operation of a power plant might be biologically more harmful than a constant, higher temperature.

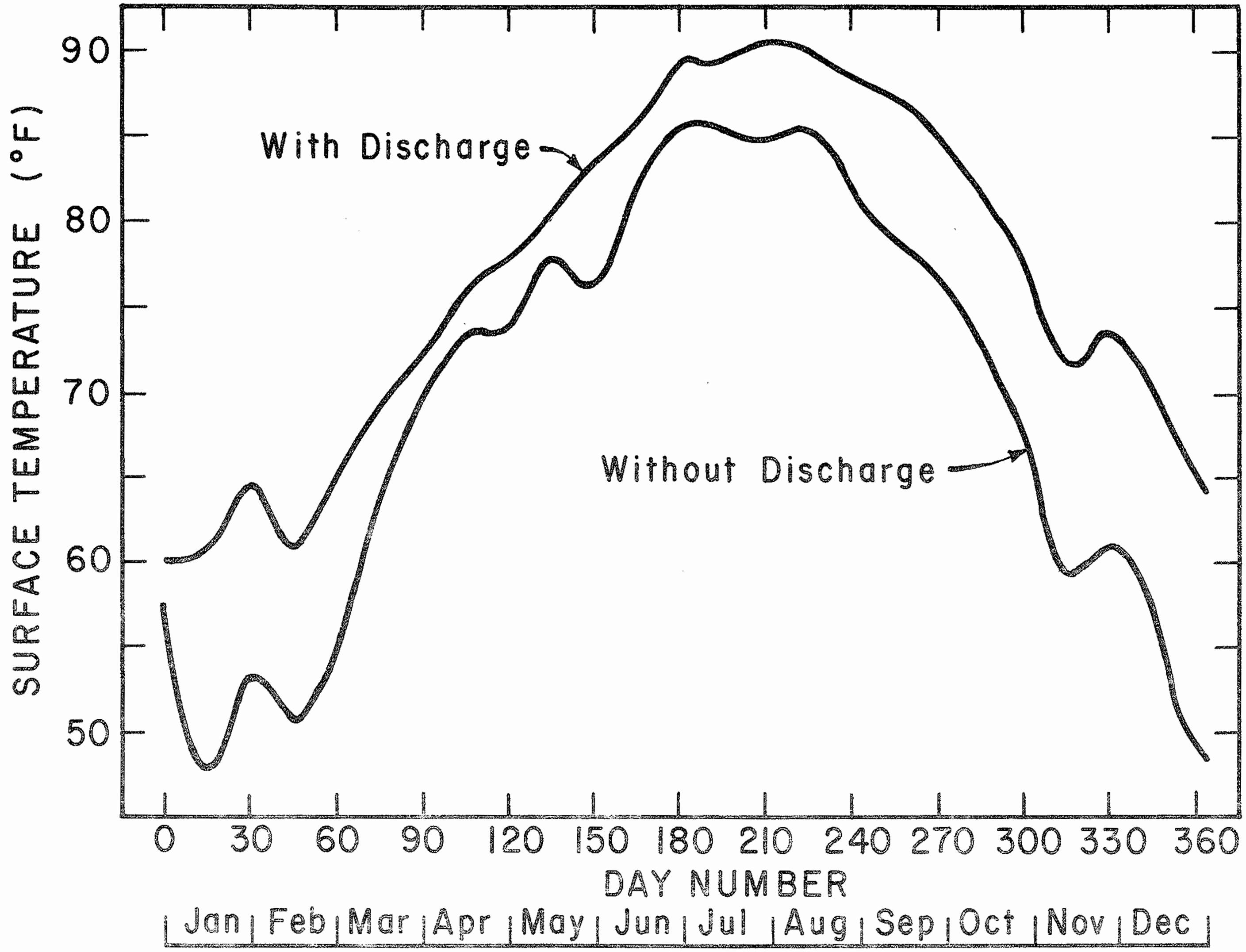

FIG. 14. SURFACE TEMPERATURE OF THE END OF THE DISCHARGE COVE WITH AND WITHOUT A THERMAL DISCHARGE

Evaluation of the Results

In Figure 14 it is also interesting to examine the day to day variations of the surface temperature in the cove with no thermal discharge. These variations re-emphasize the necessity of looking at overall trends when evaluating the results of the model, as discussed in Chapter VI.

The hydrodynamics of the thermal discharge is rather difficult to specify. Since the discharge is in the form of a fairly thick jet (six feet), it is not obvious whether the lower part of the plume will rise and become thinner because of its buoyancy or whether the plume will thicken as it cools when heat is lost to the atmosphere and cooler water is entrained in the plume. Thus, to get a first approximation of the physical effects of the heated discharge, the simplified assumptions described above were used. The yearly average differences in temperature from the surface to the bottom of each subdivision of the cove for the case of eight subdivisions with a thermal discharge and the case of no discharge are shown in Table 4. From these figures it is evident that the cove remains fairly well mixed with or without the thermal discharge. Thus, the assumed hydrodynamics does not seem to be particularly important, since all the water at a given distance from the discharge is at approximately the same temperature. It is interesting to note from the figures in Table 4 that the cove is more fully mixed with the discharge than without. This is the result of the higher surface temperature, which causes the surface to cool at all times of the year and promotes mixing as a result of the convective cooling process. The turbulence induced by jet mixing in the plume may be expected to reduce stratification even further.

Table 4

Temperature Stratification for the Discharge Cove of Lake LBJ with a Thermal Discharge

Segment Number (Segment 1 is Closest to the Discharge)	Difference in Temperature From Top to Bottom (^{o}F)
No Discharge	1.27
1	0.98
2	0.87
3	0.78
4	0.71
5	0.71
6	0.69
7	0.67
8	0.69

Although it has not been investigated in detail, the incremental temperature rise caused by the addition of a second unit to the power plant will not be as great as that caused by the first, since when another unit is added the increase in temperature will cause a greater percentage of the heat to be lost directly to the atmosphere. In two computer runs with the discharge cove divided into four subdivisions, keeping the discharge temperature constant and increasing the flow rate from 440 cfs to 613 cfs only raised the temperature at the end of the cove from 75.9° F to 77.5 °F. This represents a 23.3% increase in the temperature increase above ambient for a 28.3% increase in the discharge rate.

In this analysis the geometry of the discharge cove was assumed to be such that the cross sectional area was constant from the discharge point to the end of the cove. This meant that the depth near the discharge was assumed to be greater than it actually is. This results in too high a predicted temperature, since with shallower water in the actual case the heat will be more concentrated near the surface and more heat will be lost directly to the atmosphere instead of going to raise the temperature of the water farther from the discharge.

Another assumption which could be improved is that of the ambient lake temperature. The simulation was performed using meteorological data from a simulation of Lake Travis for 1967. Since Lake Travis and Lake LBJ have about the same temperature, the measured temperatures for Lake Travis at a 25 foot depth were used as the ambient Lake LBJ temperature. The yearly average of this temperature was the same as the surface temperature of the discharge cove with no thermal discharge.

Since the cooling water intake comes from the top 25 feet, the actual intake temperature will be less than what was assumed. Thus, using a more accurate ambient temperature will tend to lower the predicted temperatures in the discharge cove.

In evaluating the results of the simulation of the discharge cove, it is important to consider the effects of wind direction on the thermal plume. If the wind is blowing into the cove the temperature at the end of the cove will tend to be lower as the plume is retained in the cove for a longer time; however, if the wind is blowing out from the cove the temperature in the main body of water will tend to be greater. These changes do not account for differences in the evaporation rate caused by changes in the humidity which result from changes in the wind direction.

Computation time requirements for the two-dimensional simulation are longer than those of the one-dimensional model. The case of four subdivisions using a time interval of one day required about 30 seconds of CDC 6600 computation time. For eight subdivisions it was not possible to use a time step of one day without incurring numerical instabilities caused by large flow through small elements. To eliminate instabilities a time interval of six hours was used, requiring about four and a half minutes of computer time. To reduce the computer time requirements it may be possible to use a more advanced numerical solution technique which would allow the use of longer time steps.

Despite several difficulties, namely the large computation time requirements, errors caused by the assumed geometry, and the inaccuracy of the ambient lake temperature, the method of treating a thermal discharge outlined in this chapter seems to be quite useful as a starting point for predicting the effects of the cooling water discharges from a power plant on a stratified reservoir.

Chapter VIII

Conclusions

The development and use of the mathematical model to simulate the natural thermal cycle of Lake LBJ and predict the physical effects of a thermal discharge on a portion of the lake have produced a number of observations and conclusions which are summarized below.

1. From an evaluation of the state-of-the-art of one-dimensional temperature modeling of reservoirs, it was concluded that the model to simulate the natural thermal cycle of Lake LBJ should have the following characteristics:

    a. It is discretized into elements of equal thickness, extending over the entire length and width of the reservoir.

    b. It treats heat exchange at the surface due to solar radiation, atmospheric radiation, back radiation, evaporation, and convection. Each of these terms is calculated from meteorological data and the water surface temperature.

    c. It treats advection into and out of the reservoir in the horizontal direction.

    d. It treats advection and diffusion of thermal energy along the vertical axis within the reservoir.

2. The predicted results of the model have been compared with observed temperatures. Considering the complex nature of the problem of predicting the distribution of thermal energy in a deep reservoir, the model appears to give a reasonably accurate description of the annual thermal cycle of Lake LBJ. This result was not obvious at the beginning

of the investigation, since the type of model used strictly applies only to reservoirs with a small discharge-volume ratio, and models of this type had not previously been applied to lakes with as large a discharge-volume ratio as Lake LBJ's.

3. The importance of looking at overall trends when evaluating the results of the model, instead of simply comparing the observations with the predictions for a particular day, should be considered.

4. The predicted temperature profiles are very sensitive to the value of the thermal diffusion coefficient in the hypolimnion; however, the value used in the epilimnion has no significant effect on the predicted profiles. Thus, although the heat flux is relatively small in the hypolimnion, the volume of water is also small, therefore, the predicted temperature is very sensitive to the value of the diffusivity.

5. The effect of inflows and outflows on the distribution of thermal energy in Lake LBJ is not as great as might be expected, considering the fact that the average flow through time for the period of the simulation was only 35 days.

6. Due to the large inflows and outflows for Lake LBJ, it is not possible to calculate the diffusion coefficient using the method described in Chapter III.

7. When adjusting the mass transfer coefficient for the evaporative heat loss, it is important to keep in mind the coupling of the surface heat exchange and the surface temperature. Thus, if the coefficient were decreased the evaporative heat loss would be less and the surface temperature would rise. This would tend to increase the surface heat losses by convection and radiation which would lower the

temperature. Thus, the effect of reducing the evaporative heat loss would not be as great as would be expected if it were not coupled to other heat loss mechanisms.

8. For the treatment of the effects of a thermal discharge, the model has been segmented into several subdivisions in the longitudinal direction in addition to the vertical segmentation. Although this method, which is discussed in Chapter VII, has limitations, it is a good starting point for more refined analyses of the physical effects of thermal discharges from power plants on stratified reservoirs.

Chapter IX

Recommendation for Future Work

The model developed in this study has been applied to Lake LBJ with good results. It should be possible to improve the predictive ability of the model by incorporating several refinements discussed in this chapter. These refinements include more accurate input data and improvements to the mathematical description of the reservoir.

Field Research

A detailed program of field studies is needed to improve the input data to the model and to establish which aspects of the model need improvement. The data requirements are discussed below:

1. One of the most questionable pieces of input data is the coefficient of absorption of solar radiation. The value used in this study was based on the average of two measurements taken at Lake Buchanan. Since the coefficient varies with location and season, data should be obtained to determine the seasonal variation of the coefficient for Lake LBJ.

2. Other input data which could be improved are the inflow temperature data. More frequent measurements than were available for this study are needed for the temperature from Lake Inks and the Llano River. Sandy Creek makes only a minor contribution to the total inflow, so the assumption that it is at the same temperature as the Llano River should cause little error. However, a few measurements should be

taken to compare the two temperatures and possibly correct the temperature of Sandy Creek. Even with more measurements, the accuracy of the temperatures of the Llano River and Sandy Creek still remain questionable, since during periods of very high flows (during heavy rains) the temperature will generally be less than expected for the particular time of year.

3. More temperature data are needed for checking the results of computer simulation. Temperature profiles at monthly or more frequent intervals are needed. Outflow temperatures are also needed for checking the predicted values.

4. Sampling of the discharge temperature and other water quality parameters, together with profiles of these quantities in the deep pool, are needed to determine the accuracy of the simple assumption regarding the outflow velocity profile.

Profiles of temperature and other water quality parameters should also be used in an attempt to infer the hydrodynamics of the inflow from Lake Inks and from the Llano River. This data will either confirm the validity of the simple assumption regarding inflows or indicate possible improvements.

5. Temperature profiles should be taken along the entire length of the lake and also across the lake at several points to evaluate the need for extending the scope of the model to include temperature gradients in two or three dimensions. In addition, water quality profiles at various points in the lake will be helpful in defining the hydrodynamics of the reservoir. If a two or three-dimensional model is developed, the possibility of measuring velocity profiles at various points in the lake should be examined.

6. To improve the calculation of the evaporative heat flux, the wind velocity should be measured at Lake LBJ, instead of using data measured at Austin.

Refinements to the Mathematical Model

Several areas which might be improved in the mathematical model are discussed below:

1. The main factor limiting the accuracy of the model results appears to be the calculation of the energy budget terms. As described in Chapter VI, the net heat flux indicates that too little heat is being transferred through the air-water interface. The evaporative heat flux, which seems to be too large in the fall, could be reduced by employing a variable mass transfer coefficient in the calculation of evaporation, instead of one that is constant for the entire year.

2. An improved method should be incorporated for considering distributed inflows and outflows. Clay and Fruh (4) have evaluated several methods for calculating the selective withdrawal from a stratified reservoir. Methods for treating inflows are not as well established; however, Huber and Harleman (10) have presented a method which should be more realistic than that used in the present study.

If the outflow is determined by a selective withdrawal method, the shape of the velocity profile will be dependent upon the outflow rate. Since the hydro-electric power production is on a peaking schedule, the use of daily averages of the outflow rate would lead to inaccuracies in the prediction of the outflow velocity profile. Thus, it may be necessary to consider outflows on a shorter time period than one day.

3. In Lake LBJ, with large inflows and outflows, departures from a one-dimensional model can be expected. A refined two-dimensional model, in which longitudinal temperature gradients are taken into account, is needed to improve the predictive capability of the model. Except for the treatment of the inflows and outflow, impoundment hydrodynamics is ignored. To extend the model to a two-dimensional one, further refinement of the impoundment hydraulics will be necessary.

4. The model assumes that temperature is the only factor which influences the density of water. Since the density also depends upon suspended sediments and dissolved solids, incorporation of these effects would improve the prediction of the layer at which an inflow enters the reservoir.

5. It should be possible to improve the practical usefulness of the model through the use of sensitivity analysis. This process involves studying the effects of changing individual parameters or input data to determine the relative importance of various assumptions and to evaluate the influence of quality of the data on the predicted results. Three areas which should be examined to reduce input data requirements and computation time are the determination of the maximum time interval, the maximum element thickness, and the number of days over which input data can be averaged without adversely affecting the model predictions.

6. The simplified two-dimensional model described in Chapter VII could be easily refined to improve its ability to describe the physical effects of a thermal discharge on a stratified reservoir. These modifications include use of a better assumption of the hydrodynamics of the discharge, a more realistic geometry of the cove, and a more accurate

ambient lake temperature. To reduce the computation time required for the simulation, it may be possible to use a more advanced numerical solution technique, which would allow the use of a longer time step without introducing numerical instabilities.

After these refinements have been made, the effect of additional generating units on the temperature of the cove should be investigated.

7. To extend the value of the model as a tool for water quality management, its scope should be extended to include important water quality parameters, such as dissolved oxygen and nutrients.

APPENDIX A

THE COMPUTER PROGRAM

In this appendix the FORTRAN computer program used to determine the distribution of thermal energy in a deep reservoir is presented. A flow diagram of the main program is followed by a listing of the program. The program consists of the main program (PROGRAM TEMP) and three subroutines. SUBROUTINE HEAT calculates the external heat budget terms, SUBROUTINE DIFF calculates the diffusion coefficient at each elevation in the reservoir, and SUBROUTINE SOLVE solves the matrix equation for the temperature of each element in the reservoir.

An eleven month simulation of Lake LBJ, using 83 elements and a time step of one day, required about 20 seconds of CDC 6600 computer time.

A variable dictionary for the computer program is presented in Appendix B, and a description of the input data is presented in Appendix C. In Appendix D the input data used in the simulation of Lake LBJ for 1968 is given. A sample of the output of this simulation is shown in Appendix E.

Flow Diagram

PROGRAM TEMP

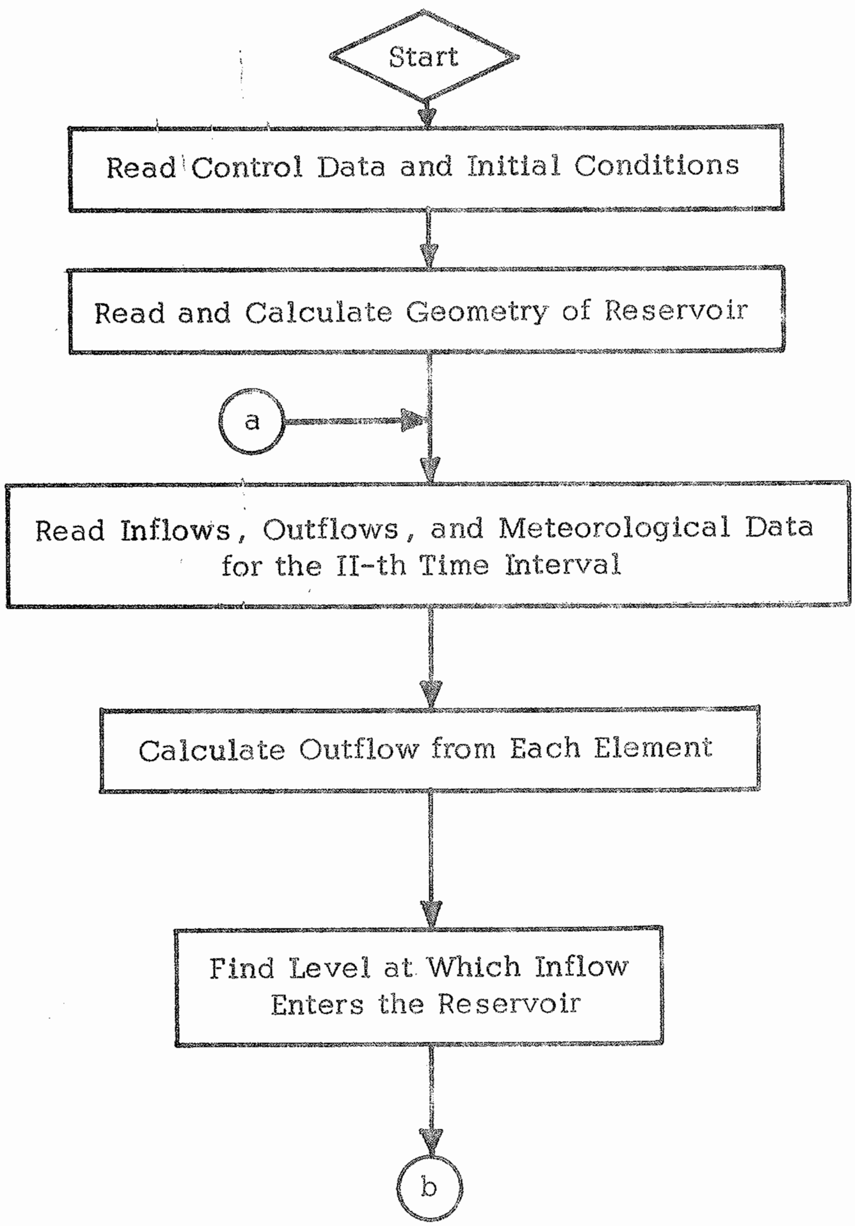

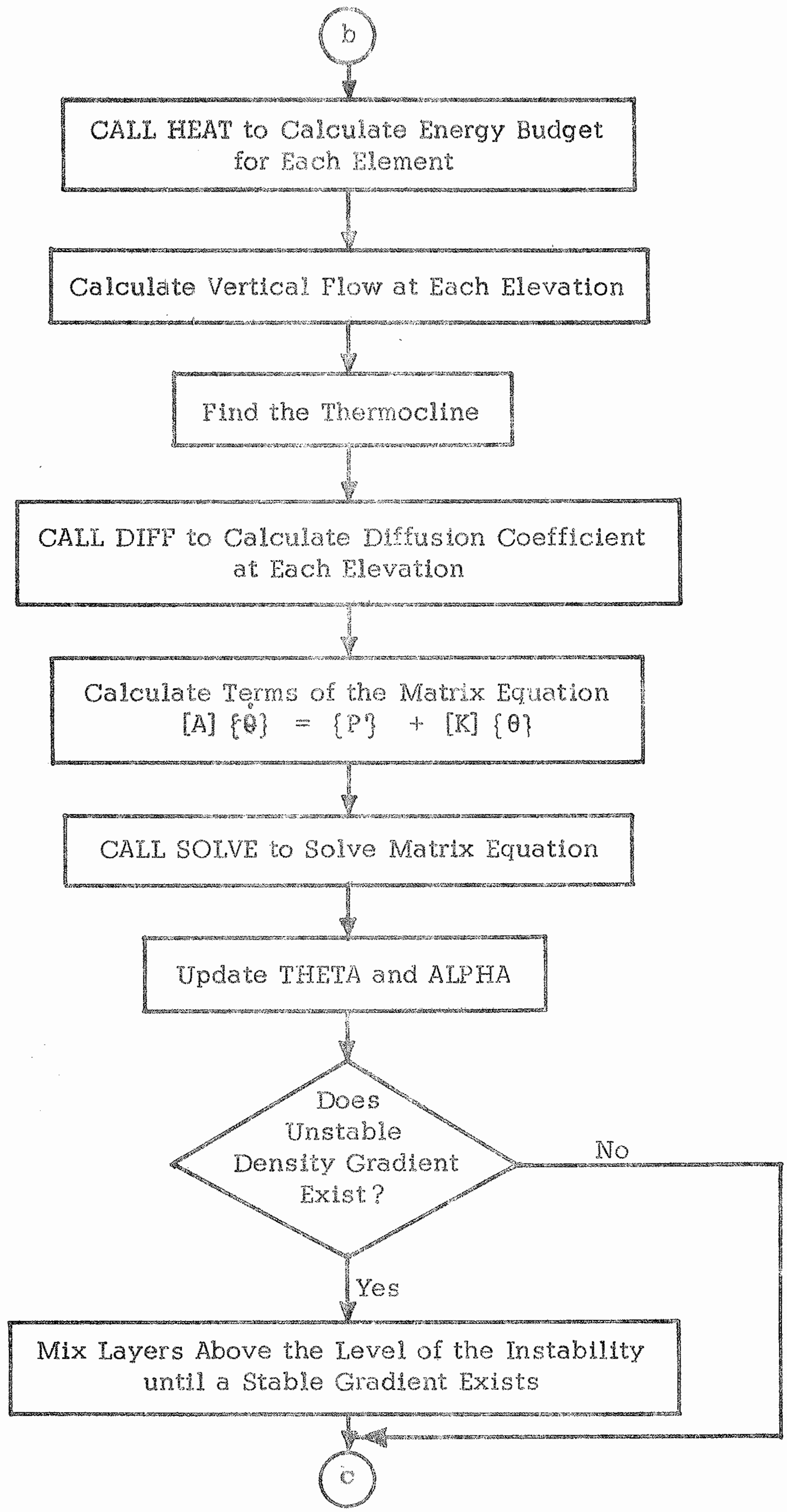
b
CALL HEAT to Calculate Energy Budget for Each Element
Calculate Vertical Flow at Each Elevation
Find the Thermocline
CALL DIFF to Calculate Diffusion Coefficient at Each Elevation
Calculate Terms of the Matrix Equation
[A] {θ̇} = {P} + [K] {θ}
CALL SOLVE to Solve Matrix Equation
Update THETA and ALPHA
Does Unstable Density Gradient Exist?
No
Yes
Mix Layers Above the Level of the Instability until a Stable Gradient Exists
c

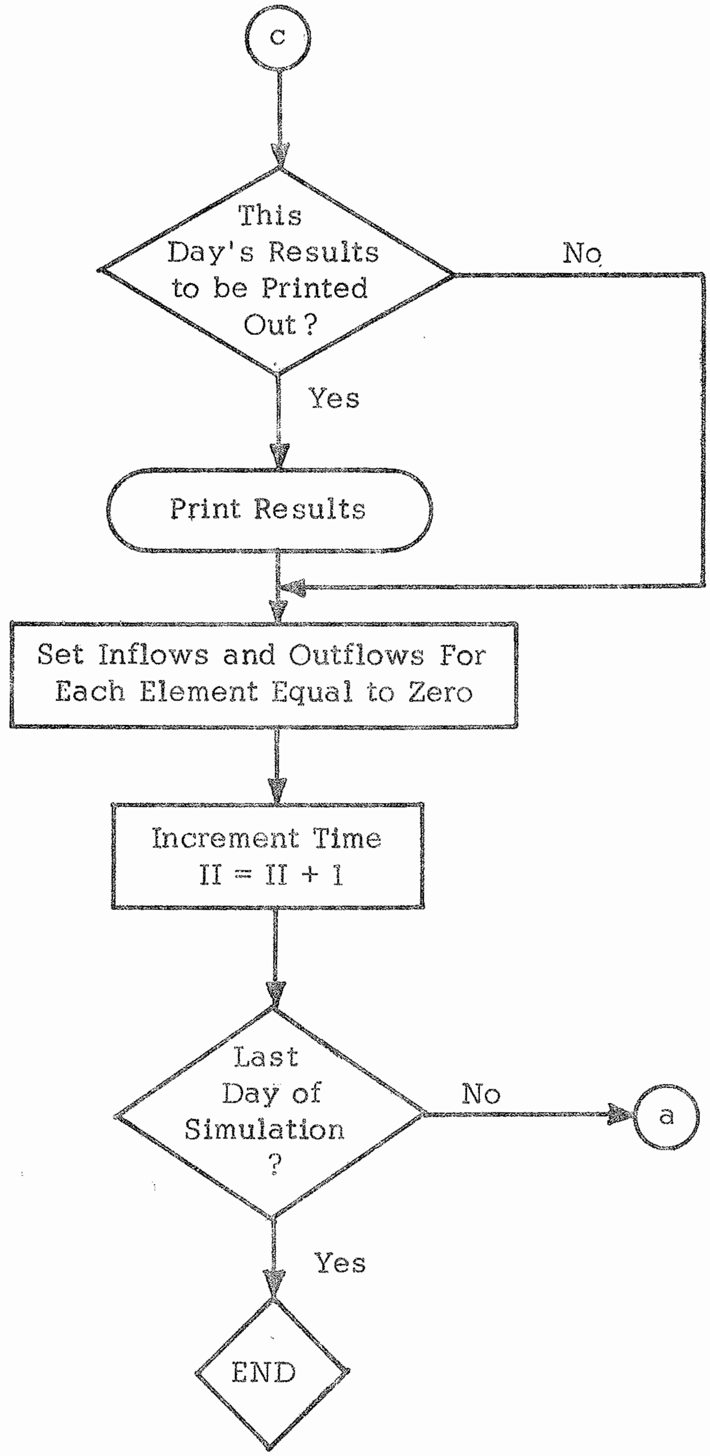
c
This Day's Results to be Printed Out ?
No
Yes
Print Results
Set Inflows and Outflows For Each Element Equal to Zero
Increment Time
II = II + 1
Last Day of Simulation ?
No
a
Yes
END

```
      PROGRAM TEMP (INPUT,OUTPUT)
      COMMON NMONTH,DT
      COMMON THETA(200),QO(200),QI(200),QV(200),THETAQI(200)
      COMMON QII(4),THETQII(4)
      COMMON ALPHA(200),PPRIME(200),S(200,3),F(200),XK(200,3)
      COMMON HPRIME(200),D(200),THETDOT(200)
      COMMON VOL(200),SURF(201),Z(200),VOLUME(200),AREA(200)
      COMMON SOLDAY,PATM,THETADB,THETAWB,W,CLOUD
      COMMON BETA,ETA,AMAX,AMIN
      COMMON ZTHERM,DEPTH,II,DELZ,ZTOP,NEL
      COMMON VOLEVAP,DELVOL,VOLTOP,VOLDIFF,SURFTOP
      COMMON HSDAY(400),HADAY(400),HBDAY(400),HEDAY(400)
      COMMON HCDAY(400),HNDAY(400)
      DIMENSION LINE(100),THETAC(200)
      DIMENSION DP(10,400),TOBS(10,400)
      DIMENSION CLOUD1(20),WIND(20)
      DIMENSION RHO(200)
      DIMENSION TINFLOW(20),VV(201),TQ(200),QSPINKS(20),QSPLBJ(20)
      DIMENSION AAA(400),BBB(400),CCC(400),DDD(400),EE1(400)
      DIMENSION NDAYOBS(400),NPR(400)
      DIMENSION THETA1(10,100),ALPHA1(10,100),THDOT1(10,100)
      DIMENSION THSURF1(10,400),THBOT1(10,400),TAVE1(10)
      DIMENSION HEAT1(10,400),HT(10),TAVE2(10),TDIFF1(10)
      DIMENSION X1(200),X2(200),X3(200),T2(200),T1(200),T2MT1(200)
      DIMENSION DTHDZ(200)
      REAL LINE
      DATA BLANK,DOT,PLUS,STAR,EQ /1H ,1H.,1H+,1H*,1H=/
    2 FORMAT (1H1)
    4 FORMAT (//)
      NOLD=1
      NWKOLD=0
      C=1.0
C
C     READ CONTROL DATA AND INITIAL CONDITIONS
C
      READ 5,KLAKE,NPRINT,NOBS,KPRINT1,KPRINT2,KPRINT3,KPRINT4,KDIFF
    5 FORMAT (I2,2I4,5I2)
      IF (KDIFF. EQ. 0) GO TO 7
      READ 6,IMIN,IMAX
```

```
 6 FORMAT (2I5)
 7 CONTINUE
   READ 8,NEL,NELMAX,NDAY1,NDAY2,KDT,NINFLOW,NDAYAVE
 8 FORMAT (7I5)
   NDAY=NDAY2-NDAY1
   NELM1=NEL-1
   NELP1=NEL+1
   DT=KDT*24.0
   DO 9 I=1,NPRINT
 9 NDAYOBS(I)=0.0
   READ 10,(NPR(I),I=1,NPRINT)
10 FORMAT (20I4)
   DO 11 I=1,400
   DO 11 JZ=1,10
   DP(JZ,I)=0.0
11 TOBS(JZ,I)=0.0
   IF (NOBS. EQ. 0) GO TO 17
   READ 10,(NDAYOBS(I),I=1,NOBS)
   DO 13 I=1,NOBS
   K=NDAYOBS(I)
   READ 12,(DP(J,K),J=1,10)
12 FORMAT (10F5.0)
13 CONTINUE
   DO 16 I=1,NOBS
   K=NDAYOBS(I)
   READ 14,(TOBS(J,K),J=1,10)
14 FORMAT (10F5.0)
   IF (KLAKE. EQ. 2. OR. KLAKE. EQ.4) GO TO 16
   DO 15 J=1,10
15 TOBS(J,K)=TOBS(J,K)*1.8+32.0
16 CONTINUE
17 CONTINUE
   IF (KLAKE. EQ. 2. OR. KLAKE. EQ. 4) GO TO 18
   GO TO 20
18 CONTINUE
   READ 19,(WIND(I),I=1,12)
   READ 19,(CLOUD1(I),I=1,12)
19 FORMAT (12F5.0)
   WIND(13)=WIND(12)
```

```
      CLOUD1(13)=CLOUD1(12)
   20 CONTINUE
      IF (KLAKE. NE. 2) GO TO 22
      READ 21,(TINFLOW(I),I=1,12)
   21 FORMAT (12F5.0)
      TINFLOW(13)=TINFLOW(12)
   22 CONTINUE
      READ 23,KREAD
   23 FORMAT (I2)
      IF (KREAD. EQ. 2) GO TO 26
      READ 24,TINIT
   24 FORMAT( F5.0)
      DO 25 J=1,NEL
   25 THETA(J)=TINIT
      GO TO 29
   26 CONTINUE
      READ 27,(THETA(J),J=1,NEL)
   27 FORMAT (13F6.0)
      DO 28 J=1,NEL
   28 THETA(J)=THETA(J)*1.8+32.0
   29 CONTINUE
      READ 31,BETA,ETA
      READ 31,ZTOP,ZBOT
   31 FORMAT (2F10.0)
      IF (KLAKE. EQ. 1. OR. KLAKE. EQ. 2) GO TO 33
      READ 32,NLAKE
   32 FORMAT (I2)
   33 CONTINUE
      IF (KLAKE. EQ. 1. OR. KLAKE. EQ. 2) NLAKE=1
C
C     PRINT INITIAL CONDITIONS
C
      PRINT 2
      PRINT 36,NEL,NDAY,KDT,NPRINT,NOBS,ZTOP
   36 FORMAT (10X* INITIAL NUMBER OF ELEMENTS IN RESERVOIR = *I3//10X* N
     1UMBER OF DAYS OF SIMULATION = *I3//10X* TIME INTERVAL = *I2* DAYS
     2*//10X* NUMBER OF DAYS PRINTED OUT = *I3//10X* NUMBER OF DAYS OF O
     3BSERVED TEMPERATURES = *I3//10X* INITIAL SURFACE ELEVATION = *F6.2
     4* FEET*)
```

```
      PRINT 4
      PRINT 37
   37 FORMAT (10X*THE NUMBERS OF THE DAYS PRINTED OUT *10X*THE NUMBERS O
     1F THE DAYS FOR WHICH OBSERVED TEMPERATURES ARE AVAILABLE*///)
      PRINT 38,((NPR(I),NDAYOBS(I)),I=1,NPRINT)
   38 FORMAT (10X,I4,50X,I4)
C
C     READ AND CALCULATE GEOMETRY OF RESERVOIR
C     VOL(J) IS VOLUME OF ELEMENT J
C     VOLUME(J) IS CUMULATIVE VOLUME INCLUDING ELEMENT J
C     SURF(J) IS SURFACE AREA AT LOWER SURFACE OF ELEMENT J
C     AREA(J) IS AVERAGE AREA OF UPPER AND LOWER SURFACES OF ELEMENT J
C     ELEMENT 1 IS AT BOTTOM OF RESERVOIR
C     Z(J) IS ELEVATION TO MIDDLE OF ELEMENT J
C
      DELZ=1.0
      NELMAXM=NELMAX-1
      Z(1)=ZBOT+DELZ/2.0
      DO 249 J=2,NELMAX
  249 Z(J)=Z(J-1)+DELZ
      DELZTOP=ZTOP-Z(NEL)+DELZ/2.0
      IF (KLAKE. NE. 1) GO TO 241
      READ 238,(VOL(J),J=1,NELMAX)
  238 FORMAT (16F5.0)
      SURF(1)=0.0
      DO 239 J=2,NELMAX
  239 SURF(J)=(VOL(J)+VOL(J-1))/(2.0*DELZ)
      DO 240 J=1,NELMAX
  240 AREA(J)=VOL(J)/DELZ
      GO TO 247
  241 CONTINUE
      IF (KLAKE. NE. 2) GO TO 243
      SURF(1)=0.0
      DO 242 J=2,NELMAX
  242 SURF(J)=2.31*EXP(0.0131*(Z(J-1)+DELZ))
      GO TO 245
  243 CONTINUE
      IF (KLAKE. EQ. 1. OR. KLAKE. EQ. 2) GO TO 1244
      SURF(1)=0.0
```

```
      DO 1242 J=2,NFLMAX
 1242 SURF(J)=363.0*J/(41.0*NLAKE)
 1244 CONTINUE
  245 CONTINUE
      DO 246 J=1,NELMAXM
      AREA(J)=(SURF(J)+SURF(J+1))/2.0
  246 VOL(J)=AREA(J)*DELZ
  247 CONTINUE
      VOLUME(1)=VOL(1)
      DO 248 J=2,NELMAXM
  248 VOLUME(J)=VOLUME(J-1)+VOL(J)
      DELZSQ=DELZ*DELZ
      VOLLAKE=VOLUME(NELM1)+VOL(NEL)*DELZTOP/DELZ
      VOLTOP=VOLLAKE-VOLUME(NELM1)
      VOLDIFF=VOLUME(NEL)-VOLLAKE
      DEPTH=ZTOP-Z(1)+DELZ/2.0
      SURFTOP=SURF(NEL)+(SURF(NELP1)-SURF(NEL))*DELZTOP/DELZ
      AREATOP=(SURFTOP+SURF(NEL))/2.0
C
C     CONVERT AREAS FROM SQ. FT. TO ACRES
C     CONVERT VOLUMES FROM CU. FT. TO ACRE-FT
C
      DO 250 J=1,NELMAXM
      AREA(J)=AREA(J)*43560.0
      VOL(J)=VOL(J)*43560.0
      VOLUME(J)=VOLUME(J)*43560.0
  250 SURF(J)=SURF(J)*43560.0
      VOLTOP=VOLTOP*43560.0
      AREATOP=AREATOP*43560.0
      VOLDIFF=VOLDIFF*43560.0
      VOLLAKE=VOLLAKE*43560.0
      SURFTOP=SURFTOP*43560.0
C
C     INITIALIZE VARIABLES
C
      DO 251 J=1,NELMAX
      RHO(J)=62.4
      ALPHA(J)=0.0
      THETDOT(J)=0.0
```

```
      THETAQI(J)=0.0
      TQ(J)=0.0
      QV(J)=0.0
      QQ(J)=0.0
      QI(J)=0.0
      X1(J)=0.0
      X2(J)=0.0
      X3(J)=0.0
      DTHDZ(J)=0.0
  251 CONTINUE
      VOLEVAP=0.0
C
C     INITIALIZE ALPHA
C
      DO 253 J=1,NEL
  253 ALPHA(J)=THETA(J)
      IF (KLAKE. EQ. 1. OR. KLAKE. EQ. 2) GO TO 256
C
C     SET INITIAL TEMPERATURES FOR 2-D SIMULATION
C
      DO 255 I=1,NLAKE
      DO 255 J=1,NEL
      THETA1(I,J)=THETA(J)
      THDOT1(I,J)=THETDOT(J)
      ALPHA1(I,J)=ALPHA(J)
  255 CONTINUE
      TAMB=THETA(NEL)
  256 CONTINUE
C
C     CALCULATE OUTFLOW WHICH GOES OVER THE LBJ AND INKS SPILLWAYS
C
      DO 257 I=1,20
      QSPINKS(I)=0.0
  257 QSPLBJ(I)=0.0
      IF (KLAKE. NE. 1) GO TO 258
C
C     CONVERT VOLUMES OF SPILL FROM ACRE FT/MONTH TO ACRE FT/DAY
C
      QSPLBJ(3)=62478.0/31.0
```

```
      QSPLBJ(5)=132026.0/31.0
      QSPINKS(3)=77889.0/31.0
      QSPINKS(4)=13754.0/30.0
      QSPINKS(5)=145177.0/31.0
  258 CONTINUE
C
C
C     BEGIN COMPUTATION FOR EACH TIME PERIOD
C
C
      DO 999 II=NDAY1,NDAY2,KDT
C
C     DETERMINE AMBIENT TEMPERATURE FOR 2-D SIMULATION
C
      IF (TOBS(3,II). LT. 5.0) GO TO 1627
      TAMP=TOBS(3,II)
 1627 CONTINUE
      NELP1=NEL+1
      NELM1=NEL-1
      NWK=(II-NDAY1)/NDAYAVE+1
      IF (KLAKE. EQ. 1. OR. KLAKE. EQ. 3) GO TO 320
C
C     READ AND AVERAGE DAILY VALUES OF LAKE TRAVIS DATA
C
      IF (NWK. EQ. NWKOLD) GO TO 313
      EEE=0.0
      FFF=0.0
      GGG=0.0
      HHH=0.0
      DO 312 I=1,NDAYAVE
  308 READ 309,I1,ZSURF,QII(1),QTRAVIS,TOBSD,SOLDAY,PATM,THETADB,THETAMP
     1,A1,A2
  309 FORMAT (I4,11X,F7.2,F7.1,5X,F7.1,F5.1,F7.1,F7.1,F5.1,F5.1,2F5.0)
      IF (I1. GT. 0) GO TO 311
      AMAX=A1
      AMIN=A2
      PRINT 2
      PRINT 310,II,AMAX,AMIN
  310 FORMAT ( 10X,*STARTING WITH DAY NUMBER *I3* THE MAXIMUM VALUE OF T
```

```
     1THE DIFFUSION COEFFICIENT IS*/15X, F9.3* AND THE MINIMUM VALUE IS *
     IF9.3* FT-FT/HR*)
      GO TO 308
  311 CONTINUE
      K=II+I-1
      AAA(K)=ZSURF
      BBB(K)=QII(1)
      CCC(K)=QTRAVIS
      DDD(K)=TOBSO
      EEE=EEE+SOLDAY
      FFF=FFF+PATM
      GGG=GGG+THETADB
      HHH=HHH+THETAWB
  312 CONTINUE
  313 CONTINUE
      ZSURF=AAA(II)
      QII(1)=BBB(II)
      QTRAVIS=CCC(II)
      TOBSO=DDD(II)
      SOLDAY=EEE/NDAYAVE
      PATM=FFF/NDAYAVE
      THETADB=GGG/NDAYAVE
      THETAWB=HHH/NDAYAVE
      PRECIP=0.
      QIN=QII(1)
      QOUT=QTRAVIS
      NMONTH=(II-1)/30+1
      W=WIND(NMONTH)
      CLOUD=CLOUD1(NMONTH)
      IF (KLAKE. EQ. 4) GO TO 333
      TINF=TINFLOW(NMONTH)
      TINC=(TINF-32.0)/1.8
      QII(1)=QII(1)*3600.0
      THETQII(1)=TINC
C
C     CALCULATE OUTFLOW FROM EACH ELEMENT FOR LAKE TRAVIS
C
      DO 315 J=50,65
  315 QQ(J)=QOUT*3600.0/16.0
```

```
  316 CONTINUE
      GO TO 333
  320 CONTINUE
C
C     READ AND AVERAGE DAILY VALUES OF LAKE LBJ DATA
C
      NWK=(II-NDAY1)/NDAYAVE+1
      IF (NWK. EQ. NWKOLD) GO TO 331
      FFF=0.0
      GGG=0.0
      HHH=0.0
      PPP=0.0
      QQQ=0.0
      RRR=0.0
      SSS=0.0
      DO 330 I=1,NDAYAVE
  326 READ 327,I1,NMONTH,SOLDAY,THETADB,THETAWB,PRECIP,PATM,W,CLOUD,
     1ZSURF,QLBJ,QINKS,QLLANO,QSANDY,A1,A2
  327 FORMAT (I3,I3,F5.0,F3.0,F3.0,F5.2,F6.2,F5.1,F4.1,F6.1,F5. ,F5.0,
     1F5.0,F5.0,7X,F5.0,F5.0)
      IF (I1. GT. 0) GO TO 329
      AMAX=A1
      AMIN=A2
      PRINT 2
      PRINT 328,II,AMAX,AMIN
  328 FORMAT ( 10X,*STARTING WITH DAY NUMBER *I2* THE MAXIMUM VALUE OF T
     1HE DIFFUSION COEFFICIENT IS*/15X, F9.3* AND THE MINIMUM VALUE IS *
     I F9.3* FT-FT/HR*)
      GO TO 326
  329 CONTINUE
      K=II+I-1
      AAA(K)=ZSURF
      BBB(K)=QLBJ
      CCC(K)=QINKS
      DDD(K)=QLLANO
      EE1(K)=QSANDY
      FFF=FFF+SOLDAY
      GGG=GGG+THETADB
      HHH=HHH+THETAWB
```

```
      PPP=PPP+PRECIP
      QQQ=QQQ+PATM
      RRR=RRR+W
      SSS=SSS+CLOUD
  330 CONTINUE
  331 CONTINUE
      ZSURF=AAA(II)
      QLBJ=BBB(II)
      QINKS=CCC(II)
      QLLANO=DDD(II)
      QSANDY=EE1(II)
      SOLDAY=FFF/NDAYAVE
      THETADP=GGG/NDAYAVE
      THETAWB=HHH/NDAYAVE
      PRECIP=PPP/NDAYAVE
      PATM=QQQ/NDAYAVE
      W=RRR/NDAYAVE
      CLOUD=SSS/NDAYAVE
      X=II
      TINKSC=-1.7784+0.22390453*X-0.0046808107*X*X
      TLLANOC=-19.481046+ 0.57918408*X-0.0020481943*X*X+0.0000 20108759*
     1X*X*X
      TSANDYC=TLLANOC
      TINKS=TINKSC*1.8+32.0
      TLLANO=TLLANOC*1.8+32.0
      TSANDY=TSANDYC*1.8+32.0
      QII(1)=QINKS*3600.0+QSPINKS(NMONTH)*43560.0/24.0
      QII(2)=QLLANO*3600.0
      QII(3)=QSANDY*3600.0
      QII(4)=QLBJ*3600.0+VOLEVAP*43560.0/DT   +QSPLBJ(NMONTH)*43560.0/24.
     10-QII(1)-QII(2)-QII(3)
      QPRECIP=PRECIP*SURFTOP/(12.0*24.0)
      QII(4)=QII(4)-QPRECIP
      QIN=(QII(1)+QII(2)+QII(3)+QII(4))/3600.0
      QOUT=QLBJ+QSPLBJ(NMONTH)*43560.0/(24.0*3600.0)
      THETQII(1)=TINKS
      THETQII(2)=TLLANO
      THETQII(3)=TSANDY
      THETQII(4)=TLLANO
```

```
      QI(NEL)=QPRECIP
      THETAQI(NEL)=THETAWB
C
C     CALCULATE OUTFLOW FROM EACH ELEMENT FOR LAKE END
C
      IF (KLAKE. EQ. 3) GO TO 333
      DEN=NEL-J4+1
      DO 332 J=J4,NEL
  332 QO(J)=QLBJ*3600.0/DEN
  333 CONTINUE
      DO 998 NN=1,NLAKE
      IF (KLAKE. EQ. 1. OR. KLAKE. EQ. 2) GO TO 341
C
C     DEFINE TEMPERATURE FOR THE NN-TH ELEMENT FOR A 2-D SIMULATION
C
      DELVOL=0.0
      QIN=0.0
      QOUT=0.0
      DO 340 J=1,NEL
      THETA(J)=THETA1(NN,J)
      ALPHA(J)=ALPHA1(NN,J)
      THETDOT(J) =THDOT1(NN,J)
  34  CONTINUE
  341 CONTINUE
      IF (KLAKE. EQ. 3. OR. KLAKE. EQ. 4) GO TO 1060
C
C     FIND TO WHICH ELEMENT INFLOW GOES
C
      DO 45 I=1,NINFLOW
      IF (QII(I). EQ. 0.0) GO TO 45
      DO 43 J=1,NEL
      IF (THETQII(I)-THETA(J)) 3044,3044,43
   43 CONTINUE
      J=NEL
 3044 TQ(J)=TQ(J)+QII(I)*THETQII(I)
      QI(J)=QI(J)+QII(I)
      THETAQI(J)=TQ(J)/QI(J)
   45 CONTINUE
      VOLIN=QI(J)*3600.0
```

```
      VOLOUT=QOUT*3600.0
      DELVOL=VOLIN-VOLOUT
 1060 CONTINUE
C
C     CALL HEAT TO CALCULATE ENERGY BUDGET FOR EACH ELEMENT
C
      CALL HEAT
      QO(NEL)=QO(NEL)+VOLEVAP*43560.0/DT  +QSPLBJ(NMONTH)*4356 .0/24.0
      IF (KLAKE. EQ. 1. OR. KLAKE. EQ. 2) GO TO 348
C
C     CALCULATE INFLOWS AND OUTFLOWS FOR 2-D SIMULATION
C
      NNM1=NN-1
      QCOOL=613.0
      NELIN=6
      NELOUT=6
      IF (NN. NE. 1) GO TO 344
      DO 342 J=1,NELIN
      K=NEL-J+1
      THETAQI(K)=TAMB+15.0
  342 QI(K)=QCOOL*3600.0/NELIN
      DO 343 J=1,NELOUT
      K=NEL-J+1
  343 QO(K)=QCOOL*3600.0/NELOUT
      GO TO 347
  344 CONTINUE
      DO 345 J=1,NELIN
      K=NEL-J+1
      THETAQI(K)=THETA1(NNM1,K)
  345 QI(K)=QCOOL*3600.0/NELIN
      DO 346 J=1,NELOUT
      K=NEL-J+1
  346 QO(K)=QCOOL*3600.0/NELOUT
  347 CONTINUE
  348 CONTINUE
```

```
C
C     CALCULATE VERTICAL FLOW AT EACH ELEVATION
C     A POSITIVE VALUE OF QV(J) REPRESENTS A FLOW UPWARD AT SURFACE J
C
      NCHANGE=0
      QV(1)=0.0
      VV(1)=0.0
      DO 46 J=2,NELP1
      QV(J)=QV(J-1)+QI(J-1)-QO(J-1)
   46 VV(J)=QV(J)/(SURF(J)*3600.0)
C
C     MAKE CHANGES ACCORDING TO WHETHER THE NUMBER OF ELEMENTS IN THE
C        RESERVOIR REMAINS THE SAME OR CHANGES
C
      TOP=(QI(NEL)-QO(NEL)+QV(NEL))*DT
      IF (TOP. GE. 0.0. AND. TOP. LE. VOLDIFF) GO TO 48
      IF (TOP. GT. VOLDIFF) GO TO 47
      IF (ABS(TOP). LT. VOLTOP) GO TO 48
C     SUBTRACT ONE ELEMENT
      QV(NEL)=-(QI(NEL)+VOLTOP/DT)
      NCHANGE=-1
      NELNEW=NEL-1
      QO(NELNEW)=QO(NELNEW)+QO(NEL)
      VOLTOP=VOL(NELM1)+(-QV(NEL)+QV(NELM1)-QO(NELM1)+QI(NELM1))*DT
      GO TO 49
C     ADD ONE ELEMENT
   47 CONTINUE
      QV(NELP1)=QV(NEL)+QI(NEL)-QO(NEL)-VOLDIFF/DT
      NCHANGE=+1
      NELNEW=NEL+1
      THETA(NELNEW)=THETA(NEL)
      THETDOT(NELNEW)=THETDOT(NEL)
      VOLTOP=TOP-VOLDIFF
      ALPHA(NELNEW)=ALPHA(NEL)
      HPRIME(NELNEW)=0.0
      THETA(NELNEW+1)=0.0
      QV(NELNEW+1)=0.0
      GO TO 49
   48 CONTINUE
```

```
C     NUMBER OF ELEMENTS REMAINS THE SAME
      VOLTOP=VOLTOP+TOP
      NCHANGE=0
      NELNEW=NEL
      THETA(NELNEW+1)=0.0
      QV(NELNEW+1)=0.0
   49 CONTINUE
      VOLDIFF=VOL(NELNEW)-VOLTOP
      ZTOP=Z(NELNEW)-DELZ/2.0+DELZ*VOLTOP/VOL(NELNEW)
      DELZTOP=ZTOP-Z(NELNEW)+DELZ/2.0
      SURFTOP=SURF(NELNEW)+(SURF(NELNEW+1)-SURF(NELNEW))*DELZTOP/DELZ
      AREATOP=(SURFTOP+SURF(NELNEW))/2.0
      VOLLAKE=VOLUME(NELNEW)-VOLDIFF
      DEPTH=ZTOP-Z(1)+DELZ/2.0
      IF (NCHANGE. EQ. +1) GO TO 150
      HPRIME(NEL)=HPRIME(NEL)/DELZTOP
      GO TO 151
  150 HPRIME(NEL-1)=HPRIME(NEL-1)/DELZ
  151 CONTINUE
C
C     FIND THE THERMOCLINE
C
      ZTHERM=Z(1)
      D2=0.0
      DO 52 J=2,NELM1
      D22=D2
   50 D2=THETA(J-1)-2.0*THETA(J)+THETA(J+1)
      IF (D22*D2) 51,52,52
   51 ZTHERM=Z(J-1)+DELZ*(ABS(D22)/ABS(D22-D2))
   52 CONTINUE
      NEL=NELNEW
      NELP1=NEL+1
      NELM1=NEL-1
      NELM2=NEL-2
C
C     CALL DIFF TO CALCULATE DIFFUSIVITY FOR EACH ELEVATION
```

```
C
      CALL DIFF
C
C
C     CALCULATE TERMS OF MATRICIES
C
C
C
C     CALCULATE TERMS OF PPRIME MATRIX
C
      THETA(NEL+1)=0.0
      QV(NEL+1)=0.0
      DO 60 J=1,NEL
      P=HPRIME(J)/(C*RHO(J))+(QI(J)*THETAQI(J)-QO(J)*THETA(J))/(AREA(J)*
     1DELZ)
      IF (QV(J+1). GT. 0.0) GO TO 53
      Q1=-QV(J+1)*THETA(J+1)
      GO TO 54
   53 Q1=-QV(J+1)*THETA(J)
   54 IF (QV(J). GT. 0.0) GO TO 55
      Q2=+QV(J)*THETA(J)
      GO TO 56
   55 Q2=+QV(J)*THETA(J-1)
   56 Q=(Q1+Q2)/DELZ
   60 PPRIME(J)=AREA(J)*P+Q
      J=NEL
      P=HPRIME(J)/(C*RHO(J))+(QI(J)*THETAQI(J)-QO(J)*THETA(J))/(AREATOP*
     1DELZTOP)
      PPRIME(J)=AREATOP*P+Q*DELZ/DELZTOP
C
C     CALCULATE TERMS OF K MATRIX
C
      DO 61 J=1,NELM1
      XK(J,1)=SURF(J)*D(J)/DELZSQ
      XK(J,2)=-(SURF(J+1)*D(J+1)+SURF(J)*D(J))/DELZSQ
   61 XK(J,3)=SURF(J+1)*D(J+1)/DELZSQ
      XK(NEL,1)=SURF(NEL)*D(NEL)/(DELZTOP*0.5*(DELZTOP+DELZ))
      XK(NEL,2)=-XK(NEL,1)
```

```
      XK(NEL,3)=0.0
C
C     CALCULATE TERMS OF S MATRIX
C
      DO 62 J=1,NEL
      S(J,1)=-XK(J,1)*DT/2.0
      S(J,2)=AREA(J)-XK(J,2)*DT/2.0
   62 S(J,3)=-XK(J,3)*DT/2.0
      S(NEL,2)=AREATOP-XK(NEL,2)*DT/2.0
C
C     CALCULATE TERMS OF F MATRIX
C
      DO 63 J=2,NELM1
      F(J)=PPRIME(J)
      DO 63 K=1,3
      L=J+K-2
   63 F(J)=F(J)+ALPHA(L)*XK(J,K)
      F(1)=PPRIME(1)+ALPHA(1)*XK(1,2)+ALPHA(2)*XK(1,3)
      F(NEL)=PPRIME(NEL)+ALPHA(NELM1)*XK(NEL,1)+ALPHA(NEL)*XK(NEL,2)
C
C     CALL SOLVE TO CALCULATE THETADOT FROM MATRIX EQUATION
C       AREA*THETADOT=PPRIME+K*THETA
C
      CALL SOLVE
C
C     UPDATE THETA AND ALPHA
C
      DO 70 J=1,NEL
      THETA(J)=ALPHA(J)+THETDOT(J)*DT/2.0
   70 ALPHA(J)=THETA(J)+THETDOT(J)*DT/2.0
C
C     MIX TOP LAYERS IF TEMPERATURE DISTRIBUTION IS UNSTABLE
C
      TEMP=0.0
      TMIX=THETA(NEL)*VOLTOP
      VOLMIX=VOLTOP
      DO 103 J=1,NELM1
```

```
      K=NEL+1-J
      TDIFF=THETA(K)-THETA(K-1)
  100 TMIX=TMIX+THETA(K-1)*VOL(K-1)
      VOLMIX=VOLMIX+VOL(K-1)
      IF (TDIFF. GE. 0.0) GO TO 104
      IF (ABS(TDIFF). LE. 0.1) GO TO 104
      TEMP=TMIX/VOLMIX
      M=J+1
      DO 102 L=1,M
      N=NEL+1-L
  102 THETA(N)=TEMP
  104 CONTINUE
  103 CONTINUE
      DO 105 J=1,NEL
  105 THETAC(J)=(THETA(J)-32.0)/1.8
C
C
C     PRINT RESULTS
C
C
      DO 576 I=1,NPRINT
      IF (NPR(I)-II) 576,501,576
C
C     PRINT INFLOWS AND OUTFLOWS
C
  501 CONTINUE
      IF (KPRINT1. EQ. 0) GO TO 545
      PRINT 2
      TOUTF=0.0
      IF (KLAKE. NE. 2) GO TO 521
      DO 520 J=50,65
  520 TOUTF=TOUTF+THETA(J)
      TOUTF=TOUTF/16.0
      TOUTC=(TOUTF-32.0)/1.8
  521 CONTINUE
      IF (KLAKE. NE. 1) GO TO 523
      DEN=NEL-54+1
      DO 522 J=54,NEL
  522 TOUTF=TOUTF+THETA(J)
      TOUTF=TOUTF/DEN
```

```
      TOUTC=(TOUTF-32.0)/1.8
  523 CONTINUE
      HTOT=0.0
      DO 524 J=1,NEL
  524 HTOT=HTOT+VOL(J)*THETA(J)
      HTOT=HTOT*62.4*1.0*0.000001*0.001
      VOLIN=QIN*24.0*3600.0/43560.0
      VOLOUT=QOUT*24.0*3600.0/43560.0
      NYEAR=II/366+1
      PRINT 530,II,NYEAR
  530 FORMAT (4X,*RESULTS FOR DAY NUMBER *I3* OF YEAR *I1/)
      PRINT 531,ZTOP,ZTHERM
  531 FORMAT (10X,*SURFACE ELEVATION = *F7.2* FEET*10X*THERMOCLINE ELEVA
     1TION = *F7.2* FEET*/)
      PRINT 534,HTOT
  534 FORMAT (10X*TOTAL THERMAL ENERGY = *F9.1* BILLION BTU*/)
      IF (KLAKE. NE. 1) GO TO 536
      VOLOUT=QLBJ*24.0*3600.0/43560.0
      VOLIN1=QII(1)*24.0/43560.0
      VOLIN2=QLLANO*24.0*3600.0/43560.0
      VOLIN3=QSANDY*24.0*3600.0/43560.0
      VOLIN4=QII(4)*24.0/43560.0
      PRINT  535,VOLIN1,TINKS,VOLIN2,TLLANO,VOLIN3,TSANDY,VOLIN4,THETQII
     1(4)
  535 FORMAT (10X,     *INFLOWS                        ACRE FEET     DEG F*/
     115X,*INKS RELEASE       *F9.0,10X,F4.1/
     215X,*LLANO RIVER        *F9.0,10X,F4.1/
     315X,*SANDY CREEK        *F9.0,10X,F4.1/
     415X,*MAKEUP             *F9.0,10X,F4.1/)
  536 CONTINUE
      IF (KLAKE. EQ. 1) GO TO 539
      PRINT 537,VOLIN
  537 FORMAT (10X,*INFLOW = *F5.0* ACRE FEET*/)
      IF (VOLIN. LT. 1.0) GO TO 539
      PRINT 538,TINF,TINC
  538 FORMAT (13X,*TEMPERATURE IN = *F4.1* DEG F = *F4.1* DEG C*/)
  539 PRINT 540,VOLOUT
  540 FORMAT (10X,*OUTFLOW = *F4.0* ACRE FEET*/)
      IF (VOLOUT. LT. 1.0) GO TO 543
```

```
      PRINT 541,TOUTF,TOUTC
  541 FORMAT (13X,*TEMPERATURE OUT = *F9.1* DEG F = *F9.1* DEG C*/)
      IF (KLAKE. EQ. 1) GO TO 543
      PRINT 542,TOBSO
  542 FORMAT (10X,*OBSERVED TEMPERATURE OUT = *F9.1/)
  543 PRINT 544,VOLEVAP
  544 FORMAT (10X,*EVAPORATION = *F9.0* ACRE FEET*////)
  545 CONTINUE
      IF (KPRINT2. EQ. 0) GO TO 555
C
C     PRINT ENERGY BUDGET TERMS
C
      PRINT 548
  548 FORMAT (10X,*EXTERNAL HEAT BUDGET IN BTU/FT-FT-DAY*/)
      PRINT 549,HSDAY(II)
  549 FORMAT (13X,*SOLAR RADIATION = *F7.2/)
      PRINT 550,HADAY(II)
  550 FORMAT (13X,*ATMOSPHERIC RADIATION = *F7.2/)
      PRINT 551,HBDAY(II)
  551 FORMAT (13X,*BACK RADIATION = *F7.2/)
      PRINT 552,HEDAY(II)
  552 FORMAT (13X,*EVAPORATION = *F7.2/)
      PRINT 553,HCDAY(II)
  553 FORMAT (13X,*CONVECTION = *F7.2/)
      PRINT 554,HNDAY(II)
  554 FORMAT (13X,*NET HEAT = *F9.2)
      PRINT 4
  555 CONTINUE
      IF (KPRINT3. EQ. 0) GO TO 575
C
C     PRINT TEMPERATURE PROFILE
C
      IF (KLAKE. EQ. 2) PRINT 2
      PRINT 560,II,NYEAR
  560 FORMAT (42X,*RESERVOIR PROFILES FOR DAY *I3* OF YEAR *I1//)
      PRINT 562
  562 FORMAT (11X,*ELEVA-     TEMPER-    TEMPER-    VERT       OUTFLOW
     1                TEMPERATURE (DEG F) *)
      PRINT 563
```

```
563 FORMAT (11X,*TION        ATURE      ATURE     VELOCITY   VOLUME*)
    PRINT 564
564 FORMAT (11X,*(FEET)     (DEG F)    (DEG C)    (FT/SEC)    (CU.FT./HR)
   1 40    45    50    55    60    65    70    75    80    85    90*)
    PRINT 565
565 FORMAT (11X,*-----       ---
   1 +--- +     +     +     +     *                                  *)
    JZ=1
    DO 574 KK=1,NEL,5
    K=NEL-KK+1
    DO 567 J=40,90
567 LINE(J)=BLANK
    LINE(40)=PLUS
    LINE(90)=PLUS
    J=THETA(K)+0.5
    LINE(J)=DOT
    IF (DP(JZ,II). GT. DEPTH) GO TO 571
    ZOB1=ZTOP-DP(JZ,II)+1.1*DELZ
    ZOB2=ZTOP-DP(JZ,II)-1.1*DELZ
    IF (Z(K). GT. ZOB1. OR.Z(K). LT. ZOB2) GO TO 570
    KZ=TOBS(JZ,II)+0.5
    IF (KLAKE. EQ. 2) KZ=TOBS(JZ,II)
    JZ=JZ+1
    IF (JZ. GT. 10) JZ=10
    IF (KZ. EQ. J) GO TO 569
    LINE(KZ)=STAR
    GO TO 570
569 LINE(J)=EQ
570 CONTINUE
571 CONTINUE
572 CONTINUE
    PRINT 573,Z(K),THETA(K),THETAC(K),VV(K),QO(K),(LINE(I),I=40,90),Z(
   1K)
573 FORMAT (10X,F5.1,7X,F4.1,6X,F4.1,3X,F10.7,2X,F8.0,6X,51A1,2X,F5.1)
574 CONTINUE
575 CONTINUE
576 CONTINUE
    NMO=(II-IDAY1)/30.0+1
    IF (NOLD. EQ. NMO) GO TO 589
```

```
      IF (KPRINT4. FQ. 0) GO TO 589
C
C     PRINT MONTHLY SUMMARY
C
      PRINT 2
      PRINT 580,NOLD
  580 FORMAT (* MONTHLY SUMMARY FOR MONTH NUMBER *I2)
      IIM1=II-1
      IIM30=II-30
      HNFT=0.0
      SOL=0.0
      ATM=0.0
      BACK=0.0
      EVAP=0.0
      CONV=0.0
      DO 581 I=IIM30,IIM1
      HNET=HNET+HNDAY(I)
      SOL=SOL+HSDAY(I)
      ATM=ATM+HADAY(I)
      BACK=BACK+HBDAY(I)
      EVAP=EVAP+HEDAY(I)
  581 CONV=CONV+HCDAY(I)
      HNET=HNET/30.0
      SOL=SOL/30.0
      ATM=ATM/30.0
      BACK=BACK/30.0
      EVAP=EVAP/30.0
      CONV=CONV/30.0
      PRINT 582,SOL
  582 FORMAT (13X,*SOLAR RADIATION = *F7.2/)
      PRINT 583,ATM
  583 FORMAT (13X,*ATMOSPHERIC RADIATION = *F7.2/)
      PRINT 584,BACK
  584 FORMAT (13X,*BACK RADIATION = *F7.2/)
      PRINT 585,EVAP
  585 FORMAT (13X,*EVAPORATION = *F7.2/)
      PRINT 586,CONV
  586 FORMAT (13X,*CONVECTION = *F7.2/)
      PRINT 587,HNET
```

```
  587 FORMAT (13X,*NET HEAT = *F9.2)
  589 CONTINUE
      IF (KDIFF. EQ. 0) GO TO 2020
C
C     CALCULATE DIFFUSION COEFFICIENT
C
      IF (II. LT. IMIN. OR. II. GT. IMAX) GO TO 2020
      DO 2002 J=2,NELM1
      X1(J)=X1(J)+HPRIME(J)/62.4
      X2(J)=X2(J)+QI(J)*THETAQI(J)-QO(J)*THETA(J)
      X3(J)=X3(J)+QV(J)*THETA(J)
      DTHDZ(J)=DTHDZ(J)+(THETA(J+1)-THETA(J-1))/(2.0*DELZ)
 2002 CONTINUE
      IF (II. NE. IMIN) GO TO 2004
      DO 2003 J=1,NEL
 2003 T1(J)=THETA(J)
 2004 CONTINUE
      IF (II. NE. IMAX) GO TO 2006
      DO 2005 J=1,NEL
      T2(J)=THETA(J)
 2005 T2MT1(J)=T2(J)-T1(J)
 2006 CONTINUE
      IF (II. NE. IMAX) GO TO 2020
      DEN=IMAX-IMIN+1
      D(1)=0.0
      DO 2007 J=2,NELM1
 2007 D(J)=D(J-1)+SURF(J)*DELZ*(T2MT1(J)/(DEN*24.0))-SURF(J)*DELZ*X1(J)/
     1DEN-X2(J)/DEN
      DO 2008 J=2,NELM1
 2008 D(J)=(D(J)+X3(J)/DEN)/(SURF(J)*DTHDZ(J)/DEN)
      PRINT 2
      PRINT 2009,IMIN,IMAX
 2009 FORMAT (5X*VALUES OF THE DIFFUSION COEFFICIENT FOR THE PERIOD OF D
     1AY *I3* TO DAY *I3//)
      PRINT 2010,((J,D(J)),J=2,NELM1)
 2010 FORMAT(10X,I4,5X,E12.5)
 2020 CONTINUE
      IF (KLAKE. EQ. 1. OR. KLAKE. EQ. 3) GO TO 9002
C
```

```
C      CALCULATE TEMPERATURES FOR 2-D SIMULATION
C
       DO 1618 J=1,NEL
       THETA1(NN,J)=THETA(J)
       ALPHA1(NN,J)=ALPHA(J)
       THDOT1(NN,J)=THETDOT(J)
  1618 CONTINUE
       THSURF1(NN,II)=THETA1(NN,NEL)
       THBOT1(NN,II)=THETA1(NN,1)
       HEAT1(NN,II)=0.0
       DO 1621 J=1,NEL
  1621 HEAT1(NN,II)=THETA(J)*VOL(J)+HEAT1(NN,II)
       HEAT1(NN,II)=HEAT1(NN,II)/VOLLAKE
   998 CONTINUE
       PRINT 3,II,THSURF1(1,II)
     3 FORMAT (10X,I4,5X,F9.2)
       IF (II. NE. 360) GO TO 999
       DO 927 I=1,NLAKE
       TAVE1(I)=0.0
       TAVE2(I)=0.0
       HT(I)=0.0
   927 CONTINUE
       DO 997 I=1,NLAKE
       DO 997 J=1,360
       HT(I)=HT(I)+HEAT1(I,J)
       TAVE2(I)=TAVE2(I)+THBOT1(I,J)
   997 TAVE1(I)=TAVE1(I)+THSURF1(I,J)
       DO 4817 I=1,NLAKE
       TAVE1(I)=TAVE1(I)/360.0
       TAVE2(I)=TAVE2(I)/360.0
       HT(I)=HT(I)/360.0
  4817 CONTINUE
       DO 4919 I=1,NLAKE
  4919 TDIFF1(I)=TAVE1(I)-TAVE2(I)
       PRINT 2
       PRINT 4920,NLAKE
  4920 FORMAT (5X*NUMBER OF SUBDIVISIONS = *I3)
       PRINT 4
       PRINT 992
```

```
  992 FORMAT (10X* NLAKE       T(S)           T(1)           T(AVE)         TDI
     1FF*)
      PRINT 995,((I,TAVE1(I),TAVE2(I),HT(I),TDIFF1(I)),I=1,NLAKE)
  995 FORMAT (10X,I3,5X,F9.3,5X,F9.3,5X,F9.3,5X,F9.3)
      PRINT 2
 9002 CONTINUE
C
C     SET INFLOWS EQUAL TO ZERO
C
      DO 110 K=1,NELP1
      TQ(K)=0.0
      QO(K)=0.0
  110 QI(K)=0.0
      NOLD=NMO
      NWKOLD=NWK
  999 CONTINUE
      CALL EXIT
      END
```

```
      SUBROUTINE HEAT
      COMMON NMONTH,DT
      COMMON THETA(200),QO(200),QI(200),QV(200),THETAQI(200)
      COMMON QII(4),THETQII(4)
      COMMON ALPHA(200),PPRIME(200),S(200,3),F(200),XK(200,3)
      COMMON HPRIME(200),D(200),THETDOT(200)
      COMMON VOL(200),SURF(201),Z(200),VOLUME(200),AREA(200)
      COMMON SOLDAY,PATM,THETADB,THETAWB,W,CLOUD
      COMMON BETA,ETA,AMAX,AMIN
      COMMON ZTHERM,DEPTH,II,DELZ,ZTOP,NEL
      COMMON VOLEVAP,DELVOL,VOLTOP,VOLDIFF,SURFTOP
      COMMON HSDAY(400),HADAY(400),HBDAY(400),HEDAY(400)
      COMMON HCDAY(400),HNDAY(400)
      DIMENSION PHI(200)
      NELM1=NEL-1
      NELM2=NEL-2
      C=1.0
      RHO=62.4
      THETAS=THETA(NEL)
C
C     CALCULATE THE EXTERNAL ENERGY BUDGET TERMS
C
      HL=1084.0-0.5*THETAS
      CL=1.0+0.17*CLOUD*CLOUD
      HA=0.97*1.713E-9*2.89E-06*(THETADB+460.0)**6*CL
      HB=0.97*1.713E-9*(THETAS+460.0)**4
      HS=0.94*SOLDAY/24.0
      EW=0.1001*EXP(0.03*THETAWB)-0.0837
      EA=EW-0.000367*PATM *(THETADB-THETAWB)*(1.0+(THETAWB-32. )/1571.0)
      ES=0.1001*EXP(0.03*THETAS)-0.0837
      HE=W*(ES-EA)*11.4*25.4/24.0
      HC=HE*0.26*(THETADB-THETAS)*1.0/((ES-EA)*25.4*1.0)
      HN=BETA*HS+HA-HB-HE+HC
      VOLEVAP=HE*DT*SURFTOP/(HL*62.4*43560.0)
      DELVOL=DELVOL*DT-VOLEVAP*43560.0
      NELP1=NEL+1
C
C     DISTRIBUTE THE EXTERNAL ENERGY BUDGET TERMS
C     IF AN ELEMENT IS SUBTRACTED, THE SURFACE EXCHANGE TAKES PLACE
```

```
C          WITH THE NEW SURFACE ELEMENT
C       IF AN ELEMENT IS ADDED, THE SURFACE EXCHANGE TAKES PLACE WITH
C          THE OLD SURFACE ELEMENT
C
        IF (DELVOL. GT. VOLDIFF) GO TO 30
        IF (DELVOL. GE. 0.0) GO TO 30
        IF (ABS(DELVOL). LT. VOLTOP) GO TO 30
C       SUBTRACT ONE ELEMENT
        HPRIME(NEL)=0.0
        HPRIME(NELM1)=HN
        ZN=Z(NELM2)+DELZ/2.0
        DO 11 J=1,NELM1
  11    PHI(J)=(1.0-BETA)*HS*EXP(-ETA*(ZN-Z(J)+DELZ/2.0))
        DO 12 J=1,NELM2
  12    HPRIME(J)=(PHI(J+1)*SURF(J+1)-PHI(J)*SURF(J))/(AREA(J)*DELZ)
        GO TO 40
C       NUMBER OF ELEMENTS REMAINS THE SAME
  30    HPRIME(NEL)=HN
        HPRIME(NEL+1)=0.0
        ZN=Z(NELM1)+DELZ/2.0
        DO 31 J=1,NEL
  31    PHI(J)=(1.0-BETA)*HS*EXP(-ETA*(ZN-Z(J)+DELZ/2.0))
        DO 32 J=1,NELM1
  32    HPRIME(J)=(PHI(J+1)*SURF(J+1)-PHI(J)*SURF(J))/(AREA(J)*DELZ)
  40    CONTINUE
C
C       CONVERT ENERGY BUDGET TERMS FROM VALUES PER HOUR TO VALUES PER DAY
C
        HSDAY(II)=HS*24.0
        HADAY(II)=HA*24.0
        HBDAY(II)=HB*24.0
        HEDAY(II)=HE*24.0
        HCDAY(II)=HC*24.0
        HNDAY(II)=(HS+HA-HE-HB+HC)*24.0
        RETURN
        END
```

```
      SUBROUTINE DIFF
C
C     CALCULATE DIFFUSION COEFFICIENT
C
      COMMON NMONTH,DT
      COMMON THETA(200),QO(200),QI(200),QV(200),THETAQI(200)
      COMMON QII(4),THETQII(4)
      COMMON ALPHA(200),PPRIME(200),S(200,3),F(200),XK(200,3)
      COMMON HPRIME(200),D(200),THETDOT(200)
      COMMON VOL(200),SURF(201),Z(200),VOLUME(200),AREA(200)
      COMMON SOLDAY,PATM,THETADB,THETAWB,W,CLOUD
      COMMON BETA,ETA,AMAX,AMIN
      COMMON ZTHERM,DEPTH,II,DELZ,ZTOP,NEL
      COMMON VOLEVAP,DELVOL,VOLTOP,VOLDIFF,SURFTOP
      COMMON HSDAY(400),HADAY(400),HBDAY(400),HEDAY(400)
      COMMON HCDAY(400),HNDAY(400)
C
C     ABOVE THE THERMOCLINE SET THE DIFFUSIVITY ACCORDING TO THE
C        EXPONENTIAL DECAY BETWEEN THE SURFACE AND THE THERMOCLINE
C     BELOW THE THERMOCLINE SET THE DIFFUSIVITY EQUAL TO THE VALUE AT
C        THE THERMOCLINE
C
      XLRATIO=+ALOG(AMIN/AMAX)/(ZTOP-ZTHERM)
      DO 100 J=1,NEL
      IF (Z(J)-DELZ/2.0-ZTHERM) 10,10,20
   10 D(J)=AMIN
      GO TO 100
   20 D(J)=AMAX*EXP(+XLRATIO*(ZTOP-Z(J)+DELZ/2.0))
  100 CONTINUE
      D(1)=0.0
      D(NEL+1)=0.0
      RETURN
      END
```

```
      SUBROUTINE SOLVE
C
C     CALCULATE THETADOT FROM MATRIX EQUATION
C       AREA*THETADOT=PPRIME+K*THETA
C
      COMMON NMONTH,DT
      COMMON THETA(200),QO(200),QI(200),QV(200),THETAQI(200)
      COMMON QII(4),THETQII(4)
      COMMON ALPHA(200),PPRIME(200),S(200,3),F(200),XK(200,3)
      COMMON HPRIME(200),D(200),THETDOT(200)
      COMMON VOL(200),SURF(201),Z(200),VOLUME(200),AREA(200)
      COMMON SOLDAY,PATM,THETADB,THETAWB,W,CLOUD
      COMMON BETA,ETA,AMAX,AMIN
      COMMON ZTHERM,DEPTH,II,DELZ,ZTOP,NEL
      COMMON VOLEVAP,DELVOL,VOLTOP,VOLDIFF,SURFTOP
      COMMON HSDAY(400),HADAY(400),HBDAY(400),HEDAY(400)
      COMMON HCDAY(400),HNDAY(400)
      F(1)=F(1)/S(1,2)
      S(1,3)=S(1,3)/S(1,2)
      DO 10 J=2,NEL
      X=1.0/(S(J,2)-S(J,1)*S(J-1,3))
      F(J)=(F(J)-S(J,1)*F(J-1))*X
   10 S(J,3)=S(J,3)*X
C
C     BACK SUBSTITUTE TO FIND THETADOT
C
      THETDOT(NEL)=F(NEL)
      DO 20 J=2,NEL
      K=NEL-J+1
   20 THETDOT(K)=F(K)-S(K,3)*THETDOT(K+1)
      RETURN
      END
```

APPENDIX B

VARIABLE DICTIONARY FOR THE COMPUTER PROGRAM

FORTRAN Notation	Description and Units
ALPHA(J)	j-th term of the α matrix
ALPHA1(NN,J)	j-th term of the α matrix for the NN subdivision of the two-dimensional simulation
AMAX	diffusivity at the surface, ft^2/hr
AMIN	diffusivity at the thermocline, ft^2/hr
AREA(J)	average area of the upper and lower surfaces of the j-th element, ft^2*
AREATOP	average area of the upper and lower surfaces of the surface element, ft^2*
ATM	monthly average atmospheric radiative heat flux, Btu/day-ft^2
A1	maximum value of the diffusivity, ft^2/hr
A2	minimum value of the diffusivity, ft^2/hr
BACK	monthly average back radiative heat flux, Btu/day-ft^2
BETA	fraction of the short-wave solar radiation absorbed in the top element
BLANK	name used to print a blank space in the plot of the temperature profile
C	specific heat of water, Btu/lb-$^{\circ}$F
CL	cloudiness factor
CLOUD	cloud cover, tenths
CLOUD1(I)	average cloud cover for the I-th month, tenths

* The geometry of the reservoir is initially read in and calculated with the units of acres and acre feet. These quantities are then converted and used in the program with the units of ft^2 and ft^3.

CONV	monthly average convective heat flux, Btu/day-ft^2
D(J)	diffusivity at the j-th surface, ft^2/hr
DELVOL	difference in the inflow and outflow, ft^3/hr
DELZ	thickness of the elements in the reservoir, ft
DELZSQ	square of the element thickness, ft^2
DELZTOP	thickness of the surface element in the reservoir, ft
DEPTH	depth of the reservoir, ft
DOT	name used to print a "." in the plot of the temperature profile
DP	depth at which an observed temperature was taken, ft
DT	time interval used in the simulation, hr
DTHDZ(J)	derivative of temperature with respect to depth for the j-th element, $^\circ$F/ft
D2	variable proportional to the second derivative of temperature with respect to depth
D22	variable proportional to the second derivative of temperature with respect to depth
EA	water vapor pressure, in. Hg.
EQ	name used to print a "=" in the plot of the temperature profile
ES	saturation vapor pressure at the water surface temperature, in. Hg.
ETA	coefficient of absorptivity of solar radiation with depth, ft^{-1}
EW	saturation vapor pressure at the wet bulb air temperature, in. Hg.
EVAP	monthly average evaporative heat flux, Btu/day-ft^2
F(J)	j-th term of the F matrix
HA	atmospheric heat flux, Btu/hr-ft^2
HADAY(I)	atmospheric heat flux for the I-th day, Btu/day-ft^2

HB	back radiative heat flux, Btu/hr-ft^2
HBDAY(I)	back radiative heat flux for the I-th day, Btu/day-ft^2
HC	convective heat flux, Btu/hr-ft^2
HCDAY(I)	convective heat flux for the I-th day, Btu/day-ft^2
HE	evaporative heat flux, Btu/hr-ft^2
HEAT1(NN,II)	volume weighted average temperature of the NN-th subdivision for the II-th day of a two-dimensional simulation, $^\circ$F
HEDAY(I)	evaporative heat flux for the I-th day, Btu/day-ft^2
HL	latent heat of vaporization of water, Btu/lb
HN	net heat flux to the top element, Btu/hr-ft^2
HNDAY(I)	net surface heat flux for the I-th day, Btu/day-ft^2
HNET	monthly average net surface heat flux, Btu/day-ft^2
HPRIME(J)	j-th term of the h' matrix
HS	short-wave solar radiative heat flux, Btu/hr-ft^2
HSDAY(I)	short-wave solar radiative heat flux for the I-th day, Btu/day-ft^2
HT(NN)	yearly volume weighted average temperature of the NN-th subdivision of a two-dimensional simulation, $^\circ$F
HTOT	total heat content of the reservoir, Btu
II	number of the day of the simulation
IMAX	day number of the end of the time period for calculating the diffusivity
IMIN	day number of the beginning of the time period for calculating the diffusivity
I1	variable which is negative if a new value for the diffusivity is to be read in
JZ	subscript used in printing out an observed temperature profile

KDIFF	variable which is used to specify whether or not the diffusivity is to be calculated
KDT	time interval used in the simulation, days
KLAKE	variable used to indicate the reservoir being simulated
KPRINT1	variable used to control what is printed out (Same for KPRINT2 through KPRINT4)
KREAD	variable used to specify whether or not the reservoir is initially isothermal
KZ	value of an observed temperature expressed as an integer, $^{\circ}F$
LINE	name used to print out a temperature profile
NCHANGE	change in the number of elements after the inflow is added and the outflow is removed
NDAY	number of days of the simulation
NDAYAVE	number of days of input meteorological data to be averaged together
NDAYOBS(I)	number of the day of the year of the I-th day for which an input temperature profile is read in
NDAY1	number of the first day of the simulation
NDAY2	number of the last day of the simulation
NEL	number of elements in the reservoir
NELIN	number of elements which an inflow enters, caused by the thermal discharge
NELMAX	maximum possible number of elements in the reservoir
NELMAXM	NELMAX - 1
NELM1	NEL - 1
NELM2	NEL - 2
NELNEW	new number of elements after the inflow is added and the outflow is removed
NELOUT	number of elements from which an outflow leaves, caused by the thermal discharge

NELP1	NEL + 1
NINFLOW	number of inflows
NLAKE	number of subdivisions in the two-dimensional simulation
NMONTH	number of the month of the year
NN	subscript used to denote the NN-th subdivision of the two-dimensional simulation
NOBS	number of days on which observed temperature profiles are read in
NPR(I)	number of the day of the year for the I-th day to be printed out
NPRINT	number of days to be printed out
NYEAR	number of the year of the simulation
P	variable used in calculating the terms in the P' matrix
PATM	barometric pressure, in. Hg.
PHI(J)	short-wave solar radiative heat flux at the j-th surface, Btu/hr-ft^2
PLUS	name used to print a "+" in the plot of the temperature
PPRIME(J)	j-th term of the P' matrix
PRECIP	precipitation, inches
Q	advective heat transport per unit depth term for the j-th element, $^\circ$F-ft^3/hr-ft
QCOOL	power plant cooling water flow, cfs
QI(J)	horizontal inflow into the j-th element, ft^3/hr
QII(I)	Flow rate of the I-th inflow, ft^3/hr
QIN	inflow to the reservoir, ft^3/hr
QINKS	flow from the release from Lake Inks, ft^3/sec
QLBJ	outflow from Lake LBJ, ft^3/sec
QLLANO	flow of the Llano River, ft^3/sec
QO(J)	horizontal outflow from the j-th element, ft^3/hr

QOUT	outflow from the reservoir, ft^3/hr
QPRECIP	precipitation, ft^3/hr
QSANDY	flow of Sandy Creek, ft^3/sec
QSPINKS(I)	flow rate over the Lake Inks spillway for the I-th month, acre ft/month
QSPLBJ(I)	flow rate over the Lake LBJ spillway for I-th month, acre ft/month
QTRAVIS	outflow from Lake Travis, ft^3/sec
QV(J)	vertical flow at the j-th surface, ft^3/hr
Q1(J)	advective heat transport term at the top of the j-th element, $^{\circ}F$-ft^3/hr
Q2(J)	advective heat transport term at the bottom of the j-th surface, $^{\circ}F$-ft^3/hr
RHO	density of water, lb/ft^3
S(J,I)	J,I term of the S matrix
SOL	monthly average short-wave solar radiative heat flux, Btu/day-ft^3
SOLDAY	short-wave solar radiative heat flux, Btu/day-ft^2
STAR	name used to print a "*" in the plot of the temperature profile
SURF(J)	area of the lower surface of the j-th element, ft^2*
SURFTOP	area of the surface of the reservoir, ft^2*
TAMB	ambient lake temperature, $^{\circ}F$
TAVE1(NN)	yearly average surface temperature for the NN-th subdivision of the two-dimensional simulation, $^{\circ}F$
TAVE2(NN)	yearly average bottom temperature for the NN-th subdivision of the two-dimensional simulation, $^{\circ}F$
TDIFF	difference in temperature between two elements, $^{\circ}F$
TDIFF1(NN)	annual average temperature difference from the top to the bottom on the NN-th subdivision for the two-dimensional simulation, $^{\circ}F$

TEMP	temperature of the mixed elements when the temperature gradient is unstable, $^{\circ}F$
THBOT1(NN,II)	temperature of the bottom element of the NN-th subdivision for the II-day of the two-dimensional simulation, $^{\circ}F$
THDOT1(NN,J)	time derivative of temperature for the j-th element of the NN-th subdivision of the two-dimensional simulation, $^{\circ}F/hr$
THETA(J)	temperature of the j-th element, $^{\circ}F$
THETAC(J)	temperature of the j-th element, $^{\circ}C$
THETADB	dry-bulb air temperature, $^{\circ}F$
THETAQI (J)	temperature of the inflow which enters the j-th element, $^{\circ}F$
THETAS	surface temperature of the reservoir, $^{\circ}F$
THETAWB	wet-bulb air temperature, $^{\circ}F$
THETA1(NN,J)	temperature of the j-th element of the NN-th subdivision of the two-dimensional simulation, $^{\circ}F$
THETDOT(J)	time derivative of temperature for the j-th element, $^{\circ}F/hr$
THETQII(I)	temperature of the I-th inflow, $^{\circ}F$
THSURF1(NN,II)	surface temperature of the NN-th subdivision of the two-dimensional simulation for the II-day, $^{\circ}F$
TINC	temperature of the inflow to Lake Travis, $^{\circ}C$
TINF	temperature of the inflow to Lake Travis, $^{\circ}F$
TINFLOW(I)	temperature of the inflow to Lake Travis for the I-th month, $^{\circ}F$
TINIT	initial temperature of the reservoir if it is isothermal, $^{\circ}F$
TINKS	temperature of the release from Lake Inks, $^{\circ}F$
TINKSC	temperature of the release from Lake Inks, $^{\circ}C$
TLLANO	temperature of the Llano River, $^{\circ}F$
TLLANOC	temperature of the Llano River, $^{\circ}C$

TMIX	variable used to calculate the temperature of the elements mixed when the temperature gradient is unstable
TOBS(JZ,II)	observed temperature at the JZ-th depth on the II-th day, $^{\circ}F$
TOBSO	observed outflow temperature, $^{\circ}F$
TOP	change in volume of the top element, ft^3
TOUTC	temperature of the outflow from the reservoir, $^{\circ}C$
TOUTF	temperature of the outflow from the reservoir, $^{\circ}F$
TQ	product of the temperature and volume of an inflow, $^{\circ}F$-ft^3/hr
TSANDY	temperature of Sandy Creek, $^{\circ}F$
T1(J)	temperature of the j-th element at the beginning of the time period for calculating the diffusivity, $^{\circ}F$
T2(J)	temperature of the j-th element at the end of the time period for calculating the diffusivity, $^{\circ}F$
T2MT1(J)	difference in the temperature of the j-th element from the end to the beginning of the time period for calculating the diffusivity, $^{\circ}F$
VOL(J)	volume of the j-th element, ft^3*
VOLDIFF	volume of the top element which does not contain water, ft^3*
VOLEVAP	volume of evaporated water, acre ft/day
VOLIN	inflow to the reservoir, acre ft/day
VOLIN1	inflow to Lake LBJ from the release from Inks Lake, acre ft/day
VOLIN2	inflow from the Llano River, acre ft/day
VOLIN3	inflow from Sandy Creek, acre ft/day
VOLIN4	inflow of the makeup, acre ft/day
VOLLAKE	calculated volume of the reservoir, ft^3*
VOLMIX	volume mixed when the temperature gradient is unstable, ft^3

VOLOBS	volume of the reservoir based on the observed surface elevation, ft^3
VOLOUT	outflow from the reservoir, acre ft/day
VOLTOP	volume of water in the top element, ft^3*
VOLUME(J)	cumulative volume up to and including the j-th element, ft^3*
VV(J)	vertical velocity at the j-th surface, ft/sec
W	wind speed, mi/hr
Wind	wind speed mi/hr
XK(J,I)	J,I term of the K matrix
XLRATIO	decay coefficient for the absorption of solar radiation with depth, ft^{-1}
Z(J)	elevation of the bottom of the reservoir, ft. above m.s.l.
ZBOT	elevation of the bottom of the reservoir, ft. above m.s.l.
ZN	elevation of the bottom of the second to top element of the reservoir, ft above m.s.l.
ZSURF	observed elevation of the surface of the reservoir, ft. above m.s.l.
ZTHERM	elevation of the thermocline, ft. above m.s.l.
ZTOP	calculated elevation of the surface of the reservoir, ft. above m.s.l.

APPENDIX C

INPUT VARIABLES TO THE COMPUTER PROGRAM

Card 1, FORMAT I2,2I4,5I2

KLAKE = 1 for a simulation of Lake LBJ.

= 2 for a simulation of Lake Travis.

= 3 for a simulation of Lake LBJ discharge cove using Lake LBJ meteorological data.

= 4 for a simulation of Lake LBJ discharge cove using Lake Travis meteorological data.

NPRINT = number of days to be printed out.

NOBS = number of days for which observed temperature profiles are read in.

KPRINT1 = 0 for no printout of the inflows and outflows.

= 1 for a printout of the inflows and outflows.

KPRINT2 = 0 for no printout of the energy budget terms.

= 1 for a printout of the energy budget terms.

KPRINT3 = 0 for no printout of the temperature profile.

= 1 for a printout of the temperature profile.

KPRINT4 = 0 for no printout of the monthly summary.

= 1 for a printout of the monthly summary.

KDIFF = 0 for no calculation of the diffusivity.

= 1 for a calculation of the diffusivity.

Card 2, FORMAT 2I5

IMIN = day number of the first day of the calculation of the diffusivity.

IMAX = day number of the last day of the calculation of the diffusivity. If KDIFF = 0 omit this card

Card 3, FORMAT 7I5

NEL = initial number of elements in reservoir.

NELMAX = maximum possible number of elements in reservoir.

NDAY1 = number of the first day of the simulation.

NDAY2 = number of the last day of the simulation.

KDT = time interval in days.

NINFLOW= number of inflows.

NDAYAVE= number of days of input meteorological data to be averaged together. (Inflows are not averaged)

Card Group 4, FORMAT 20I4

NPR(I) = numbers of the days to be printed out, where I=1, NPRINT.

Card Group 5, FORMAT 20I4

NDAYOBS(I) = numbers of the days for which observed temperatures are read in, where I=1, NOBS. If no observed temperatures are read in, omit Card Groups 5, 6, and 7.

Card Group 6, FORMAT 10F5.0

DP(J,K,) = depth for each observed temperature, starting with the closest to the surface, where J = 1,10 and K = the number of the day of the observation. Put each day's depths on a different card in order of increasing K. Maximum of ten observations per day. Depths are in feet.

Card Group 7, FORMAT 10F5.0

TOBS(J,K) = observed temperature, read in the same manner as Card Group 6. If KLAKE = 1 or 3, °C. If KLAKE = 2 or 4, °F

Card Group 8, **,**** FORMAT 12F5.0

WIND(I) = average wind velocity for each month of the simulation, in mi/hr, I = 1,12.

Card Group 9, **,**** FORMAT 12F5.0

CLOUD1(I) = average cloudiness factor for each month in tenths, I = 1,12.

Card 10, ** FORMAT 12F5.0

TINFLOW(I) = average inflow temperature for each month in °F, I=1,12

Card 11, FORMAT I2

KREAD = 1 if the lake is initially isothermal.

= 2 if the lake is not initially isothermal.

Card 12, FORMAT F5.0

TINIT = initial temperature of the reservoir, °F. If the reservoir is not intially isothermal, use Card Group 13 and not Card 12.

Card Group 13, FORMAT 13F6.0

THETA (J) = Initial temperature of the j-th element, ^{o}C. If the reservoir is initially isothermal, use Card 12 and not Card Group 13.

Card 14, FORMAT 2F10.0

BETA = fraction of the short-wave solar radiation absorbed in the top elements.

ETA = coefficient of absorptivity of short-wave solar radiation with depth, ft^{-1}.

Card 15, FORMAT 2F10.0

ZTOP = initial elevation of the surface of the reservoir, ft above m.s.l.

ZBOT = elevation of the bottom of the reservoir, ft above m.s.l.

Card 16,***,**** FORMAT I2

NLAKE =number of subdivision of discharge cove.

Card Group 17, * FORMAT 16F5.0

VOL(J) = volume of each element in acre feet, J=1, NELMAX.

Card 18, FORMAT I4, 66X, 2F5.0

I1	=	-10 to read in the initial or a new value of the diffusivity
	≠	-10 to use the same value of the diffusivity that was used on the previous day.
AMAX	=	value of the diffusivity at the surface, ft^2/hr
AMIN	=	value of the diffusivity at the thermocline, ft^2/hr.

(When the first or a new value of the diffusivity is read in, place this card before Card 19 or 20 for the day on which the diffusivity is to be changed)

Card Group 19, *, *** FORMAT I3,I3,F5.0,2F3.0,F5.2,F6.2 F5.1,F4.1,F6.1,4F5.0

I1	=	number of the day of the year.
NMONTH	=	number of the month.
SOLDAY	=	short-wave solar radiation, Btu/day-ft^2.
THETADB	=	dry-bulb temperature, $^\circ F$.
THETAWB	=	wet-bulb temperature, $^\circ F$.
PRECIP	=	precipitation, inches.
PATM	=	barometric pressure, in. Hg.
W	=	wind speed, mi/hr.
CLOUD	=	cloud cover, tenth.
ZSURF	=	observed surface elevation, ft. above m.s.l.
QLBJ	=	outflow from Lake LBJ, ft^3/sec.
QINKS	=	outflow from Lake Inks, $ft^3 sec$.
QLLANO	=	flow of Llano River, ft^3/sec.
QSANDY	=	flow of Sandy Creek, $ft^3 sec$.

(Repeat this card for each day of the simulation)

Card Group 20, **, **** FORMAT I4,11X,F7.2,F7.1,5X,F7.1,F5.1,
F7.1,F7.1,F5.1,F5.1

I1	=	number of the day of the year.
ZSURF	=	observed surface elevation, ft. above m.s.l.
QII(1)	=	inflow, ft^3/sec.
QTRAVIS	=	outflow, ft/sec.
TOBSO	=	observed outflow temperature, $^{\circ}F$.
SOLDAY	=	short-wave solar radiation, Btu/day-ft^2.
PATM	=	barometric pressure, in. Hg.
THETADB	=	dry-bulb temperature, $^{\circ}F$.
THETAWB	=	wet-bulb temperature, $^{\circ}F$.

(Repeat this card for each day of the simulation)

---

* Card used if KLAKE = 1.

** Card used if KLAKE = 2.

*** Card used if KLAKE = 3.

**** Card used if KLAKE = 4.

APPENDIX D

INPUT FOR THE LAKE LBJ SIMULATION

Lake LBJ Capacity Table

(From Reference 17)

LAKE ELEV.	VOLUME AC.FT.	DIFF. AC.FT.	LAKE ELEV.	VOLUME AC.FT.	DIFF. AC.FT.
836	234,418		817	94,304	
		10,802			4,663
835	223,616		816	89,641	
		10,402			4,503
834	213,214		815	85,138	
		9,996			4,349
833	203,218		814	80,789	
		9,578			4,197
832	193,640		813	76,592	
		9,154			4,051
831	184,486		812	72,541	
		8,720			3,907
830	175,766		811	68,634	
		8,276			3,769
829	167,490		810	64,865	
		7,842			3,634
828	159,648		809	61,231	
		7,434			3,500
827	152,214		808	57,731	
		7,053			3,368
826	145,161		807	54,363	
		6,701			3,237
825	138,460		806	51,126	
		6,375			3,107

Lake LBJ Capacity Table

(From Reference 17), continued

LAKE ELEV.	VOLUME AC.FT.	DIFF. AC.FT.	LAKE ELEV.	VOLUME AC.FT.	DIFF. AC.FT.
824	132,085		805	48,019	
		6,078			2,980
823	126.007		804	45,039	
		5,807			2,853
822	120,200		803	42,186	
		5,565			2,727
821	114,635		802	39,459	
		5,350			2,604
820	109,285		801	36,855	
		5,163			2,481
819	104,122		800	34,374	
		4,993			2,360
818	99,129		799	32,014	
		4,825			2,242
817	94,304		798	29,772	
798	29,772		779	4,854	
		2,127			567
797	27,645		778	4,287	
		2,015			511
796	25,630		777	3,776	
		1,906			461
795	23,724		776	3,315	
		1,804			413
794	21,920		775	2,902	
		1,710			369

Lake LBJ Capacity Table

(From Reference 17), continued

LAKE ELEV.	VOLUME AC.FT.	DIFF. AC.FT.	LAKE ELEV.	VOLUME AC.FT.	DIFF. AC.FT.
793	21,210		774	2,533	
		1,620			329
792	18,590		773	2,204	
		1,530			293
791	17,060		772	1,911	
		1,442			261
790	15,618		771	1,650	
		1,358			233
789	14,260		770	1,417	
		1,277			209
788	12,983		769	1,208	
		1,197			188
787	11,786		768	1,020	
		1,118			169
786	10,668		767	851	
		1,042			153
785	9,626		766	698	
		969			138
784	8,657		765	560	
		897			126
783	7,760		764	434	
		826			118
782	6,934		763	316	
		758			110
781	6,176		762	206	

Lake LBJ Capacity Table

(from Reference 17), continued

LAKE ELEV.	VOLUME AC.FT.	DIFF. AC.FT.	LAKE ELEV.	VOLUME AC.FT.	DIFF. AC.FT.
		693			104
780	5,483		761	102	
		629			102
779	4,854		760	0	

Observed Temperature Profiles for
the Deep Pool of Lake LBJ
(From Reference 8)

Sea Level Elevation (feet)	Date 2/24/68	4/27/68	6/19/68	7/20/68	10/19/68	2/1/69
825	10.2	22.0	29.1	29.2	24.2	
						13.0
815	9.8	21.4		27.8	24.2	
		20.5	24.8			
805	9.3	20.5	24.0	27.8	23.7	
		19.0	23.5			
795	9.3	17.5		26.8	23.7	
			22.5	25.4		12.5
785	9.3	16.5		22.9	23.7	
			22.0			
775	9.3	15.5	21.0	21.5	23.7	
765	9.3	15.3	20.5	20.0	23.7	
		14.7			21.0	12.0
755	9.3	14.0	20.0	19.0	20.5	
			18.0			
745		11.7	17.5	17.6	19.5	
			17.0	17.1	19.0	11.5
735						

Volumes of Flows Over Lake LBJ and Lake Inks Spillways for February, 1968 through February, 1969

(Flows are in acre feet/month)

(From Reference 16)

March	62,478	March	77,889
May	132,026	April	13,754
		May	145,177

For all other months during this period there was no flow over the spillway.

(a) Day Number
(b) Month Number
(c) Solar Radiative Flux, Btu/day-ft^2
(d) Dry-Bulb Temperature, $^\circ$F
(e) Wet-Bulb Temperature, $^\circ$F
(f) Precipitation, inches
(g) Barometric Pressure, in. Hg.
(h) Wind Speed, mi/hr
(i) Cloud Cover, tenths
(j) Surface Elevation, Ft. above m.s.l.
(k) Flow Through Lake LBJ Penstock, ft^3/sec
(l) Flow Through Lake Inks Penstock, ft^3/sec
(m) Flow of Llano River, ft^3/sec
(n) Flow of Sandy Creek, ft^3/sec

(a)	(b)	(c)	(d)	(e)	(f)	(g)	(h)	(i)	(j)	(k)	(l)	(m)	(n)
55	2	1741	42	31	0.00	29.52	8.5	0.0	824.8	1372	793	424	75
56	2	1648	52	41	0.00	29.49	5.9	0.0	824.8	91	647	406	64
57	2	1523	58	38	0.00	29.63	8.2	0.0	825.1	194	156	388	67
58	2	1523	59	40	0.00	29.51	10.6	0.7	825.3	716	0	371	59
59	2	342	53	46	0.01	29.31	17.4	0.9	825.3	1868	228	367	64
60	2	1865	41	22	0.00	29.69	14.7	0.1	824.9	630	302	367	67
61	3	1337	43	25	0.00	29.62	8.6	0.7	824.9	1658	817	346	53
62	3	1243	56	42	0.00	29.34	7.6	0.9	824.8	1387	1215	330	54
63	3	1710	47	31	0.00	29.69	17.0	0.6	824.9	1808	1169	326	46
64	3	939	43	23	0.00	29.74	8.2	1.0	824.9	1780	1247	315	45
65	3	435	46	39	0.27	29.47	6.6	1.0	824.8	1373	1218	315	51
66	3	995	54	46	0.03	29.34	5.5	0.6	824.8	1522	1018	334	61
67	3	1399	56	49	0.00	29.43	6.9	0.4	824.8	1151	742	338	61
68	3	311	60	56	0.03	29.36	6.6	1.0	824.8	303	266	326	48
69	3	1648	70	56	0.38	29.18	8.2	0.6	825.0	1329	39	323	67

(a)	(b)	(c)	(d)	(e)	(f)	(g)	(h)	(i)	(j)	(k)	(l)	(m)	(n)
70	3	1274	65	54	0.26	29.03	7.3	0.7	824.8	629	335	846	112
71	3	342	47	45	0.88	29.09	20.1	1.0	825.2	4200	2272	7960	2180
72	3	1710	46	28	0.00	29.50	25.0	0.5	825.6	4920	2514	2800	1070
73	3	1834	46	30	0.00	29.68	8.3	0.3	825.3	4569	2933	1260	454
74	3	1554	53	41	0.00	29.53	12.2	0.8	825.1	4719	2533	930	356
75	3	901	63	52	0.00	29.50	9.1	0.9	825.1	4600	2533	793	254
76	3	1741	64	52	0.00	29.59	7.1	0.4	825.4	4800	2523	725	196
77	3	808	63	56	0.00	29.44	11.2	1.0	825.6	4717	2533	671	178
78	3	560	68	60	0.00	29.30	14.8	1.0	825.6	5611	2533	642	148
79	3	373	67	64	0.01	29.27	10.9	1.0	825.2	4772	2552	677	157
80	3	653	55	54	0.23	29.28	16.8	1.0	824.9	6876	2458	2330	492
81	3	901	45	31	0.00	29.55	20.6	1.0	825.2	9419	2485	1860	381
82	3	2052	50	26	0.00	29.65	15.1	0.2	825.1	9459	2478	1310	290
83	3	2145	48	31	0.00	29.74	7.3	0.1	825.2	9312	2466	982	175
84	3	2021	57	41	0.00	29.56	10.5	0.2	825.1	6682	2543	781	145
85	3	1741	60	48	0.00	29.43	10.5	0.4	824.7	6290	2523	695	85
86	3	1803	63	52	0.00	29.41	14.2	0.6	824.2	2166	2543	642	83
87	3	497	67	56	0.00	29.48	11.4	1.0	825.0	3762	2533	603	83
88	3	715	68	59	0.00	29.56	7.6	1.0	825.1	3632	2552	586	77
89	3	653	69	61	0.00	29.50	8.2	1.0	825.1	3428	2458	586	77
90	3	1026	73	61	0.00	29.35	11.2	0.9	825.0	2760	2343	575	49
91	3	1212	72	60	0.00	29.29	12.9	0.9	825.1	2470	2484	564	67
92	4	995	63	55	0.40	29.44	8.8	1.0	825.2	3332	2198	548	64
93	4	622	69	63	0.02	29.21	10.2	1.0	825.1	3850	1961	737	62
94	4	808	74	64	0.01	29.02	7.9	0.8	824.7	2560	2181	762	62
95	4	2300	58	40	0.00	29.37	14.0	0.2	824.8	2314	2227	625	49
96	4	2269	54	30	0.00	29.59	11.2	0.1	824.9	3302	1780	537	28
97	4	2145	61	42	0.00	29.39	10.2	0.4	824.6	2646	2135	496	24
98	4	1399	73	63	0.03	29.24	10.2	1.0	824.5	2504	1247	491	18
99	4	777	73	66	0.00	29.20	5.9	1.0	824.3	1831	2044	486	11
100	4	964	66	59	0.25	29.44	9.9	1.0	824.5	2615	2013	1730	55
101	4	1430	67	57	0.00	29.57	10.5	0.7	824.7	7683	2523	4700	699
102	4	435	64	52	0.00	29.57	6.8	0.7	824.8	7923	2439	2600	282
103	4	1616	64	59	0.76	29.36	9.6	0.9	824.4	4900	2501	1780	178
104	4	1772	74	64	0.00	29.34	12.5	0.8	824.7	3695	2495	1490	200
105	4	1927	70	61	0.00	29.44	12.2	0.5	824.9	3068	2215	1110	148
106	4	746	67	49	0.00	29.41	7.6	0.2	825.0	4130	2181	900	112
107	4	591	73	65	0.00	29.19	13.1	0.9	824.7	3549	2261	826	95
108	4	684	74	67	0.00	29.19	9.5	1.0	824.5	4398	2347	793	91
109	4	715	75	69	0.00	29.23	8.8	1.0	824.3	2378	2485	756	91
110	4	746	75	67	0.00	29.19	11.5	1.0	824.4	2312	2400	2390	91
111	4	622	73	65	0.21	29.30	6.0	1.0	825.0	4470	2289	1740	102
112	4	933	72	66	0.02	29.28	5.2	1.0	825.0	3118	2033	2750	91
113	4	497	73	67	0.00	29.18	10.9	0.9	825.3	5524	2475	1710	85
114	4	777	62	47	0.17	29.38	14.7	0.9	825.1	4963	2494	1220	87
115	4	2456	60	36	0.00	29.53	8.3	0.0	825.1	5268	2477	967	77
116	4	2362	62	44	0.00	29.34	8.5	0.1	824.7	3725	2494	846	59

(a)	(b)	(c)	(d)	(e)	(f)	(g)	(h)	(i)	(j)	(k)	(l)	(m)	(n)
117	4	1772	70	60	0.00	29.18	10.8	0.6	824.8	2320	1542	733	47
118	4	1989	77	65	0.00	29.19	10.4	0.5	824.8	3731	2200	749	42
119	4	870	72	65	0.00	29.31	8.8	1.0	824.5	2479	2205	713	40
120	4	2362	68	49	0.00	29.51	13.1	0.4	824.6	1397	2214	695	37
121	4	2176	66	45	0.00	29.48	5.3	0.3	825.0	3211	2411	671	35
122	5	2238	68	53	0.00	29.32	7.8	0.1	825.0	4134	2437	648	31
123	5	1772	74	62	0.00	29.26	10.4	0.6	824.6	2810	2456	621	28
124	5	1679	73	65	1.17	29.23	11.1	0.8	824.7	3959	2376	631	20
125	5	2114	71	61	0.00	29.25	10.2	0.4	824.5	2850	2494	660	182
126	5	1710	73	60	0.59	29.30	9.2	0.7	824.6	2418	2475	614	89
127	5	995	69	61	0.00	29.28	11.9	0.8	824.8	3932	2456	2970	53
128	5	622	71	66	0.02	29.30	6.6	0.9	825.0	5721	2495	1070	51
129	5	1492	73	66	0.05	29.39	8.9	0.8	824.5	4439	2456	719	42
130	5	1368	77	62	0.02	29.33	9.6	0.9	824.2	3184	2466	642	33
131	5	901	70	66	1.86	29.20	8.8	1.0	824.2	9571	2439	2210	1390
132	5	187	64	62	1.51	29.18	6.8	1.0	825.2	9300	2380	7900	2640
133	5	591	70	65	0.00	29.24	9.2	1.0	825.3	7554	2371	3260	881
134	5	1119	78	71	0.01	29.25	12.2	0.9	825.2	7302	2324	1550	495
135	5	933	80	72	0.00	29.31	10.9	1.0	824.9	7433	2379	1200	345
136	5	1648	81	71	0.00	29.22	12.5	0.7	824.4	6972	2427	952	258
137	5	808	79	70	0.00	29.15	10.2	1.0	824.2	6017	2912	833	200
138	5	653	72	66	1.96	29.13	8.8	0.9	824.8	5405	2485	1170	192
139	5	2425	68	56	0.00	29.30	8.8	0.0	824.9	6530	2428	1910	400
140	5	2331	70	55	0.00	29.41	10.1	0.1	825.1	6742	2393	997	148
141	5	2331	70	54	0.00	29.47	8.5	0.2	824.8	5928	2485	756	102
142	5	1984	73	60	0.00	29.34	5.1	0.6	824.4	2377	2495	666	83
143	5	1585	80	67	0.00	29.19	15.7	0.7	824.8	4263	2494	619	77
144	5	1523	81	68	0.00	29.14	14.1	0.6	824.9	2226	2465	586	72
145	5	1523	82	69	0.00	29.20	9.4	0.6	824.8	2770	2350	553	77
146	5	1430	82	70	0.00	29.25	8.1	0.6	824.0	2900	2450	532	67
147	5	1306	79	69	0.00	29.17	10.2	0.8	825.0	2701	2483	496	58
148	5	1616	69	62	1.56	29.18	10.9	0.9	825.1	4993	2456	737	263
149	5	2394	71	61	0.00	29.34	5.5	0.0	824.9	4128	2350	893	221
150	5	2269	78	64	0.00	29.34	7.5	0.1	824.7	3796	2418	575	82
151	5	1803	82	69	0.00	29.27	10.9	0.6	824.9	2373	2263	481	49
152	5	1554	79	69	0.00	29.20	12.5	0.8	824.7	2176	2309	447	41
153	6	1337	78	67	0.54	29.25	9.4	0.9	824.7	2891	2437	438	54
154	6	1327	73	65	0.14	29.28	7.2	0.8	824.8	2412	2437	1030	98
155	6	1523	73	65	0.00	29.25	8.9	0.8	825.0	3965	2456	886	77
156	6	777	74	67	0.20	29.21	9.2	0.8	824.9	3703	2446	597	62
157	6	1088	75	66	0.19	29.19	6.5	0.3	824.8	3329	2230	730	132
158	6	1430	77	69	0.00	29.16	7.8	0.9	825.0	3560	1542	1160	196
159	6	1492	81	71	0.00	29.18	9.1	0.8	824.9	3541	2088	631	102
160	6	1554	82	70	0.00	29.20	9.5	0.6	824.7	2418	1789	496	33
161	6	1523	83	71	0.00	29.23	11.4	0.5	824.7	0	1606	443	14
162	6	1492	84	72	0.00	29.24	9.4	0.6	825.3	3730	1662	401	12
163	6	1896	84	71	0.00	29.28	6.9	0.4	824.9	2522	2205	352	16
164	6	2114	85	72	0.00	29.33	7.2	0.3	824.5	1315	2413	328	12

(a)	(b)	(c)	(d)	(e)	(f)	(g)	(h)	(i)	(j)	(k)	(l)	(m)	(n)
165	6	1927	84	70	0.00	29.23	4.9	0.2	825.0	2372	2408	319	8
166	6	1865	84	69	0.00	29.28	7.3	0.2	824.9	2385	2408	292	8
167	6	1399	83	71	0.00	29.34	8.5	0.7	824.9	2718	2408	271	8
168	6	1896	83	70	0.00	29.37	6.9	0.4	824.9	2748	2398	253	7
169	6	1057	81	63	0.30	29.35	6.5	0.9	824.8	3092	2398	464	579
170	6	1274	79	69	0.00	29.21	5.6	0.9	825.0	3077	2446	496	178
171	6	1057	78	68	0.08	29.23	7.2	1.0	825.1	261	142	315	41
172	6	1274	76	69	0.16	29.23	9.6	0.9	825.2	1479	206	257	50
173	6	1554	79	69	0.01	29.25	8.1	0.9	824.8	461	702	240	94
174	6	995	78	69	0.07	29.27	6.6	0.9	825.0	712	157	230	3
175	6	466	74	70	0.71	29.24	9.8	1.0	824.9	0	0	230	19
176	6	1554	81	71	0.17	29.12	10.6	0.7	825.0	1097	1172	234	21
177	6	1585	79	74	0.51	29.19	10.4	0.7	825.1	2355	1026	218	21
178	6	1648	75	65	0.02	29.34	10.2	0.8	824.7	385	388	230	30
179	6	2394	74	62	0.00	29.36	5.9	0.1	824.9	930	407	221	23
180	6	1927	83	71	0.00	29.26	13.7	0.6	824.9	96	389	203	17
181	6	1896	84	71	0.00	29.26	15.8	0.6	824.9	0	0	189	10
182	6	1865	84	72	0.00	29.35	15.7	0.5	824.9	0	0	169	9
183	7	1896	83	71	0.00	29.42	9.5	0.4	825.0	1853	1131	156	9
184	7	2052	83	69	0.03	29.46	7.5	0.5	824.8	999	392	148	9
185	7	1616	82	68	0.00	29.48	9.1	0.6	824.7	0	537	148	9
186	7	1896	80	65	0.00	29.46	11.4	0.5	824.9	0	0	161	0
187	7	2145	78	59	0.00	29.43	8.1	0.5	824.9	1435	779	161	0
188	7	2362	77	57	0.00	29.46	8.2	0.5	824.7	0	195	148	0
189	7	2145	79	63	0.00	29.39	4.2	0.5	824.8	0	0	156	9
190	7	1057	81	69	0.35	29.29	7.6	0.8	824.8	1017	883	311	10
191	7	933	76	69	2.43	29.31	6.8	0.7	824.9	0	0	460	151
192	7	2021	79	68	0.00	29.37	4.5	0.2	825.1	1432	445	315	27
193	7	1989	80	70	0.30	29.37	4.6	0.3	825.0	1975	387	221	18
194	7	1368	78	70	0.00	29.35	9.3	0.7	824.5	0	859	200	17
195	7	1834	82	70	0.00	29.29	10.8	0.7	824.9	0	0	386	18
196	7	2145	84	71	0.00	29.35	14.0	0.7	825.0	0	0	310	27
197	7	2269	84	72	0.00	29.42	11.7	0.6	825.1	1392	604	260	10
198	7	1585	85	71	0.00	29.40	9.5	0.6	824.9	430	547	191	9
199	7	1989	84	70	0.00	29.35	8.1	0.6	825.0	1575	751	175	7
200	7	2238	83	70	0.00	29.34	7.6	0.5	824.8	1574	1110	159	6
201	7	1927	84	70	0.00	29.38	6.5	0.6	824.7	138	528	146	6
202	7	1554	85	70	0.00	29.40	7.5	0.6	824.9	0	0	134	15
203	7	1554	84	70	0.00	29.40	7.6	0.4	824.9	0	0	146	0
204	7	1772	85	70	0.00	29.42	8.9	0.2	824.9	518	301	143	5
205	7	1989	85	69	0.00	29.37	10.1	0.4	824.9	597	609	134	4
206	7	1896	85	69	0.00	29.38	10.2	0.5	825.0	548	381	129	4
207	7	1523	83	71	0.00	29.43	7.6	0.7	824.9	0	[illegible]	125	4
208	7	1554	84	70	0.00	29.47	7.2	0.5	824.9	0	0	122	3
209	7	1896	84	69	0.00	29.50	7.2	0.3	824.9	0	0	116	3
210	7	2052	84	68	0.00	29.48	5.9	0.1	825.0	104	0	110	3
211	7	1648	84	67	0.00	29.44	7.2	0.4	824.9	1179	990	104	3

(a)	(b)	(c)	(d)	(e)	(f)	(g)	(h)	(i)	(j)	(k)	(l)	(m)	(n)
212	7	2052	86	68	0.00	29.37	11.5	0.5	824.9	1199	1119	100	3
213	7	1896	86	68	0.00	29.39	12.9	0.4	824.9	1475	1114	95	3
214	8	1865	84	69	0.00	29.44	7.9	0.4	824.7	819	1105	95	2
215	8	1492	83	69	0.00	29.43	7.6	0.3	824.8	881	1160	87	2
216	8	1803	84	68	0.00	29.43	6.5	0.5	824.9	467	593	82	2
217	8	1554	84	68	0.00	29.42	6.9	0.6	824.9	0	0	80	2
218	8	1368	82	70	0.31	29.42	4.9	0.6	824.9	1478	1043	80	3
219	8	1865	84	70	0.00	29.45	5.5	0.4	824.8	2231	1294	79	2
220	8	1927	84	70	0.00	29.44	6.5	0.2	824.4	870	1326	79	2
221	8	1989	86	69	0.00	29.39	7.8	0.4	824.6	728	1140	79	2
222	8	2145	86	70	0.00	29.35	9.9	0.5	824.7	1052	815	77	2
223	8	2269	86	69	0.00	29.32	9.4	0.3	824.6	0	782	74	2
224	8	1865	86	69	0.00	29.31	7.8	0.4	824.9	0	96	92	2
225	8	2083	87	69	0.00	29.25	9.1	0.5	825.0	933	334	204	5
226	8	1834	87	70	0.00	29.24	10.2	0.6	824.8	1160	960	134	6
227	8	1896	86	69	0.00	29.25	11.5	0.6	824.8	516	784	247	25
228	8	1648	88	71	0.00	29.28	13.8	0.6	824.9	1338	788	281	7
229	8	1616	88	70	0.00	29.33	13.1	0.5	824.8	1360	491	138	5
230	8	1306	85	71	0.10	29.36	10.1	0.6	824.6	1404	1118	108	4
231	8	1834	84	67	0.00	29.31	10.2	0.3	824.5	0	163	96	3
232	8	1212	85	70	0.00	29.32	9.5	0.5	824.6	0	814	84	3
233	8	1212	84	70	0.00	29.40	8.3	0.6	824.8	985	827	77	2
234	8	1492	85	69	0.00	29.45	7.3	0.4	824.8	684	835	74	2
235	8	2114	85	68	0.00	29.44	7.6	0.2	824.8	520	706	70	2
236	8	1989	85	67	0.00	29.38	8.2	0.2	824.9	817	341	67	2
237	8	1679	85	67	0.00	29.39	6.5	0.3	824.7	162	614	64	1
238	8	1803	84	67	0.00	29.42	7.1	0.2	824.9	162	580	66	1
239	8	1616	85	65	0.00	29.40	4.9	0.2	824.8	1037	342	63	1
240	8	1399	84	63	0.00	29.38	7.5	0.3	824.8	432	757	66	1
241	8	2114	80	55	0.00	29.37	7.8	0.0	824.9	0	506	61	1
242	8	1927	79	56	0.00	29.37	6.5	0.3	825.0	387	344	69	1
243	8	1306	80	59	0.00	29.38	7.2	0.6	824.9	593	484	79	1
244	8	839	78	66	0.33	29.38	4.9	1.0	824.7	0	0	82	2
245	9	1523	80	64	0.00	29.33	5.6	0.9	824.7	0	0	77	2
246	9	528	73	68	0.05	29.29	5.9	1.0	824.7	0	0	86	3
247	9	1616	83	71	0.03	29.20	11.9	0.6	824.8	485	816	87	2
248	9	1492	81	73	1.42	29.24	13.1	0.8	824.9	543	602	100	2
249	9	715	73	66	0.53	29.41	8.5	0.9	824.9	477	624	105	2
250	9	1430	78	67	0.00	29.49	7.8	0.7	825.0	1091	193	91	2
251	9	1399	80	69	0.00	29.42	5.0	0.8	824.7	483	909	91	2
252	9	1927	84	71	0.00	29.33	8.6	0.5	824.8	515	851	87	2
253	9	1274	82	66	0.00	29.33	7.3	0.4	825.0	1247	690	82	2
254	9	1710	76	54	0.00	29.40	10.5	0.8	824.8	0	0	79	2
255	9	1989	72	53	0.00	29.42	7.9	0.1	824.8	191	0	74	2
256	9	1896	71	55	0.00	29.40	5.9	0.3	824.7	0	428	72	2
257	9	746	70	60	0.03	29.36	4.8	0.8	824.8	0	102	70	2
258	9	311	67	64	0.84	29.27	6.6	1.0	824.8	1252	0	215	109

(a)	(b)	(c)	(d)	(e)	(f)	(g)	(h)	(i)	(j)	(k)	(l)	(m)	(n)
259	9	1834	78	69	0.02	29.10	7.6	0.5	824.7	810	208	438	241
260	9	1585	82	72	0.02	29.07	11.5	0.6	824.7	520	0	319	77
261	9	1492	71	59	0.41	29.21	12.4	0.4	824.6	0	0	224	33
262	9	1896	70	51	0.00	29.33	5.8	0.0	824.7	0	0	166	9
263	9	1958	73	56	0.00	29.25	7.9	0.0	824.8	0	0	132	10
264	9	1306	83	72	0.05	29.27	9.8	0.8	824.9	0	0	108	9
265	9	1461	83	72	0.00	29.33	10.1	0.6	824.8	0	0	96	9
266	9	1274	80	71	0.00	29.38	6.3	0.6	824.9	0	0	89	8
267	9	1274	82	70	0.00	29.38	8.1	0.7	824.9	153	0	95	9
268	9	1150	79	67	0.02	29.37	7.1	0.6	824.9	0	55	111	9
269	9	1523	75	63	0.00	29.41	11.1	0.4	825.0	0	0	177	9
270	9	1865	73	56	0.00	29.41	9.1	0.0	825.1	0	0	146	8
271	9	1834	71	51	0.00	29.29	7.1	0.0	825.1	0	0	141	8
272	9	1399	71	55	0.00	29.36	5.6	0.2	825.2	0	0	138	8
273	9	1679	73	56	0.00	29.48	6.6	0.1	825.2	0	0	122	7
274	9	1337	74	58	0.00	29.53	6.0	0.1	825.2	552	0	108	7
275	10	1616	75	59	0.00	29.29	5.0	0.1	825.1	325	0	100	5
276	10	1461	79	64	0.00	29.26	10.5	0.4	825.0	816	492	98	5
277	10	1212	77	65	0.00	29.40	10.4	0.8	824.9	231	0	94	4
278	10	435	66	56	0.17	29.49	5.1	1.0	824.9	0	0	96	5
279	10	777	74	65	0.08	29.24	6.6	0.8	824.9	0	295	98	9
280	10	1585	73	66	0.00	29.19	7.9	0.2	825.0	0	0	93	8
281	10	715	72	65	0.01	29.25	7.3	0.0	825.0	0	0	97	6
282	10	839	80	70	0.00	29.24	10.4	0.8	825.0	1472	524	100	7
283	10	839	79	70	0.26	29.31	11.4	0.9	824.8	998	657	101	14
284	10	1585	79	59	0.00	29.44	11.2	0.5	824.7	0	0	98	7
285	10	684	72	65	0.03	29.39	5.9	1.0	824.7	0	36	95	5
286	10	964	80	69	0.00	29.39	8.8	0.7	824.8	0	0	94	4
287	10	1430	81	68	0.00	29.37	8.1	0.5	824.8	0	0	93	4
288	10	1150	81	69	0.00	29.36	8.9	0.7	824.9	1314	1240	92	3
289	10	1026	80	68	0.00	29.29	10.4	0.6	824.9	998	257	90	4
290	10	933	76	65	0.00	29.13	7.9	0.7	824.6	0	0	88	4
291	10	1554	65	43	0.00	29.35	14.7	0.1	824.7	0	0	87	2
292	10	1337	64	38	0.00	29.42	7.6	0.5	824.7	0	0	86	3
293	10	1492	66	46	0.00	29.41	6.3	0.4	824.7	0	0	85	4
294	10	1243	72	57	0.00	29.42	5.8	0.5	824.7	0	0	84	4
295	10	1026	68	54	0.00	29.37	6.5	0.2	824.7	0	0	84	4
296	10	808	72	62	0.05	29.33	5.9	0.4	824.7	193	0	83	27
297	10	1212	75	58	0.00	29.30	6.9	0.6	824.7	0	0	88	45
298	10	1492	63	41	0.00	29.50	13.5	0.1	824.7	0	0	90	29
299	10	1461	61	39	0.00	29.53	6.3	0.2	824.8	0	0	86	5
300	10	1399	66	46	0.00	29.46	8.8	0.0	824.8	0	0	83	5
301	10	1274	67	51	0.00	29.46	6.0	0.3	824.8	0	0	81	5
302	10	1243	67	36	0.00	29.51	6.5	0.3	824.8	0	0	80	5
303	10	1243	68	53	0.00	29.38	6.5	0.0	824.9	0	0	79	5
304	10	839	73	61	0.00	29.33	8.9	0.5	824.9	0	0	80	5
305	10	839	76	64	0.00	29.36	10.9	0.5	824.9	0	0	80	4

(a)	(b)	(c)	(d)	(e)	(f)	(g)	(h)	(i)	(j)	(k)	(l)	(m)	(n)
306	11	777	73	61	0.00	29.45	7.6	0.4	824.9	0	0	80	4
307	11	839	75	62	0.03	29.36	11.7	0.7	824.9	0	0	80	4
308	11	964	57	46	0.00	29.44	16.5	0.4	825.0	0	0	78	4
309	11	1150	57	43	0.00	29.35	8.1	0.2	825.0	0	0	74	4
310	11	839	61	54	0.00	29.16	5.5	0.6	824.9	0	0	75	4
311	11	1243	61	47	0.00	29.28	12.1	0.1	824.9	0	0	75	4
312	11	964	55	40	0.00	29.52	12.4	0.7	824.9	0	0	75	4
313	11	155	44	39	0.49	29.53	15.1	1.0	824.9	0	0	91	7
314	11	1274	45	36	0.00	29.39	8.9	0.5	825.0	0	0	108	10
315	11	933	55	40	0.00	29.15	13.5	0.2	825.0	0	0	115	7
316	11	1274	47	25	0.00	29.60	14.0	0.0	825.1	0	0	121	6
317	11	1119	49	30	0.00	29.54	7.6	0.2	825.1	0	0	116	6
318	11	964	60	50	0.00	29.31	10.9	0.5	825.1	0	0	110	6
319	11	622	59	61	0.00	29.22	13.4	0.9	825.1	0	0	106	6
320	11	1057	63	55	0.55	29.18	8.0	0.5	825.1	412	31	114	6
321	11	808	58	40	0.00	29.22	6.2	0.4	825.1	0	0	116	6
322	11	1150	60	46	0.00	29.22	10.1	0.2	825.1	0	0	118	6
323	11	1150	54	26	0.00	29.56	12.1	0.2	825.1	0	0	114	5
324	11	1212	49	29	0.00	29.61	6.8	0.0	825.2	0	0	110	5
325	11	1150	53	37	0.00	29.65	5.9	0.0	825.2	0	0	105	5
326	11	1119	57	45	0.00	29.60	6.8	0.0	825.2	0	0	102	5
327	11	591	59	54	0.00	29.47	6.5	0.7	825.3	0	0	100	5
328	11	839	70	59	0.00	29.38	8.9	0.7	825.3	0	0	101	6
329	11	1150	57	37	0.00	29.57	12.4	0.3	825.3	0	0	[illegible]	5
330	11	1057	54	42	0.00	29.45	9.8	0.4	825.3	402	0	[illegible]	5
331	11	435	64	57	1.33	29.17	15.2	1.0	825.2	688	0	106	7
332	11	311	45	43	0.94	29.23	15.0	0.8	825.1	1465	0	142	71
333	11	1119	49	36	0.00	29.40	8.6	0.0	824.8	0	0	185	70
334	11	342	44	35	0.00	29.66	10.1	0.8	824.9	0	182	184	42
335	11	31	43	40	1.57	29.50	10.8	1.0	825.1	482	280	222	105
336	12	1181	48	41	0.00	29.33	10.1	0.4	825.1	702	0	638	324
337	12	280	45	46	0.01	29.33	4.0	0.9	825.1	562	0	426	111
338	12	1088	46	33	0.00	29.55	16.4	0.1	825.1	400	0	299	46
339	12	1057	48	30	0.00	29.50	8.3	0.2	825.1	498	0	233	[illegible]
340	12	995	49	37	0.00	29.37	4.9	0.1	825.[illegible]	114	0	195	24
341	12	1088	48	33	0.00	29.38	7.5	0.1	825.1	480	0	169	19
342	12	1119	47	26	0.00	29.73	15.2	0.1	825.0	96	0	154	15
343	12	1119	41	22	0.00	29.83	8.5	0.0	825.0	0	0	143	14
344	12	342	45	38	0.00	29.66	4.8	0.0	825.1	404	0	137	14
345	12	187	56	51	0.00	29.70	6.3	1.0	824.9	102	0	134	14
346	12	404	60	58	0.00	29.50	9.2	1.0	825.0	66	0	121	15
347	12	1057	61	53	0.02	29.26	11.7	0.8	825.0	387	0	131	15
348	12	1088	49	26	0.00	29.61	11.4	0.2	825.0	363	0	127	13
349	12	1150	42	21	0.00	29.81	9.2	0.1	824.9	0	0	123	13
350	12	1181	44	22	0.00	29.73	7.3	0.0	824.9	0	0	118	11
351	12	311	48	41	0.00	29.47	7.2	0.7	824.9	310	0	115	11
352	12	435	66	58	0.00	29.26	14.1	0.9	824.9	0	0	118	13

(a)	(b)	(c)	(d)	(e)	(f)	(g)	(h)	(i)	(j)	(k)	(l)	(m)	(n)
353	12	591	60	45	0.00	29.16	15.0	0.8	824.9	165	0	119	11
354	12	839	51	24	0.00	29.37	6.8	0.7	824.9	440	0	113	10
355	12	218	49	39	0.09	29.33	6.6	1.0	824.9	465	0	112	10
356	12	218	61	59	0.14	29.10	7.2	1.0	824.7	0	0	118	13
357	12	684	47	30	0.29	29.42	12.8	0.9	824.8	0	0	131	15
358	12	1159	40	18	0.00	29.76	8.1	0.0	824.8	529	0	130	11
359	12	1119	44	27	0.00	29.66	7.6	0.0	824.7	92	0	123	1
360	12	659	54	47	0.00	29.38	10.4	0.3	824.8	0	0	120	1
361	12	373	65	59	0.00	29.14	13.5	1.0	824.9	0	0	121	1
362	12	839	60	46	0.00	28.99	21.6	0.5	824.8	0	0	129	1
363	12	964	51	31	0.00	29.33	5.8	0.2	824.9	282	0	112	9
364	12	870	55	43	0.00	29.28	9.6	0.4	824.8	0	0	115	9
365	12	435	56	49	0.00	29.31	9.4	1.0	824.8	0	0	113	9
366	12	715	24	19	0.00	29.75	16.4	0.9	824.9	853	0	110	8
367	1	435	23	13	0.06	29.84	8.6	0.9	824.6	0	0	112	9
368	1	218	41	38	0.13	29.57	6.6	1.0	824.6	0	0	123	11
369	1	218	44	42	0.03	29.51	12.4	1.0	824.7	0	1619	125	11
370	1	995	34	16	0.00	29.72	12.5	0.4	825.3	1134	956	122	9
371	1	1088	40	22	0.00	29.52	8.5	0.1	825.3	0	0	119	9
372	1	933	51	34	0.00	29.36	5.9	0.4	825.3	218	0	119	9
373	1	933	57	40	0.00	29.28	7.8	0.5	825.3	0	0	120	9
374	1	1057	63	49	0.00	29.96	11.9	0.0	825.3	0	0	119	9
375	1	1057	43	16	0.00	29.39	20.4	0.3	825.3	0	0	114	8
376	1	653	39	12	0.00	29.56	12.1	0.7	825.4	0	0	110	7
377	1	901	45	17	0.00	29.54	6.8	0.8	825.4	0	0	109	8
378	1	995	46	29	0.00	29.46	6.3	0.6	825.4	0	0	109	8
379	1	497	52	46	0.00	29.52	5.3	1.0	825.4	0	205	111	8
380	1	249	59	53	0.00	29.51	7.8	1.0	825.5	0	0	113	9
381	1	311	64	57	0.17	29.35	8.8	1.0	825.6	0	0	117	10
382	1	870	69	58	0.01	29.29	7.6	0.8	825.6	0	0	123	11
383	1	435	64	60	0.00	29.26	7.5	0.7	825.7	0	0	124	11
384	1	404	55	50	0.00	29.34	10.6	1.0	825.7	0	0	123	1
385	1	808	50	42	0.00	29.44	10.5	0.9	825.8	221	0	121	1
386	1	311	56	51	0.00	29.28	6.6	1.0	825.7	1281	0	120	9
387	1	1150	70	51	0.00	29.17	8.8	0.4	825.3	0	0	156	9
388	1	1119	66	48	0.00	29.08	7.8	0.1	825.4	0	0	159	8
389	1	1088	64	35	0.00	29.15	8.5	0.3	825.4	0	0	137	8
390	1	1057	46	19	0.00	29.52	17.7	0.7	825.5	1175	0	122	7
391	1	1119	43	23	0.00	29.61	8.2	0.4	825.1	324	246	114	7
392	1	404	56	46	0.00	29.39	9.9	1.0	825.1	0	0	112	8
393	1	497	66	60	0.00	29.18	10.4	1.0	825.2	132	200	114	9
394	1	404	71	63	0.00	29.20	12.9	1.0	825.2	181	0	117	9
395	1	404	73	66	0.00	29.24	14.0	1.0	825.3	169	0	120	10
396	1	497	62	46	0.02	29.46	12.1	1.0	825.2	477	0	119	11
397	1	218	50	43	0.01	29.44	9.4	1.0	825.2	173	0	121	13
398	2	342	51	49	0.02	29.26	6.5	1.0	825.1	0	0	125	13

APPENDIX E

SAMPLE OUTPUT FOR THE LAKE LBJ SIMULATION

RESULTS FOR LAKE LBJ FOR DAY NUMBER 118 OF 1968

SURFACE ELEVATION = 824.79 FEET

THERMOCLINE ELEVATION = 812.33 FEET

TOTAL THERMAL ENERGY = 25677.3 BILLION BTU

INFLOWS	ACRE FEET	DEG F
INKS RELEASE	4822	64.6
LLANO RIVER	1496	74.6
SANDY CREEK	83	74.6
MAKEUP	1089	74.6

OUTFLOW = 7400 ACRE FEET

TEMPERATURE OUT = 67.9 DEG F = 20.0 DEG C

EVAPORATION = 59 ACRE FEET

EXTERNAL HEAT BUDGET IN BTU/FT-FT-DAY

SOLAR RADIATION = 1869.66

ATMOSPHERIC RADIATION = 2881.11

BACK RADIATION = 3106.49

EVAPORATION = 615.91

CONVECTION = 208.11

NET HEAT = 1296.48

ELEVA-TION (FEET)	TEMPER-ATURE (DEG F)	TEMPER-ATURE (DEG C)	VERTICAL VELOCITY (FT/SEC)	OUTFLOW VOLUME (CU.FT./HR)
824.5	71.5	22.0	-.0000043	553970
822.5	70.6	21.4	-.0000037	447720
820.5	70.1	21.2	-.0000030	447720
818.5	69.8	21.0	-.0000020	447720
816.5	69.5	20.8	-.0000009	447720
814.5	69.1	20.6	.0000004	447720
812.5	68.7	20.4	.0000018	447720
810.5	68.3	20.1	.0000035	447720
808.5	67.8	19.9	.0000054	447720
806.5	67.2	19.6	.0000077	447720
804.5	66.7	19.3	.0000103	447720
802.5	66.1	18.9	.0000134	447720
800.5	65.6	18.6	.0000172	447720
798.5	65.1	18.4	.0000216	447720
796.5	64.7	18.1	-.0000015	447720
794.5	64.2	17.9	0.0000000	0
792.5	63.8	17.7	0.0000000	0
790.5	63.4	17.4	0.0000000	0
788.5	63.0	17.2	0.0000000	0
786.5	62.6	17.0	0.0000000	0
784.5	62.2	16.8	0.0000000	0
782.5	61.8	16.6	0.0000000	0
780.5	61.4	16.3	0.0000000	0
778.5	61.0	16.1	0.0000000	0
776.5	60.7	15.9	0.0000000	0
774.5	60.2	15.7	0.0000000	0
772.5	59.8	15.5	0.0000000	0
77 .5	59.4	15.2	0.0000000	0
768.5	58.9	14.9	0.0000000	0
766.5	58.3	14.6	0.0000000	0
764.5	57.7	14.3	0.0000000	0
762.5	57.1	13.9	0.0000000	0
760.5	56.5	13.6	0.0000000	0
758.5	55.9	13.3	0.0000000	0
756.5	55.4	13.0	0.0000000	0
754.5	54.9	12.7	0.0000000	0
752.5	54.6	12.5	0.0000000	0
750.5	54.3	12.4	0.0000000	0
748.5	54.0	12.2	0.0000000	0
746.5	53.8	12.1	0.0000000	0
744.5	53.7	12.1	0.0000000	0
742.5	53.7	12.0	0.0000000	0

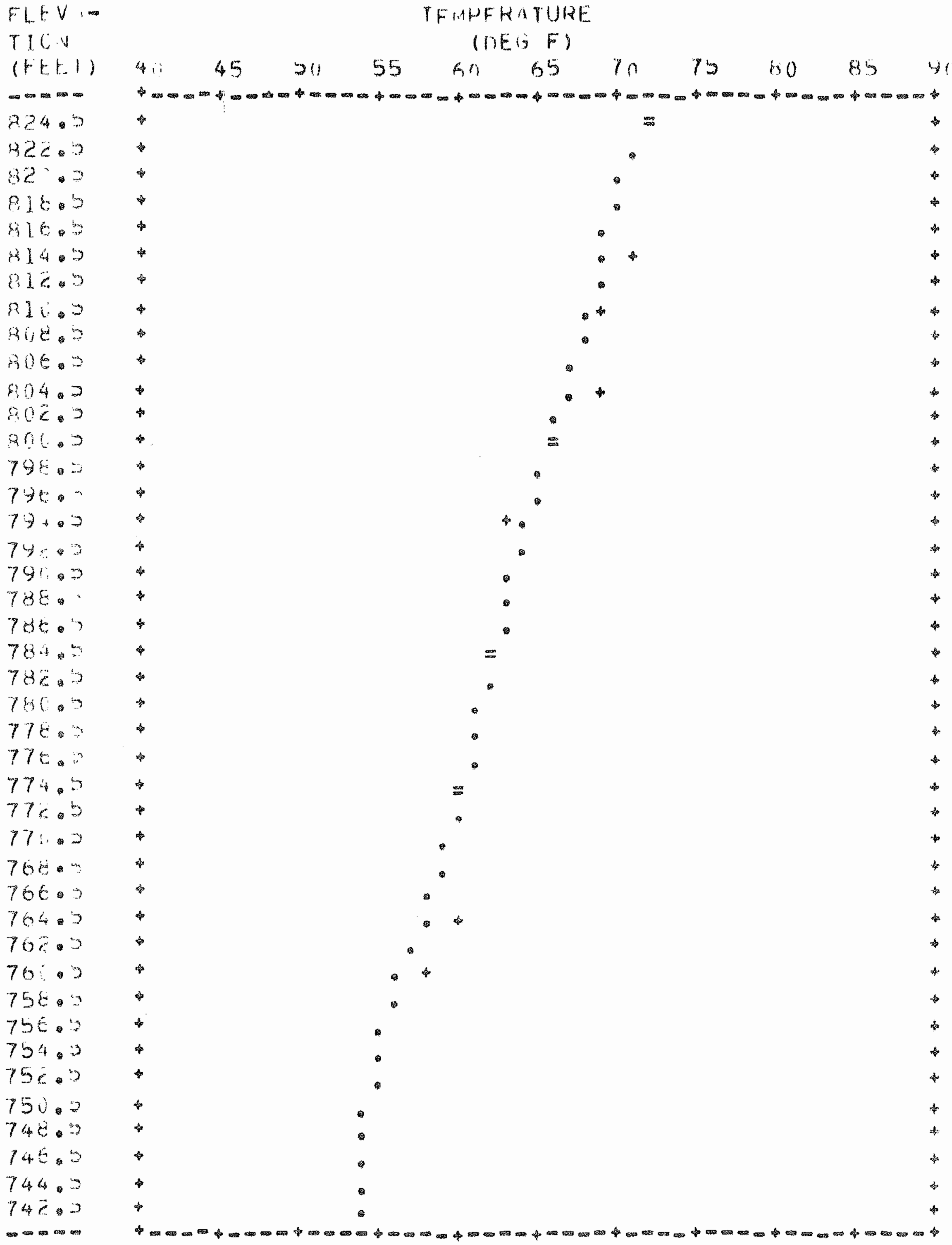

LEGEND

- . CALCULATED TEMPERATURE
- \+ OBSERVED TEMPERATURE
- = CALCULATED AND OBSERVED TEMPERARTURES ARE THE SAME

APPENDIX F

METHOD OF SOLVING THE MATRIX EQUATION $[S]\{\dot{\theta}\} = \{F\}$ FOR $\{\dot{\theta}\}$

The method used for solving the matrix equation

$$[S(t+\Delta t)]\{\dot{\theta}(t+\Delta t)\} = \{F(t+\Delta t)\} \quad \ldots\ldots \text{(F.1)}$$

for $\dot{\theta}(t+\Delta t)$ is presented by Ralston and Wilf (20, p. 233). Writing out a few terms of the matrix:

$$\begin{matrix} S_{12} & S_{13} & & & \\ S_{21} & S_{22} & S_{23} & & \\ & S_{31} & S_{32} & S_{33} & \\ & & & \cdot & \\ & & & \cdot & \\ & & & \cdot & \\ & & & S_{n1} & S_{n2} \end{matrix} \quad \begin{matrix} \dot{\theta}_1 \\ \dot{\theta}_2 \\ \dot{\theta}_3 \\ \cdot \\ \cdot \\ \vdots \\ \dot{\theta}_n \end{matrix} \quad = \quad \begin{matrix} F_1 \\ F_2 \\ F_3 \\ \cdot \\ \cdot \\ \cdot \\ F_n \end{matrix}$$

Note that the subscripts of the S matrix are not in standard matrix notation. This notation, which is also used in the computer program, is employed to reduce storage requirements by not having a storage location for the elements of the S matrix which are always equal to zero. Since the matrix S is tridiagonal, the algorithm used for solving equation F.1 is very simple and fast. The procedure is as follows:

1. Set $\bar{F}_1 = \dfrac{F_1}{S_{1,2}}$ and $\bar{S}_{1,3} = \dfrac{S_{1,3}}{S_{1,2}}$.

2. Operate from the second row to the last row, n, using the relations given below for j = 2,3,...n. Compute

$$\bar{F}_j = \frac{F_j - S_{j,1}\bar{F}_{j-1}}{S_{j,2} - S_{j,1}S_{j-1,3}} \quad ,$$

$$\bar{S}_{j,3} = \frac{S_{j,3}}{S_{j,2} - S_{j,1}\bar{S}_{j-1,3}} \quad .$$

3. For the last row, n,

$$\dot{\theta}_n = \bar{F}_n \quad .$$

4. Operate from row n-1 to row 1 to find $\dot{\theta}_j$ by

$$\dot{\theta}_j = \bar{F}_j - \bar{S}_{j,3}\dot{\theta}_{j+1} \quad .$$

REFERENCES

1. Bohan, J. P. and J. L. Grace, "Mechanics of Flow from Stratified Reservoirs in the Interest of Water Quality", U. S. Army Engineering Waterways Experiment Station, Corps of Engineers, Vicksburg, Mississippi, July 1969.

2. Brady, Derek K., Willard L. Graves, Jr., and John C. Geyer, "Surface Heat Exchange at Power Plant Cooling Lakes", Cooling Water Studies for Edison Electric Institute, The Johns Hopkins University, November 1969.

3. Christianson, Alden G. and Bruce A. Tichenor, "Industrial Waste Guide on Thermal Pollution", U. S. Department of the Interior, Federal Water Pollution Control Administration Pacific Northwest Water Laboratory, Corvallis, Oregon, September 1968.

4. Clay, Herman M. Jr., and E. Gus Fruh, "Selective Withdrawal at Lake Livingston - An Impoundment Water Quality Model Emphasizing Selective Withdrawl", CRWR Report No. 66, The University of Texas at Austin, November 1970.

5. Dake, J. M. K. and D. R. F. Harleman, "Thermal Stratification in Lakes: Analytical and Laboratory Studies", Water Resources Research, Vol. 5. No. 2, April 1969, pp. 484-495.

6. Edinger, John E. and John C. Geyer, "Heat Exchange in the Environment", Cooling Water Studies for Edison Electric Institute, The Johns Hopkins University, June 1965.

7. Fruh, E. Gus, " 'Before' and 'After' Studies of the Effects of Thermal Discharges into Lake Lyndon B. Johnson", Draft Proposal, Center for Research in Water Resources, The University of Texas at Austin, 1970.

8. Fruh, E. Gus and E. M. Davis, "Limnological Investigations of Texas Impoundments for Water Quality Purposes - Limnological and Water Quality Data for the Highland Lakes, 1968", CRWR Report No. 40, The University of Texas at Austin, March 1969.

9. Gebhard, Thomas G. and Frank D. Masch, "Evaluation of Micro-Models for Near Surface Dispersion in Reservoirs", CRWR Report No. 46, The University of Texas at Austin, July 1969.

10. Huber, W. C. and D. R. F. Harleman, "Laboratory and Analytical Studies of the Thermal Stratification of Reservoirs", M.I.T. Hydrodynamics Laboratory Technical Report No. 112, October 1968.

11. Hutchinson, G. E., A Treatise on Limnology, Vol. I. -- Geography, Physics, and Chemistry, John Wiley and Sons, Inc., New York, 1957.

12. Koh, R. C. Y., "Viscous Stratified Flow Towards a Line Sink," W. M. Keck Laboratory Report No. KH-R-6, California Institute of Technology, January 1964.

13. Krenkel, Peter A. and Frank L. Parker, ed., Biological Aspects of Thermal Pollution, Proceedings of the National Symposium on Thermal Pollution, Portland, Oregon, June 3-5, 1968, Vanderbilt University Press, 1969.

14. Lee, Chin-Yuan and Frank D. Masch, "Macro-Turbulence from Wind Waves", CRWR Report No. 47, The University of Texas at Austin, July 1969.

15. Lower Colorado River Authority, "Lake Lyndon B. Johnson and Alvin Wirtz Dam", Undated Pamphlet.

16. Lower Colorado River Authority, Unpublished records of hydro-electric operation, 1971.

17. Lower Colorado River Authority, Unpublished records of the geometry of Lake LBJ, 1971

18. Markofsky, Mark and D. R. F. Harleman, "A Predictive Model for Thermal Stratification and Water Quality in Reservoirs", M. I. T. Hydrodynamics Laboratory Technical Report No. 134, January 1971.

19. Parker, Frank L. and Peter A. Krenkel, Thermal Pollution: Status of the Art, Report No. 3, Department of Environmental and Water Resources Engineering, Vanderbilt University, December 1969.

20. Ralston, Anthony and Herbert S. Wilf, ed., Mathematical Methods for Digital Computers, Vol II, John Wiley and Son, Inc., New York, 1967.

21. Raphael, Jerome M., "Prediction of Temperature in Rivers and Reservoirs", Proceedings of A. S. C. E., Vol. 88, No. PO2, July 1962, pp. 157-181.

22. Sundaram, T. R., C. C. Easterbrook, K. R. Piech, and G. Rudinger, "An Investigation of the Physical Effects of Thermal Discharges into Cayuga Lake ", Cornell Aeronautical Laboratory, Inc., November, 1969.

23. Sundaram, R. R. and R. G. Rehm, "Formation and Maintenance of Thermoclines in Stratified Lakes Including Effects of Power-Plant Thermal Discharges", AIAA Paper No. 70-238, January 1970.

24. Tennessee Valley Authority, "Notes on the Warming of Lake Water by Solar Radiation Absorption Based on Cherokee Reservoir Water Quality Study -- 1967", Division of Water Control Planning, Engineering Laboratory, Norris, Tennessee, March 1969.

25. Texas Water Commission, "Base Flow Studies, Llano River, Texas -- Quantity and Quality", Bulletin No. 6505, Austin, Texas, March 1965.

26. Texas Water Development Board, "Dams and Reservoirs in Texas -- Historical and Descriptive Information ", Report No. 48, Austin, Texas, June 1967.

27. Texas Water Development Board, "Simulation of Water Quality in Streams and Canals", Report No. 128, Austin, Texas, May 1971.

28. Texas Water Development Board, Unpublished records of daily values of short-wave solar radiation at Austin, Texas, 1971.

29. United States Department of Commerce, "Local Climatological Data -- Austin, Texas ", 1968 and 1969.

30. United States Department of the Interior, Geological Survey, "Water Resources Data for Texas ", Part 1, Surface Water Records for the 1968 and 1969 Water Years, 1969 and 1970.

31. Ward, J. C., "Annual Variation of Stream Water Temperature", Proceedings of A. S. C. E., Vol. 89 No. SA6, December 1963, pp. 1-16.

32. Water Resources Engineers, Inc., "Prediction of Thermal Energy Distribution in Streams and Reservoirs", Final Report, Prepared for the Department of Fish and Game, State of California, August 1968.

33. Wunderlich, W. O. and R. A. Elder, "The Mechanics of Stratified Flow in Reservoirs", Tennessee Valley Authority, Division of Water Control Planning, Engineering Laboratory, Norris, Tennessee, April 1967.